OPTIMAL DYNAMIC BALANCING AND DESIGN OF PLANAR MECHANISMS

Ph.D. Thesis

KAILASH CHAUDHARY

(2011RME7145)

DEPARTMENT OF MECHANICAL ENGINEERING

MALAVIYA NATIONAL INSTITUTE OF TECHNOLOGY

JAIPUR

JLN MARG, JAIPUR – 302017, INDIA

AUGUST, 2016

OPTIMAL DYNAMIC BALANCING AND DESIGN OF PLANAR MECHANISMS

KAILASH CHAUDHARY

(2011RME7145)

Thesis submitted

as a partial fulfillment of the requirements of the degree of

Doctor of Philosophy

to the

Department of Mechanical Engineering

Malaviya National Institute of Technology Jaipur

Jaipur – 302017, India

August, 2016

Certificate

This is to certify that the thesis entitled **Optimal Dynamic Balancing and Design of Planar Mechanisms** being submitted by **Mr. Kailash Chaudhary** to the Malaviya National Institute of Technology Jaipur for the award of the degree of **Doctor of Philosophy** is a bonafide record of original research work carried out by him under my supervision in conformity with rules and regulations of the institute.

The results contained in this thesis have not been submitted, in part or in full, to any other University or Institute for the award of any Degree or Diploma.

Dr. Himanshu Chaudhary
Associate Professor
Mechanical Engineering Department
Malaviya National Institute of
Technology Jaipur
Jaipur-302017, India

Acknowledgements

I would like to express my deep and sincere gratitude to my thesis supervisor, Dr. Himanshu Chaudhary, for his invaluable guidance and support. He is an excellent teacher and his knowledge and logical way of thinking has been of great value for me. This research is impossible without his inspiring guidance, experience, and subject knowledge.

I also take this opportunity to express my heartfelt thanks to the members of Departmental Research Evaluation Committee (DREC), Dr. T. C. Gupta, Dr. Dinesh Kumar and Dr. Amit Singh, who spared their valuable time and experiences to evaluate my research plan and the synopsis. I would also like to thank Prof. G. S. Dangayach, Head of the Mechanical Engineering Department, and his office team for helping in all administrative works regarding the thesis.

My friends, Manoj Gupta, Chitresh Nayak, Vimal Pathak, Sagar Kumar and Ramanpreet Singh made my stay memorable in the department. Finally, but not the least I am very thankful to my parents, wife Monika and sons Veer and Vansh who have surrendered their priority and time for me.

Kailash Chaudhary

Department of Mechanical Engineering

Malaviya National Institute of Technology Jaipur

Abstract

A novel two stage optimization methodology is proposed for dynamic balancing and link's shape design of planar mechanisms in this thesis. The shaking force and shaking moment developed due to the inertia-induced forces need to be reduced for smooth operation of the mechanisms as well as to improve their dynamic performance. In the first stage of the formulation, the balancing of shaking force and shaking moment is presented. The shaking force and shaking moment solely depend on link's masses and their distribution for the prescribed motion of the mechanism. The mass distribution of each moving link is modeled as an equimomental set of point-masses. The point-mass parameters are chosen as the design variables and the constraints are defined to ensure the feasibility of the mechanism links. The optimization problem is formulated to minimize the shaking force and shaking moment for the complete cycle of the mechanism operation. The optimization problem is solved using popular evolutionary optimization technique, Genetic algorithm (GA), and Teaching-learning-based-optimization (TLBO) algorithm. It is found that TLBO is computationally more efficient than GA as it finds the optimum results with less number of function evaluations than GA.

The optimum inertial parameters obtained from the first stage optimization are the desired inertial properties. Links shapes are synthesized systematically using closed parametric curve such as cubic B-spline in the second stage of the optimization method for the desired inertial properties. The control points of cubic B-spline curve are taken as the design variables for link shape formation. The constraints on design variables are proposed for both symmetrical and non-symmetrical shapes in the optimization problem formulation. The proposed method of balancing and shape synthesis can be applied to any planar single and multiloop mechanism with revolute as well as prismatic joints. Its effectiveness is demonstrated by applying it to four-bar, five-bar, six-bar and slider-crank mechanisms.

Contents

Certificate i

Acknowledgements ii

Abstract iii

Contents iv

List of Figures vii

List of Tables xi

List of Symbols and Abbreviations xiii

Chapter 1 Introduction 1

1.1 Balancing of Mechanisms 5

1.2 Link Shape Synthesis 7

1.3 Contributions of the Research 8

1.4 Thesis Organization 8

1.5 Summary 10

Chapter 2 Literature Survey 11

2.1 Complete Shaking Force Balancing 11

2.2 Complete Shaking Force and Shaking Moment Balancing 13

2.3 Partial Shaking Force and Shaking Moment Balancing 18

2.3.1 Method of harmonic balancing 18

2.3.2 Extension of method of linearly independent Vectors 19

2.3.3 Optimum design of counterweights 21

2.3.4 Optimum mass distribution using equimomental system of point-masses 22

2.3.5 Optimum mass distribution to reduce effect of joint clearances 24
2.3.6 Non-linear constraint optimization using natural orthogonal complement method 25
2.3.7 Mixed mass redistribution method 25
2.3.8 Balancing through integrating kinematic and dynamic characteristics 26
2.3.9 Sensitivity analysis 26
2.4 Methods for Link Shape Synthesis 28
2.4.1 Small element superposing method 28
2.4.2 Voxel-based discretization 28
2.4.3 Evolutionary structural optimization method 29
2.4.4 Gradient-based method 30
2.4.5 Topology optimization method 30
2.4.6 Shapes for specific path and motion 31
2.5 Optimization Techniques 31
2.6 Summary 32
Chapter 3 Optimization Techniques 34
3.1 Definitions of Different Terms Used In Optimization Techniques 37
3.2 Genetic Algorithm 39
3.3 Teaching-Learning-Based Optimization Algorithm 46
3.4 Applications 55
3.5 Summary 56
Chapter 4 Optimal Dynamic Balancing 57
4.1 Equations of Motion of Rigid Link Moving In a Plane 57

4.2 Equimomental Systems of Point-masses 60

4.3 Shaking Force and Shaking Moment 65

4.4 Optimization Problem Formulation 67

4.5 Planar Mechanisms 69

4.5.1 Four-bar mechanism 70

4.5.2 Five-bar mechanism 81

4.5.3 Stephenson six-bar mechanism 85

4.5.4 Slider-crank mechanism 89

4.6 Multi-cylinder Engine 95

4.7 Summary 98

Chapter 5 Optimal Link Shape Synthesis 99

5.1 Link Shape 99

5.2 Optimization Problem Formulation 104

5.3 Planar Mechanisms 108

5.3.1 Four-bar mechanism 110

5.3.2 Five-bar mechanism 118

5.3.3 Stephenson six-bar mechanism 119

5.3.4 Slider-crank mechanism 122

5.4 Summary 125

Chapter 6 Conclusions 127

References 130

Appendix A MATLAB codes for generating shape 142

Appendix B MATLAB codes for calculating inertial properties of a shape 150

Papers published based on this work 155

Brief Biodata of the author 157

List of Figures

Fig. 1.1	Applications of planar mechanism	4
Fig. 1.2	Complete force and moment balancing of four-bar mechanism with physical pendulum coupler and inertia counterweights on rotating links (Norton, 2011)	6
Fig. 2.1	Complete force balancing of planar four-bar mechanism using counterweights (Berkof and Lowen, 1969)	12
Fig. 2.2	Complete balancing of planar four-bar mechanism using geared counter-inertias (Esat and Bahai, 1999)	15
Fig. 2.3	Dynamic balancing of planar six-bar mechanism using cam operated counterweight (Kamenskii, 1968a, b)	15
Fig. 2.4	Complete shaking force and shaking moment balancing through mass redistribution and addition of inertia counterweights (Feng, 1990)	16
Fig. 2.5	Complete shaking force and shaking moment balancing of slider-crank mechanism based on the copying properties of the pantograph (Arakelian and Smith, 1999)	17
Fig. 2.6	Self-balanced slider-crank mechanism (Arakelian, 2006)	17
Fig. 2.7	First harmonic balancing of the shaking moment in planar four-bar mechanism (Arakelian and Dahan, 2001)	20
Fig. 2.8	Balancing of planar four-bar mechanism using three counterweights (Tricamo and Lowen, 1983a, b)	21
Fig. 2.9	Partial balancing of planar ten-bar mechanism using sector-type counterweights (Verschuure, 2009)	22
Fig. 2.10	Planar four-bar mechanism with joint clearance (Erkaya and Uzmay, 2009)	24
Fig. 2.11	Balancing of four-bar mechanism by designing bi-material moving links (Soong and Hsu, 2007)	27
Fig. 2.12	Small element superposing method for finding link shape (Feng et al., 2002)	29
Fig. 2.13	Optimum shape for piston-crank mechanism using gradient-based method (Azegami et al., 2013)	30

Fig. 2.14	Geometry synthesis through topology optimization (Yoganand and Sen, 2011)	31
Fig. 3.1	Flow chart of the genetic algorithm	42
Fig. 3.2	Crossover site selection	44
Fig. 3.3	Parent's crossover to produce children	44
Fig. 3.4	Bitwise mutation	45
Fig. 3.5	Flow chart of the TLBO algorithm	52
Fig. 4.1	The *i*th rigid link moving in XY plane	58
Fig. 4.2	Equimomental system of point-masses for *i*th rigid link	62
Fig. 4.3	Definitions of various parameters for a multiloop mechanism	66
Fig. 4.4	Four-bar mechanism detached from its frame	71
Fig. 4.5	Variation in shaking force with time for one complete crank cycle. Case (1), (2), (5) and (6) without converting link #2 into physical pendulum; Case (3) and (4) with link #2 as physical pendulum in four-bar mechanism	74
Fig. 4.6	Variation in shaking moment with time for one complete crank cycle. Case (1), (2), (5) and (6) without converting link #2 into physical pendulum; Case (3) and (4) with link #2 as physical pendulum in four-bar mechanism	75
Fig. 4.7	Variation in driving torque with time for one complete crank cycle. Case (1), (2), (5) and (6) without converting link #2 into physical pendulum; Case (3) and (4) with link #2 as physical pendulum in four-bar mechanism	76
Fig. 4.8	Variations in the dynamic quantities of original and optimally balanced four-bar mechanism using GA and TLBO for complete cycle of operation	79
Fig. 4.9	Pareto front for four-bar mechanism	80
Fig. 4.10	Convergence plot comparing GA and TLBO values for four-bar mechanism	80
Fig. 4.11	Planar five-bar mechanism detached from its frame	81
Fig. 4.12	Variations in the dynamic quantities of original and optimally balanced five-bar mechanism using GA and TLBO for complete cycle of operation	83

Fig. 4.13	Pareto front for five-bar mechanism	84
Fig. 4.14	Convergence plot comparing GA and TLBO values for five-bar mechanism	85
Fig. 4.15	Variations in the dynamic quantities of original and optimally balanced Stephenson six-bar mechanism using GA and TLBO for complete cycle of operation	88
Fig. 4.16	Pareto front for Stephenson six-bar mechanism	89
Fig. 4.17	Convergence of objective function in GA and TLBO for Stephenson six-bar mechanism	89
Fig. 4.18	Planar slider-crank mechanism detached from its frame	91
Fig. 4.19	Variations in the dynamic quantities of original and optimally force balanced slider-crank mechanism for complete cycle of operation	92
Fig. 4.20	Variations in the dynamic quantities of original and optimally balanced slider-crank mechanism using GA and TLBO for complete cycle of operation	93
Fig. 4.21	Pareto front for slider-crank mechanism	95
Fig. 4.22	Convergence of objective function in GA and TLBO for slider-crank mechanism	95
Fig. 4.23	Crank orientations in four-cylinder inline engine	96
Fig. 4.24	Bearing forces in four-cylinder inline engine	97
Fig. 4.25	Force on bearing C in four-cylinder inline engine	98
Fig. 5.1	Closed cubic B-spline curve and its control points	101
Fig. 5.2	Closed cubic B-spline curve representing link shape and its control points where P_i and P_j are two opposite points about x-axis	106
Fig. 5.3	Design variables to find optimum link shape of planar mechanisms	108
Fig. 5.4	Two stage optimization scheme to balance mechanism and shape synthesis	109
Fig. 5.5	Original and optimally designed mechanisms corresponding to different cases for four-bar mechanism [all figures drawn on scale]	112
Fig. 5.6	CAD model of optimally designed four-bar mechanism	117

Fig. 5.7	Fully force and moment balanced inline four-bar mechanism (Farmani et al., 2011)	117
Fig. 5.8	Original and optimally designed five-bar mechanism [figure drawn on scale]	118
Fig. 5.9	CAD model of optimally designed five-bar mechanism	119
Fig. 5.10	Original and optimized link shapes of Stephenson six-bar mechanism [figure drawn on scale]	120
Fig. 5.11	CAD model of optimally designed Stephenson six-bar mechanism	121
Fig. 5.12	Balancing of shaking force and shaking moment in Stephenson six-bar mechanism using counterweights (Verschuure et al., 2007)	121
Fig. 5.13	Original and optimally designed force balanced planar slider-crank mechanism [figure on scale]	122
Fig. 5.14	CAD model of optimally designed force balanced slider-crank mechanism	123
Fig. 5.15	Original and optimally designed planar slider-crank mechanism [figure drawn on scale]	124
Fig. 5.16	CAD model of optimally designed planar slider-crank mechanism	125
Fig. 5.17	Complete force and moment balancing of slider-crank mechanism using cam attached counterweights (Arakelian and Briot, 2010)	125
Fig. A.1	The control points of a circle	142
Fig. A.2	Circle generated using linear B-spline curve segments	145
Fig. A.3	Circle generated using quadratic B-spline curve segments	146
Fig. A.4	Circle generated using cubic B-spline curve segments	148
Fig. A.5	Circle generated using linear, quadratic and cubic B-spline curve segments	149

List of Tables

Table 3.1	Initial population for genetic algorithm example	43
Table 3.2	Selection of solutions to generate new generation	43
Table 3.3	Final population at the end of one iteration of genetic algorithm	45
Table 3.4	Controlling parameters for different evolutionary optimization algorithms	47
Table 3.5	Initial population generation for TLBO example	53
Table 3.6	Modified population in Teacher phase	53
Table 3.7	Modified population at the end of Teacher phase	54
Table 3.8	Modified population in Learner phase	55
Table 3.9	Modified population at the end of Learner phase	55
Table 4.1	Original parameters of four-bar mechanism	71
Table 4.2	Equimomental point-mass parameters for Normalised four-bar mechanism links	71
Table 4.3	Values of dynamic quantities in the original and optimally balanced four-bar mechanism	73
Table 4.4	Link parameters of the optimally balanced four-bar mechanism	73
Table 4.5	Normalized RMS values of dynamic quantities in the original and optimally balanced four-bar mechanism using GA and TLBO (case 2)	78
Table 4.6	Normalised optimum equimomental point-mass parameters for balanced four-bar mechanism (case 2)	78
Table 4.7	Parameters of original and optimally balanced four-bar mechanism	81
Table 4.8	Parameters of original and optimally balanced planar five-bar mechanism	82
Table 4.9	Normalized RMS values of dynamic quantities in the original and optimally balanced five-bar mechanism using GA and TLBO	84
Table 4.10	Normalised optimum equimomental point-mass parameters for balanced five-bar mechanism	85
Table 4.11	Parameters of original and optimally balanced planar Stephenson six-bar mechanism	86
Table 4.12	Normalized RMS values of dynamic quantities in the original and	87

	optimally balanced Stephenson six-bar mechanism using GA and TLBO	
Table 4.13	Normalised optimum equimomental point-mass parameters for balanced Stephenson six-bar mechanism	87
Table 4.14	Original and optimum parameters of statically and dynamically balanced planar slider-crank mechanism	90
Table 4.15	Normalized dynamic quantities for planar slider-crank mechanism	94
Table 4.16	Optimum equimomental point-mass parameters for balanced slider-crank mechanism	94
Table 4.17	Normalized bearing forces in four-cylinder inline engine	97
Table 5.1	Design variables for optimally designed four-bar mechanism (all parameters are in meters)	113
Table 5.2	Design variables for optimally designed five-bar mechanism (all parameters are in meters)	119
Table 5.3	Design variables for optimally designed Stephenson six-bar mechanism (all parameters are in meters)	120
Table 5.4	Design variables for optimally designed slider-crank mechanism (all parameters are in meters)	124
Table B.1	Inertial properties of the circle	154

List of Symbols and Abbreviations

$\mathbf{a}_i$	position vector of the origin O_{i+1} of the $(i+1)^{th}$ link, from origin O_i of the ith link
a_i	magnitude of $\mathbf{a}_i$, link length
A	area of region defining link shape
C_i	the mass center of ith link
$\mathbf{d}_i$	position vector of the mass center C_i of ith link, from origin O_i
D	boundary of region defining link shape
$\mathbf{f}_i^c$	resultant force acting on the ith link at center of mass C_i
$\mathbf{f}_{sh}$	shaking force in the complete mechanism
$\bar{f}$	normalized shaking force in the complete mechanism
$\mathbf{I}_i^c$	the centroidal inertia tensor with respect to C_i
l_{ij}	distance of jth point mass from origin O_i of ith link
k_i	radius of gyration of ith link about origin O_i
m_i	mass of ith link
m_{ij}	mass of jth point mass of ith link
$\mathbf{n}_i^c$	resultant of the pure moment and the moment of forces about C_i
$\mathbf{n}_{sh}$	shaking moment in mechanism about a fixed point perpendicular to the plane of motion
$\bar{n}$	normalized shaking moment in the complete mechanism
O_i	origin of ith link where local coordinate frame $O_i\ X_i\ Y_i$ fixed to the link
O_{i+1}	origin of (i+1)st link
P_i	ith control point of closed parametric curve
t	thickness of links

$\mathbf{v}_i$	linear velocity of origin O_i of ith link
$\mathbf{v}_i^c$	linear velocity of mass center C_i of ith link
$\dot{\mathbf{v}}_i$	linear acceleration of origin O_i of ith link
$\dot{\mathbf{v}}_i^c$	linear acceleration of mass center C_i of ith link
w_1, w_2	weighting factors for multiple objective functions
$\mathbf{x}_i$	design vector for the ith link
$\mathbf{x}$	design vector for complete mechanism
α_i	angular position of ith link
θ_i	angular position of mass center C_i of ith link in the local frame
θ_{ij}	angular position of point mass m_{ij} in the local frame
ω_i	angular velocity of ith link
$\dot{\omega}_i$	angular acceleration of ith link
ρ	material density of link's material

Vectors are shown by bold characters

Chapter 1

Introduction

The prime objective of this research work is to develop a unified methodology for dynamic balancing and link design of the planar mechanisms. The planar mechanisms have wide applications in industrial machinery, automotive and robotics (Fig. 1.1). These mechanisms are designed considering dynamics and kinematics to fulfill the specific requirement of the different applications. To design a mechanism on the basis of the dynamic constraints, the important properties considered are shaking force, shaking moment and driving torque.

The balancing of inertia forces and moments in mechanisms is referred to dynamic balancing. The unbalanced inertia force and moment shake the mechanism known as the shaking force and the shaking moment. They are responsible for increased vibration and noise level, increased energy consumption and loss of functional accuracy as well as mechanical life. Thus these quantities are to be minimized to improve the dynamic performance, to reduce the vibrations, noise and wear and to smooth the input torque.

The dynamic balancing requires trade-off between these competing shaking force and shaking moment. Thus, the mechanism balancing problem can be formulated as an optimization problem to minimize simultaneously shaking force and shaking moment with proper constraints imposed to assure the feasibility of the mechanism. The mass and its distribution of each moving link of the mechanism contribute to the shaking force and shaking moment and hence play a significant role in the balancing. Thus determination of inertial properties and shape of the link consists of two distinct problems.

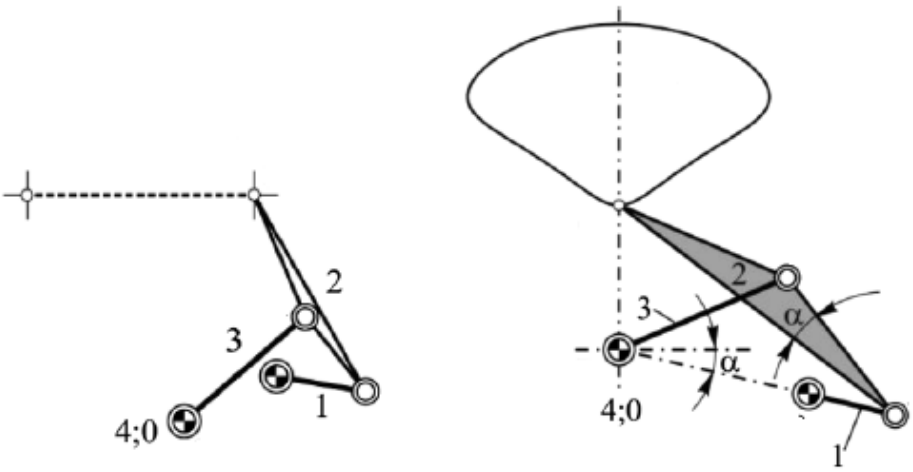

(a) Planar four-bar mechanism for generating (1) straight line displacement and (2) symmetric coupler curve (Husing et al., 2015)

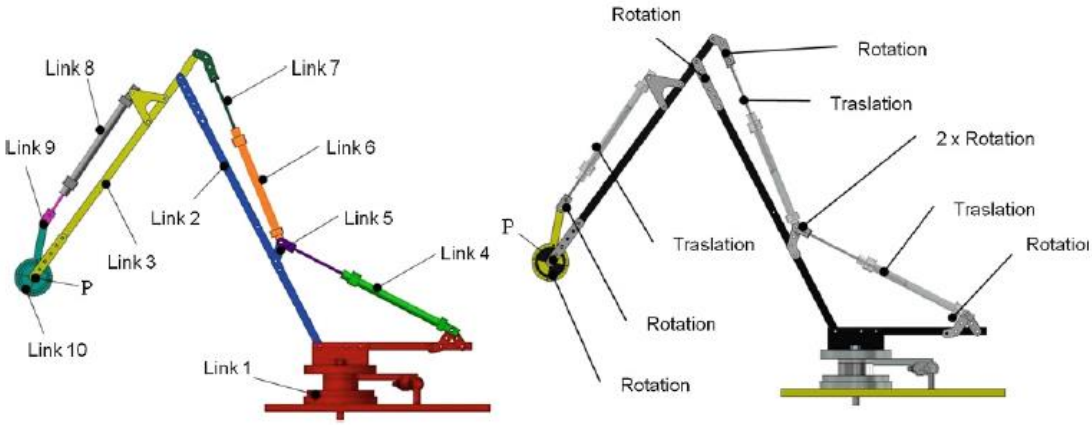

(b) Planar ten-bar mechanism for designing a manipulator arm (Soriano et al., 2015)

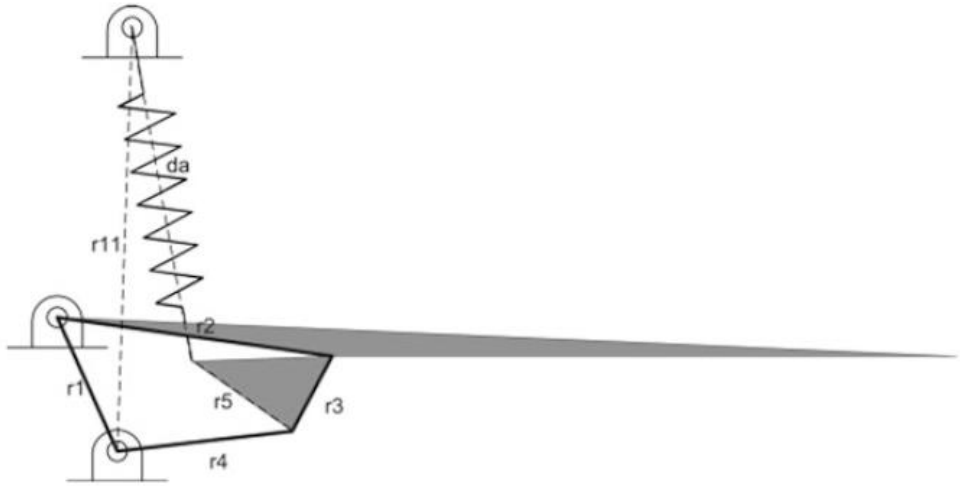

(c) Planar four-bar mechanism for designing a motorcycle rear suspension systems (Castillo et al., 2013)

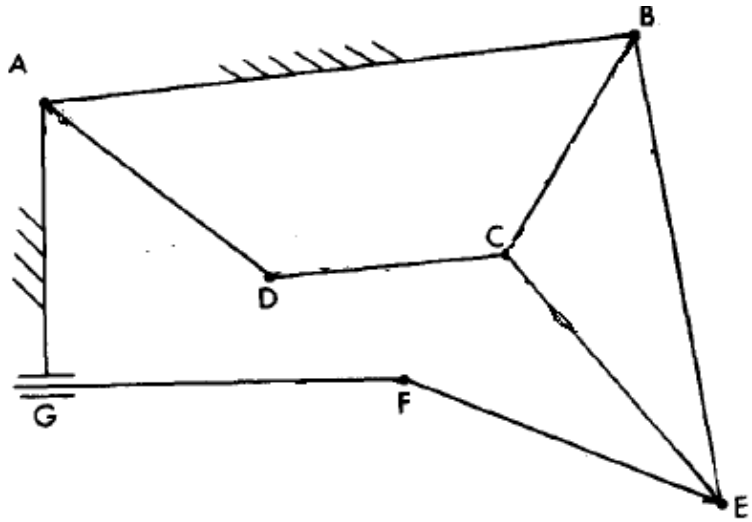

Link AD rotates at constant speed and the paper is fed by link FG

(d) Planar six-bar mechanism used for feeding paper in duplicating machine (Walker and Oldham, 1978)

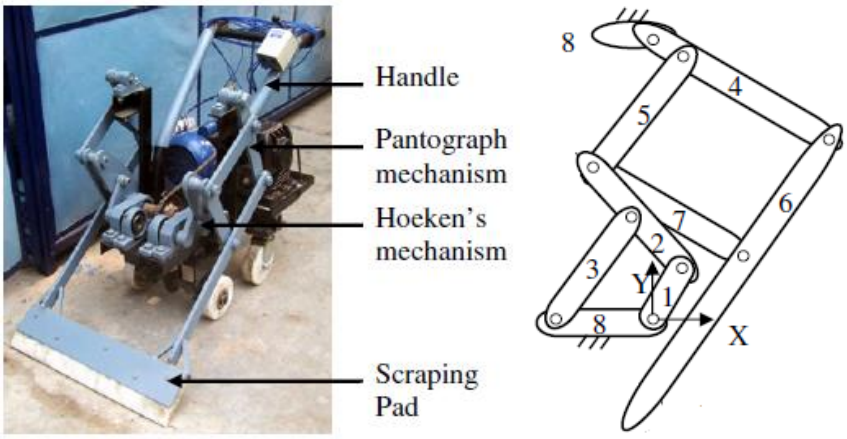

(e) Carpet scraping machine with planar multiloop mechanism (Chaudhary and Saha, 2008)

Fig. 1.1 *Applications of planar mechanism*

The optimization problem for dynamic balancing of the mechanism and its links shape synthesis is formulated in two successive stages in this research work. There are several algorithms available to solve any optimization problem. Among the various optimization algorithms, Genetic Algorithm (GA) and Teaching-Learning-Based-Optimization algorithm (TLBO) are explored for the balancing problem. These optimization algorithms find solution near to the global optimum solution without providing initial guess solution to start the algorithm.

The algorithms are compared in terms of convergence to reach to the global optimum solution. To demonstrate the effectiveness of the proposed methodology, several mechanisms are considered to balance and to find shapes of links. The mechanisms consist of single-loop and/or multiloop with binary and ternary links, namely, four-, five- and six-bar and slider-crank mechanisms are optimally balanced and their links' shapes are obtained.

1.1 Balancing of Mechanisms

The interaction between a mechanism and its surrounding is an important aspect to be considered by the machine designers. Most of the modern machinery uses the high speed mechanisms. The resultant inertial forces and moments of the moving links of these mechanisms are termed as shaking force and shaking moment. These inertial forces and moments have no opposite reaction forces to cancel out internally in the mechanism. Finally they transmit to the frame on which the mechanism is mounted. As a consequence, resulting vibrations, wear, noise and fatigue adversely affect the dynamic performance of the mechanism. All the applied and constraint forces have equal and opposite reaction forces and they vanish within system including frame. There will be no reaction force for the inertia forces and moments and hence they need to be balanced. The mechanism balancing also helps in reducing the fluctuations in the input torque required to maintain a constant drive speed.

The shaking force and shaking moment depend upon the masses and their distribution, and accelerations of the moving links of the mechanism under study. The shaking force can be balanced either by redistributing the link masses or by adding the counterweights which results in overall increase in mass of the balanced mechanism. However, the complete balancing of shaking moment is not possible using mass redistribution alone. Therefore, the balancing of the shaking moment along with the shaking force can be achieved by using the additional links having opposite motion that makes the balanced mechanism very complex as shown in Fig. 1.2.

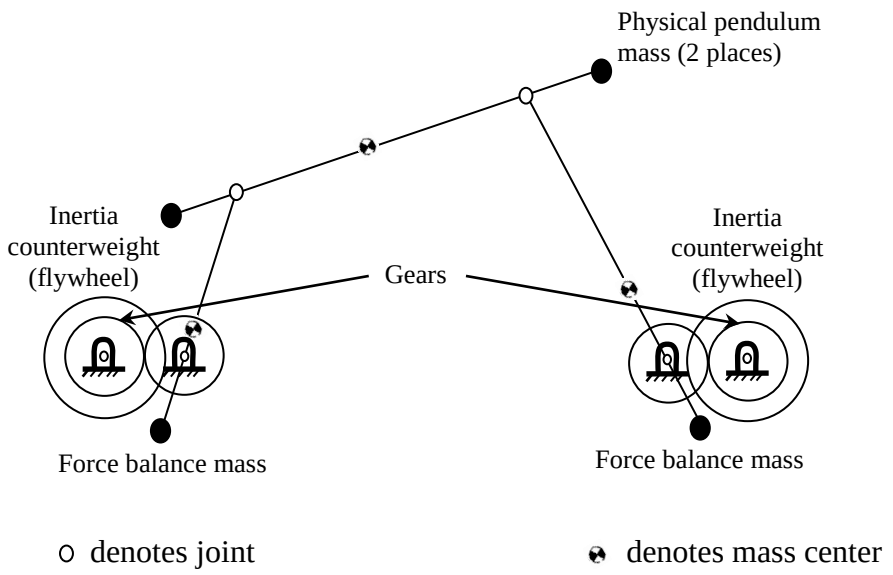

Fig. 1.2 *Complete force and moment balancing of four-bar mechanism with physical pendulum of coupler and inertia counterweights on rotating links (Norton, 2011)*

Thus the complete balance of shaking force and shaking moment is not recommended in most of the studies. To overcome this difficulty, some methods suggest reducing the shaking force and shaking moment simultaneously using the optimization methods. The researchers all over the world are continuously trying to explore the new ideas and techniques to balance the shaking force and shaking moment in the planar mechanisms though a good amount of research in this area has been carried out in the past.

In most of the methods available in the literature, the analytical method is derived for complete force balance for simple mechanisms and cannot be extended for the complex mechanisms. Few optimization methods use the dynamically equivalent systems to balance the mechanisms by finding the optimum inertial parameters of the mechanism, i.e., the mass, the mass moment of inertia and the mass center location. The convex optimization method is also used to optimally design the counterweights to balance the mechanisms. Some other methods are based on the mixed mass

redistribution approach in which the principles of mass distribution and counterweight addition are combined to achieve dynamic balancing in the planar mechanisms.

1.2 Link Shape Synthesis

One of the crucial problems in mechanism is to determine link's shape for the desired inertial properties corresponding to minimum shaking force and shaking moment. The links must carry the applied and constraint dynamic loads during the operation of the balanced mechanism. To synthesize the links' shapes for the specified inertial properties, machine designer normally find shapes iteratively from the initial guess designs. Methods such as small element superposing method, voxel-based discretization, evolutionary structural optimization method, gradient-based method and topology optimization method are proposed in the literature. These methods require a pre-defined design domain, i.e., initial guess shape, to start with and do not include the dynamic balance requirements.

Thus, the optimization methods available in the literature are used separately (1) for the dynamic balancing of the planar mechanisms and (2) for synthesizing their link shapes. This motivates to develop a methodology to find the links' shapes which balance the planar mechanisms dynamically through simultaneous reductions in shaking force and shaking moment.

In this thesis, the computer-aided design principles are used to form the links' shapes. The closed parametric curves, i.e., cubic B-spline curves are used to define shapes' boundaries. The inertial properties of the resulting links' shapes should be same as those of the balanced mechanism.

1.3 Contributions of the Research

The contributions of this research work are summarized as follows:

1. The problem of dynamic balancing and formation of links' shapes for the planar multiloop mechanisms is proposed as an optimization problem.
2. Planar mechanisms are balanced by finding the optimum mass distribution for their links instead of using the counterweights and/or additional members.
3. A novel design methodology for links of the optimally balanced mechanisms using computer aided design principles is proposed.
4. Evolutionary optimization techniques are explored to find the optimum solution for the proposed optimization problem.
5. Teaching-learning-based optimization algorithm (TLBO) is applied for the mechanism balancing. It is established that TLBO is computationally more efficient than the popular optimization algorithm, genetic algorithm (GA).

1.4 Thesis Organisation

This thesis contains six chapters arranged as follows:

Chapter 1: Introduction

The objective and motivation of the research work to develop a method for the dynamic balancing and link shape synthesis is presented in this chapter. It introduces the mechanism balancing and link shape synthesis approaches. It also highlights the major contributions of the research work and outlines the organization of the thesis.

Chapter 2: Literature Survey

The various methods developed for complete force balance, complete force and moment balance, partial force and moment balance including the optimization methods as well as the methods used for link shape synthesis are discussed in this

chapter. The drawbacks and limitations of these methods are mentioned to identify the research gap.

Chapter 3: Optimization Techniques

This chapter discusses about the traditional and evolutionary optimization algorithms. It differentiates the various parameters required to search the solution in the entire design space for these optimization algorithms. The popular evolutionary optimization algorithms, Genetic algorithm (GA), and teaching-learning-based optimization algorithm (TLBO), are explained and their applications are discussed in this chapter.

Chapter 4: Optimal Dynamic Balancing

The dynamics for the planar mechanisms along with the equimomental system of point-masses used to simplify it are explained in this chapter. The optimization problem is formulated to dynamically balance the planar mechanism and numerical examples of planar four-, five- and six-bar and slider-crank mechanism are solved to minimize the shaking force and shaking moment. The method to reduce the loads on main bearings of an inline multi-cylinder engine is also presented.

Chapter 5: Link Shape Synthesis

This chapter presents the formulation of the optimization problem for the link shape synthesis. The numerical problems of planar four-, five- and six-bar and slider-crank mechanism which are solved for the dynamic balancing in the chapter 4 are solved to find the optimum link shapes in this chapter.

Chapter 6: Conclusions

The results obtained in this research work are summarized in this chapter. It also addresses the contributions and future scope of the research work.

1.5 Summary

The dynamic balancing and link shape synthesis for the planar mechanisms are introduced in this chapter. It describes the motivation and objective of the research work and also outlines the thesis contributions. It also contains brief information about the six chapters of the thesis.

Chapter 2

Literature Survey

This chapter reviews the various methods developed for balancing of the planar mechanisms and synthesizing the link shapes. The methods used for complete force balance, complete force and moment balance, partial force and moment balance including the optimization methods as well as the methods used for the link shape synthesis are reviewed. Several review papers such as Kamenskii (1968a), Lowen and Berkof (1968), Lowen et al. (1983), Kochev (2000), Arakelian and Smith (2005), Wijk et al. (2009), and Arakelian and Briot (2015) throw light on the quantum of work carried out on the dynamic balancing of the mechanisms.

2.1 Complete Shaking Force Balancing

The complete shaking force balancing known as static balancing requires the total center of mass of a mechanism to be fixed. The two common approaches used to achieve this are the redistribution of the link masses and use of the counterweights for the mechanism links.

The analytical methods have been developed to trace and keep the total mass center of the mechanism fixed. Shchepetilnikov (1968) presented the method of '*Principal Vectors*' in which the position of the mass center is described using the vectors directed along the links of the mechanism. Similarly, Berkof and Lowen (1969) introduced the '*Method of Linearly Independent Vectors*' for the complete force balancing of four and six-bar planar mechanisms with arbitrary link mass distribution (Fig. 2.1). The balancing conditions are presented for the internal mass redistribution and for the counterweight addition. In this method, the links masses are redistributed in such a way that it eliminates the time-dependent terms coefficients in an equation representing the trajectory of the total center of mass of the mechanism.

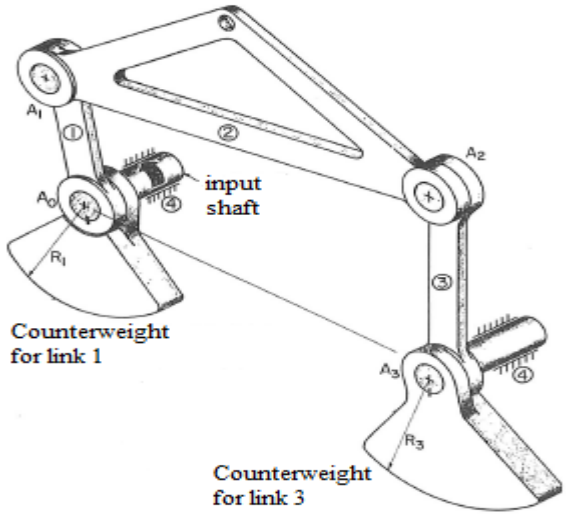

Fig. 2.1 *Complete force balancing of planar four-bar mechanism using counterweights (Berkof and Lowen, 1969)*

This results in a fixed center of mass of the mechanism and thus the complete shaking force balancing is achieved.

Tepper and lowen (1972) extended this method and proved that the counterweights required for the complete force balance of an *n*-link planar mechanism are half of the total number of the links. They developed the '*Contour Theorem*' to differentiate between the mechanisms which can be fully force balanced and those which cannot. Contour theorem examines the nature of the paths from the individual links to the ground. It was found that the pinned planar mechanisms can always be force balanced as they do not have time-dependent coefficient in the center of mass equation. Based on the same approach, Walker and Oldham (1978, 1979) presented the complete force balancing conditions for various types of planar mechanisms with multi-degrees of freedom. The counterweights are used to balance the mechanism containing both the revolute and the prismatic joints. They presented the criteria for deciding the number of the counterweights required for complete force balancing and for the selection of the links to which the counterweight are to be attached. As an extension of the method proposed by Berkof and Lowen (1969), Kochev (1988) used

the ordinary vector algebra for deriving the conditions for full force balancing in the planar mechanisms. Thus, the linear balancing conditions are presented in the Cartesian form in this method. A computer program is also developed to completely balance the shaking force in the mechanisms based on the *Method of Linearly Independent Vectors* which also controls the increment in the shaking moment through properly designing the counterweights (Smith, 1975). In another approach, the balancing conditions are presented to reduce the root-mean-square (RMS) and maximum value of the shaking force in the mechanisms which is known as the best uniform balancing (Han, 1967).

Chiou and Davies (1997) minimized the shaking force in a press machine by designing a cam mechanism. Force balancing along with the trajectory tracking is achieved in a five-bar real-time controllable (RTC) mechanism using the adjusting kinematics parameter (AKP) approach (Ouyang et al., 2003, Ouyang and Zhang, 2005). Similar to the robot manipulators, the RTC mechanism is driven by the servomotors and can be scheduled and planned in real-time. The AKP approach was found better than the counterweight method as far as the reduction in the servomotors torques and joint forces are concerned.

The effect of the complete force balance on the other dynamic properties was studied by Kamenskii (1968a) and Lowen et al. (1974). It was found that the complete force balance increases the shaking moment and driving torque for the mechanism. Therefore, only force balancing is not useful and the moment balance is also needed to balance the mechanism completely.

2.2 Complete Shaking Force and Shaking Moment Balancing

To achieve the dynamic balance in the mechanisms, the shaking moment is completely balanced by eliminating the angular momentum of the moving links along

with the full force balance. The complete elimination of the total angular momentum using the link mass distribution and/or adding the counterweights is not possible (Kochev, 2000). Therefore, normally the shaking moment is reduced by adding disk counterweights (Tepper and Lowen, 1972; Feng, 1990, 1991; Chiou et al., 1998), cam-actuated oscillating counterweight (Kamenskii, 1968b), physical pendulum (Berkof, 1973), counter-rotating disks (Lowen et al., 1983), inertia counterweight (Tricamo and Lowen, 1983a, b), geared counterweights (Esat and Bahai, 1999; Ye and Smith, 1994), duplicate mechanism (Arakelian and Smith, 1999) and moment balancing idler loops (Bagci, 1982). Moore et al. (2009) presented the different sets of the design parameters that dynamically balance a four-bar mechanism without using the counter-rotations.

Berkof (1973) developed a method in which the coupler mass is dynamically substituted by the concentrated masses located at the rotating links to completely balance the force and moment in the mechanisms. In this method, the coupler is treated as a massless link having two concentrated masses and thus only the rotating links need to be balanced for complete balancing of the mechanism. Considering the dynamic replacement of point masses for the moving links described as the mass flow concept, the complete balancing of the planar mechanisms can be obtained (Ye and Smith, 1994).

As an extension to the method of linearly independent vectors for full force balance, Elliot and Tesar (1977, 1982) presented a theory to balance shaking force and shaking moment in the complex planar mechanisms. Esat and Bahai (1999) extended the method developed by Tepper and Lowen (1972) and found that for a fully force balanced mechanism; the moment can be completely eliminated using the geared counter-inertias (Fig. 2.2). Kochev (1992) suggested the balancing of the

shaking moment in a force balanced mechanism by prescribing the input speed fluctuations using non-circular gears.

Kamenskii (1968a, b) used the cam mechanism to completely balance the shaking force and shaking moment in the planar mechanisms (Fig. 2.3). The reduction of the inertia forces is achieved by using a cam-counterweight arrangement where the cam driven masses keep the mechanism's center of mass fixed.

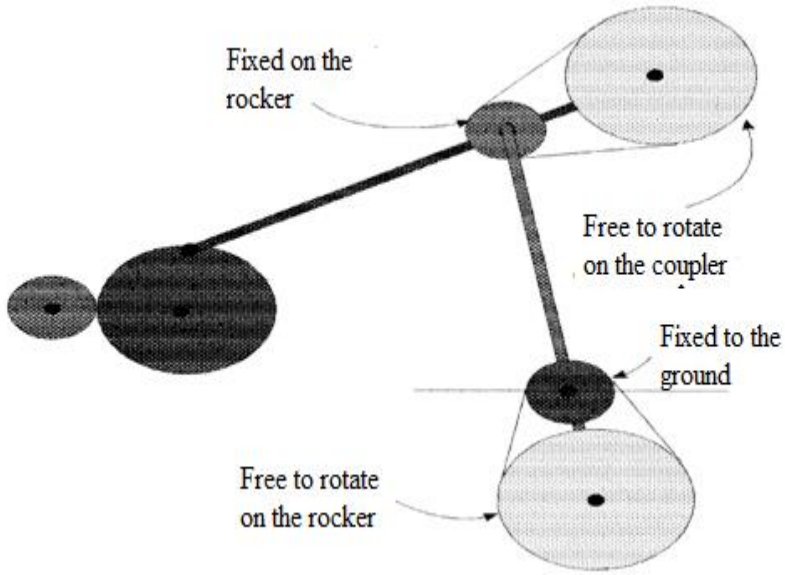

Fig. 2.2 *Complete balancing of planar four-bar mechanism using geared counter-inertias (Esat and Bahai, 1999)*

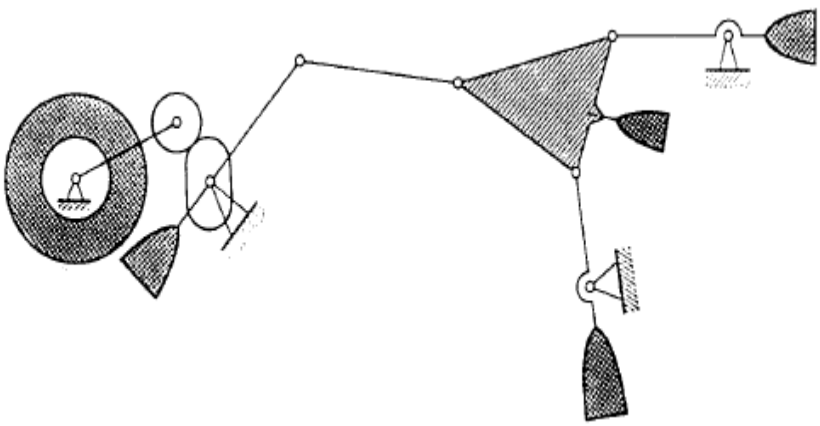

Fig. 2.3 *Dynamic balancing of planar six-bar mechanism using cam operated counterweight (Kamenskii, 1968a, b)*

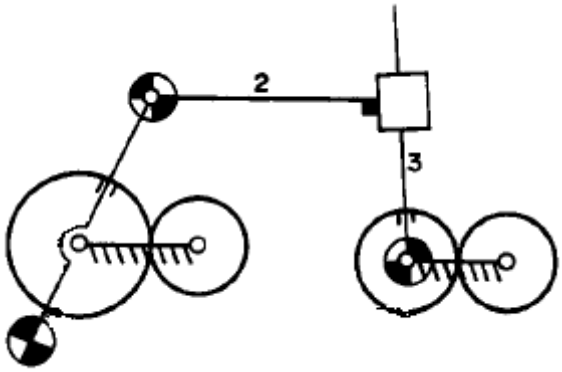

Fig. 2.4 *Complete shaking force and shaking moment balancing through mass redistribution and addition of inertia counterweights (Feng, 1990)*

Feng (1990, 1991) developed a method for complete force and moment balance of the planar mechanisms combining mass redistribution and addition of the geared inertia counterweights (Fig. 2.4). The analytical conditions for complete force and moment balance for 17 types of eight-bar mechanism and 26 types of four-, five- and six-bar mechanism with prismatic pairs are presented in this method.

Arakelian and Smith (1999, 2005) proposed a method to completely balance the planar mechanisms using the counterweights connected through toothed-belt transmission system and gears. This arrangement generates an equal and opposite movement to mechanism's center of mass movement and hence completely balance the mechanism (Fig. 2.5). Similarly, Arakelian (2006) presented a method to improve the balancing of a double slider-crank mechanical system (Fig. 2.6). The shaking force is balanced in this method by using the two slider-crank mechanisms having equal and opposite movements. The shaking moment is balanced in this mechanism by the design modification of the second connecting rod of the double slider-crank mechanical system.

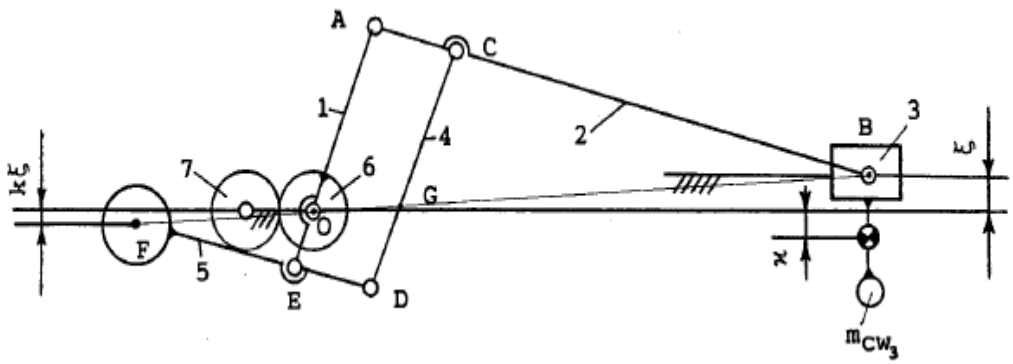

Fig. 2.5 *Complete shaking force and shaking moment balancing of slider-crank mechanism based on the copying properties of the pantograph (Arakelian and Smith, 1999)*

Arakelian and Briot (2010) used counterweight with cam mechanism to balance a slider-crank mechanism. The torque reduction in this mechanism is achieved through the spring that is used to maintain contact with the balancing cam mechanism.

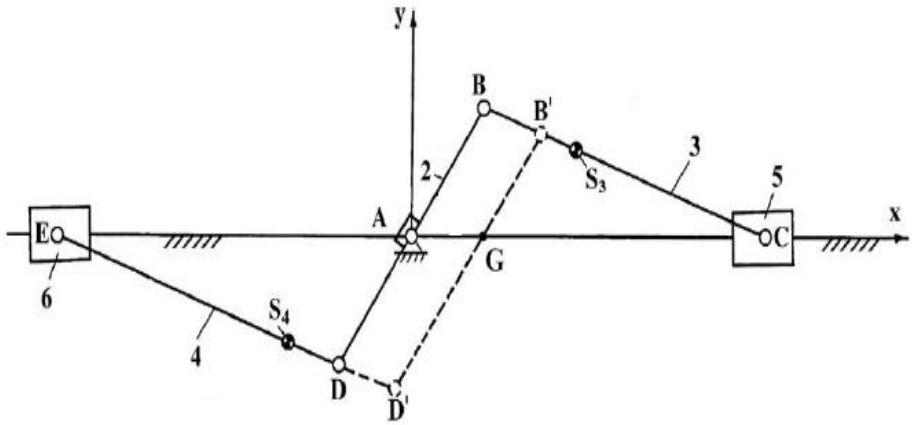

Fig. 2.6 *Self-balanced slider-crank mechanism (Arakelian, 2006)*

Bagci (1979, 1982) solved the balancing problem of planar mechanisms containing multiple prismatic pairs that cannot be fully force balanced using the balancing criteria presented by Tepper and lowen (1972). He termed it as “force transmission irregularities” and used the “idler loop” concept with counter-rotating disks to completely balance the force and moment in the mechanism. Dresig and Dien (2011) proposed a method to completely balance the shaking force and shaking moment using a single rigid body known as the *balancing body*. In this method, the inertia

forces and moments both for the mechanism and the balancing body are eliminated by controlling the motion of the balanced body.

Gosselin et al. (2009) proposed an analytical method for static and dynamic balancing in the mechanisms. In this method, the balancing conditions are presented by the algebraic equations using joint angular velocities and complex variables. Thus, by using the computer algebra, the necessary and sufficient conditions are derived to completely balance the shaking force and shaking moment in the mechanism.

The effects of the dynamic balancing on the elastodynamic properties of the mechanisms are investigated in (Raghu and Balasubramonian, 1990; Xi and Sinatra, 1997; Yu and Jiang, 2007; Martini et al., 2013, 2014). It is found that these methods increase the overall mass, space, cost and complexity in the mechanisms, and most of them are applicable to the simple mechanisms only. Hence, complete force and moment balancing is achieved by producing shaking moment that counteract the moment in the original mechanism.

2.3 Partial Shaking Force and Shaking Moment Balancing

Instead of complete balancing of shaking force and shaking moment independently, minimization of them simultaneously is more useful from the design point of view. The optimization methods used to simultaneously minimize the shaking force and shaking moment in planar mechanism can be categorised as:

2.3.1 Method of harmonic balancing

A method based on the harmonic analysis is used to balance the harmonics of the shaking forces and shaking moments in which the forces and moments are formulated using Gaussian least-square formulation and Fourier series (Norton, 2011). Han (1967) presented a least-square approach to balance the complex mechanisms in which a counterweight connected to the input shaft results in first harmonic balancing

of the inertia induced forces and moments. Stevensen (1973) presented a method for the complete balancing of a harmonic unbalance of the machine, including inertia forces, moments of the inertia forces, and inertia torques, utilizing six weights on three shafts in the machine parallel to the coordinate axes and rotating at the speed of the harmonic. Similarly, Tsai (1984) used two Oldham couplings to balance second harmonics of the shaking force and shaking moment. This type of balancer runs at the primary speed of the machine whereas the Lanchester balancer runs at double of the primary speed to get the same balancing effect (Hsieh and Tsai, 2009). A method was developed based on the harmonic balancing to find the region boundaries to locate the additional shafts by Davies and Niu (1994). Arakelian and Dahan (2001) presented a method to achieve the first harmonic balancing of the shaking moment by using the counterweight connected to the input shaft in such a way that the counterweight rotation axis remains at an offset to the input shaft axis (Fig. 2.7).

2.3.2 Extension of method of linearly independent vectors

Based on the fact that the in a force balanced mechanism, the shaking moment reduces to a pure torque, Berkof and Lowen (1971a, b) developed the theory of shaking moment optimization. In this method, RMS value of the shaking moment is minimized for a force balanced in-line planar four-bar mechanism. The link mass distribution ratios as the functions of the link length ratios are defined as the design variables. This method was the extension of previously developed force balancing method by Berkof and Lowen (1969).

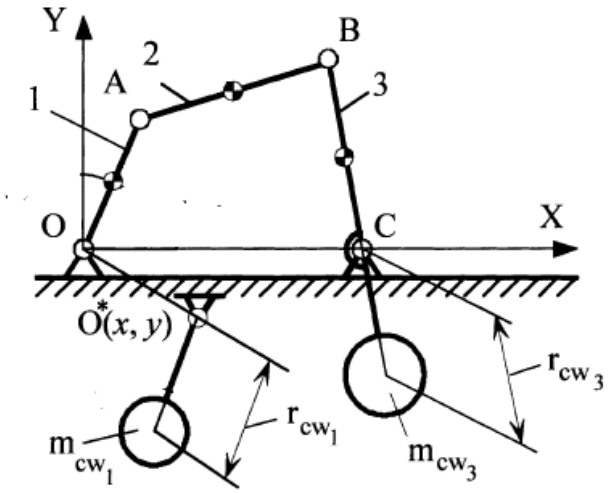

Fig. 2.7 *First harmonic balancing of the shaking moment in planar four-bar mechanism (Arakelian and Dahan, 2001)*

The angular momentum principle is used to define the shaking moment of a force balanced four-bar mechanism. It was shown that the shaking moment cannot be completely balanced without using additional links, but a partial moment balance may be obtained by the desired internal mass rearrangement. Carson and Stephens (1978) extended this method by considering feasible limits for the link parameters. The optimum mass distribution is found for the mechanism links to balance it, and the kinematic design criterion is satisfied by fixing the link length ratios. Similarly, Haines (1981) optimized the RMS values of the shaking moment and the driving torque for a force balanced mechanism by constraining the link parameters within the physical limits.

Tepper and Lowen (1975) presented a method for partial force balancing of four-bar mechanisms, which allows control over the increase in ground bearing forces. They presented a trade-off method, wherein the RMS shaking force of constant input speed, a general four-bar mechanism is optimized while the increase of the RMS ground bearing forces is limited using Lagrange multiplier formulation. They presented an optimization method that represent feasible trade-off techniques for

optimizing the RMS shaking force of a four-bar mechanism while keeping the RMS ground bearing forces lower than those of the fully force balanced mechanism.

2.3.3 Optimum design of counterweights

A partial force balancing method for a planar four-bar mechanism was developed by Tricamo and Lowen (1983a, b) which allows the prescribed maximum shaking force. The simultaneous minimization of shaking moment, input torque and bearing forces is achieved by using the three-counterweight technique (Fig. 2.8). This method determines the parameters of the three counterweights that must be attached to the input, coupler, and output links, respectively.

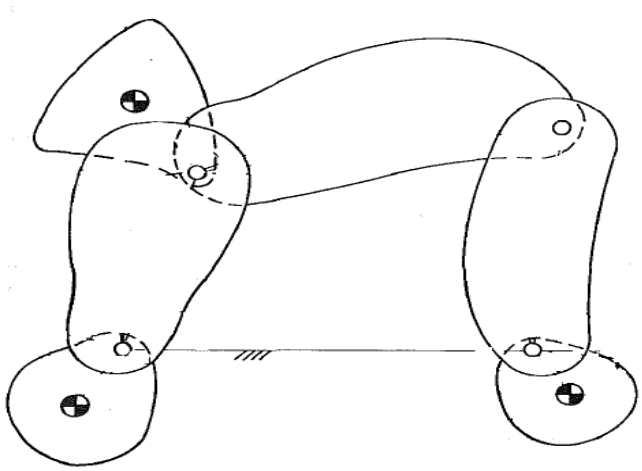

Fig. 2.8 *Balancing of planar four-bar mechanism using three counterweights (Tricamo and Lowen, 1983a, b)*

Demeulenaere et al. (2004, 2006, and 2010) developed a convex optimization technique to determine the counterweight parameters to balance the planar mechanisms. This technique is used to design point-mass counterweights and minimum-inertia counterweights for the planar mechanisms. The counterweight parameters are chosen as the design variables while the upper and lower limits on mass and center of mass coordinates are presented as the convex constraint functions. The ratio of RMS values of the optimized dynamic force to the original dynamic force

known as *balancing effect index* is defined as the objective function. Verschuure (2009) extended this method and introduced a set of auxiliary parameters, μ-parameters that are a function of the classical mass parameters to describe a counterweight. Due to the introduction of these parameters, an analytical derivation of the mechanism kinematics and dynamics is not necessary for this method (Fig. 2.9).

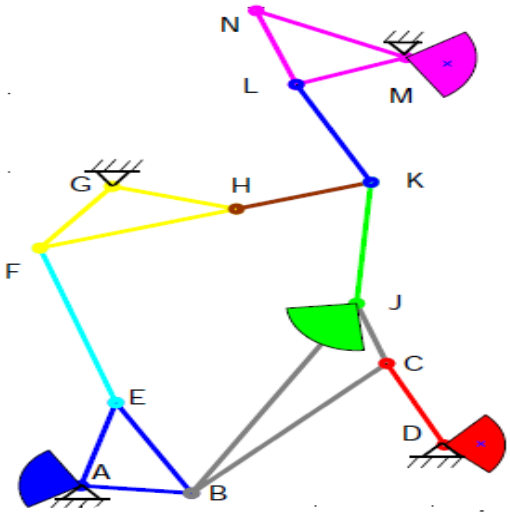

Fig. 2.9 *Partial balancing of planar ten-bar mechanism using sector-type counterweights (Verschuure, 2009)*

Farmani et al. (2011) formulated the mechanism balancing problem as a multi-objective optimization problem based on the concepts of inertia counterweights and physical pendulum developed by Berkof (1973) which completely balance all linear and rotary mass effects. The thickness of counterweights and disks for both input and output links of a planar four-bar mechanism are considered as the objective functions and minimized using Particle Swarm Optimization (PSO) and Genetic Algorithm (GA). The multiple optimum solutions were found for the optimization problem and then a fuzzy decision maker was used to select the best solution.

2.3.4 Optimum mass distribution using equimomental system of point-masses

Gill and Freudenstein (1983a, b) developed a design procedure for the optimum mass distribution of the links of high-speed spherical four-bar mechanisms. This analysis

includes a quadratic-programming technique that allows an optimum trade-off between shaking forces, shaking moments, bearing reactions, and input-torque fluctuation. They replaced the mass distribution of a rigid link with a fixed point by four equivalent point masses to simplify inertia-force calculations. Rahman (1996) extended this method to the general spatial mechanisms. The previous method was limited to one particular type i.e. spherical mechanism. Lee and Cheng (1984) used a two point-mass model for combined balancing of shaking force, shaking moment, and torque by developing the optimality criterion using Lagrangian and Newtonian formulations. They formulated an optimization problem for the mechanism balancing and solved the same by Heuristic Optimization Technique of Lee and Freudenstein (1976a, b). This method presents the trade-offs among shaking force, shaking moment, input-torque fluctuations and bearing reactions by redistributing the link masses and adding counterweights. Thus, the optimum balancing of the mechanism can be achieved in the design stage. The two-point mass model developed by Wiederich and Roth (1976) for momentum conservation was adopted for the modeling of the inertial properties of the mechanism.

Chaudhary and Saha (2007, 2008 and 2009) solved the mechanism balancing problem as an optimization problem by finding the optimum mass distribution of the mechanism links along with constraining the mechanism parameters within the feasible limits. Thus, the shaking force and shaking moment are minimized simultaneously by optimizing links inertial properties, i.e., mass, location of center of mass and moment of inertia. In this method, the inertia properties of the mechanism are represented by the equimomental point-mass systems that are dynamically equivalent to the rigid moving links of the mechanisms. The equimomental point-mass systems are used to identify the design variables and to formulate the constraints

for the optimization problem formulation. They proposed three equimomental point-masses for each link of the planar mechanisms (Chaudhary and Saha, 2006). To determine the shaking force and the shaking moment, the equimomental point-masses parameters are used to formulate the dynamic equations of motion for the mechanisms. An optimization problem is formulated for finding the optimum mass distribution of the mechanism links that minimizes the shaking force and shaking moment. The point-mass parameters are defined as the design variables and limits on links masses, and inertias are presented as the constraints for the optimization problem. The objective function is defined as the weighted sum of the dimensionless RMS values of the shaking force and shaking moment calculated using Newton-Euler equations of motions.

2.3.5 Optimum mass distribution to reduce effect of joint clearances

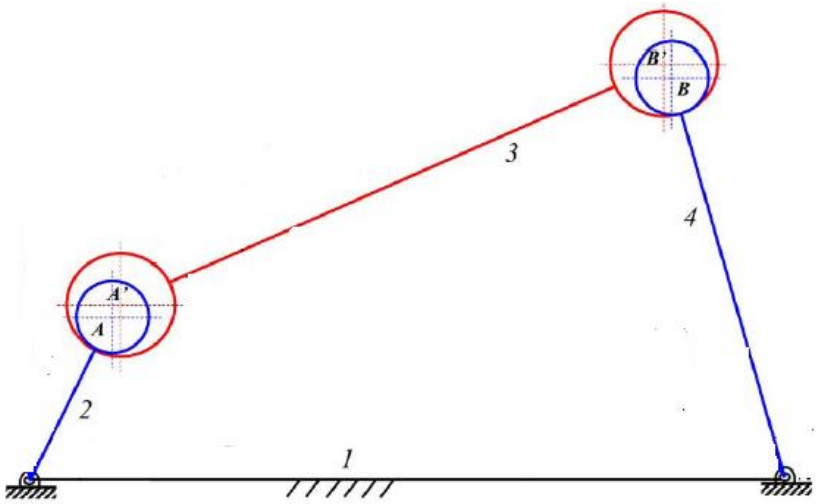

Fig. 2.10 *Planar four-bar mechanism with joint clearance (Erkaya and Uzmay 2009)*

For the mechanisms with a clearance at joints as shown in Fig. 2.10, the changes in the direction and magnitude of the joint forces produce the vibrations and thus considered as the critical design parameters (Zhe and Shixian, 1992). An optimization method is developed to minimize the adverse dynamic effects produced due to the

joint clearances (Park and Kwak, 1987). In this method, the magnitude and location of the counterweight added to the mechanism are selected as the design variables. Similarly, Feng et al. (2002) reduced the joint forces by finding the optimum mass distribution for the link masses. The change in direction and amplitude of the joint forces is calculated using the Lagrange's equations of motion and presented as the objective function whereas the inertial parameters of the moving links, i.e., the mass, the location of mass center and the moment of inertia are taken as the design variables. Erkaya and Uzmay (2008, 2009) presented an optimization method to reduce the effect of joint clearance on the shaking force and shaking moment in the planar mechanism. The weighted sum of differences of force and moment values with and without the clearance is defined as the objective function to be minimized. The link lengths and their center of mass locations are defined as the design variables with proper lower and upper limits to solve this optimization problem.

2.3.6 Non-linear constraint optimization using natural orthogonal complement method

An optimization method was developed to balance a five-bar mechanism using natural orthogonal complement dynamic modeling (Ilia and Sinatra, 2007, 2009). The shaking force is minimized through conventional optimization method, i.e., non-linear constraint optimization. The center of mass parameters of moving links were chosen as the design variables while the natural orthogonal complement method was used for dynamic analysis of the mechanism.

2.3.7 Mixed mass redistribution method

The mixed mass redistribution method combining the principles of the mass redistribution and addition of counterweights is applied for reducing the shaking force and shaking moment in the mechanisms (Guo et al., 2000; Feng et al., 2000). The

mass, moment of inertia and location of mass center of the moving links along with the mass and mass center location of the counterweights were taken as the design variables.

2.3.8 Balancing through integrating kinematic and dynamic characteristics

Yan and Soong (2001 and 2004) presented an optimization method integrating kinematic synthesis, dynamic balancing design, and the design of the input link's motion trajectory. The trajectory of the crank displacement is represented by a Bezier curve while the kinematic and dynamic properties of the mechanism are included in the objective function using appropriate weighting factors. Thus, the kinematic design requirements are satisfied along with the reduction in the shaking force and shaking moment for the mechanism. This method was further extended using the bi-material moving links (Soong and Hsu, 2007). The moving links of the mechanism are designed by joining two different materials with optimum link length proportions as shown in Fig. 2.11.

2.3.9 Sensitivity analysis

Sensitivity analysis is the study of the uncertainty in the output of a mathematical model to different sources of uncertainty in its inputs. Li (1998) presented a method to analyse the sensitivity of the shaking force and shaking moment to the design variables for a planar mechanism. The objective function includes shaking force, shaking moment and the sensitivity terms such as the ratio of shaking moment to mass center distance of links; is minimized by optimizing the inertial parameters of the links treated as the design variables. Alici and Shirinzadeh (2006) formulated an optimization problem to dynamically balance the planar parallel manipulators. In this method, the objective function is defined as the sum-squared values of shaking moment, driving torques, bearing forces and the angular momentum deviation. The

constraints are imposed on the geometric as well as the inertial properties along with the full force balancing condition for the mechanism.

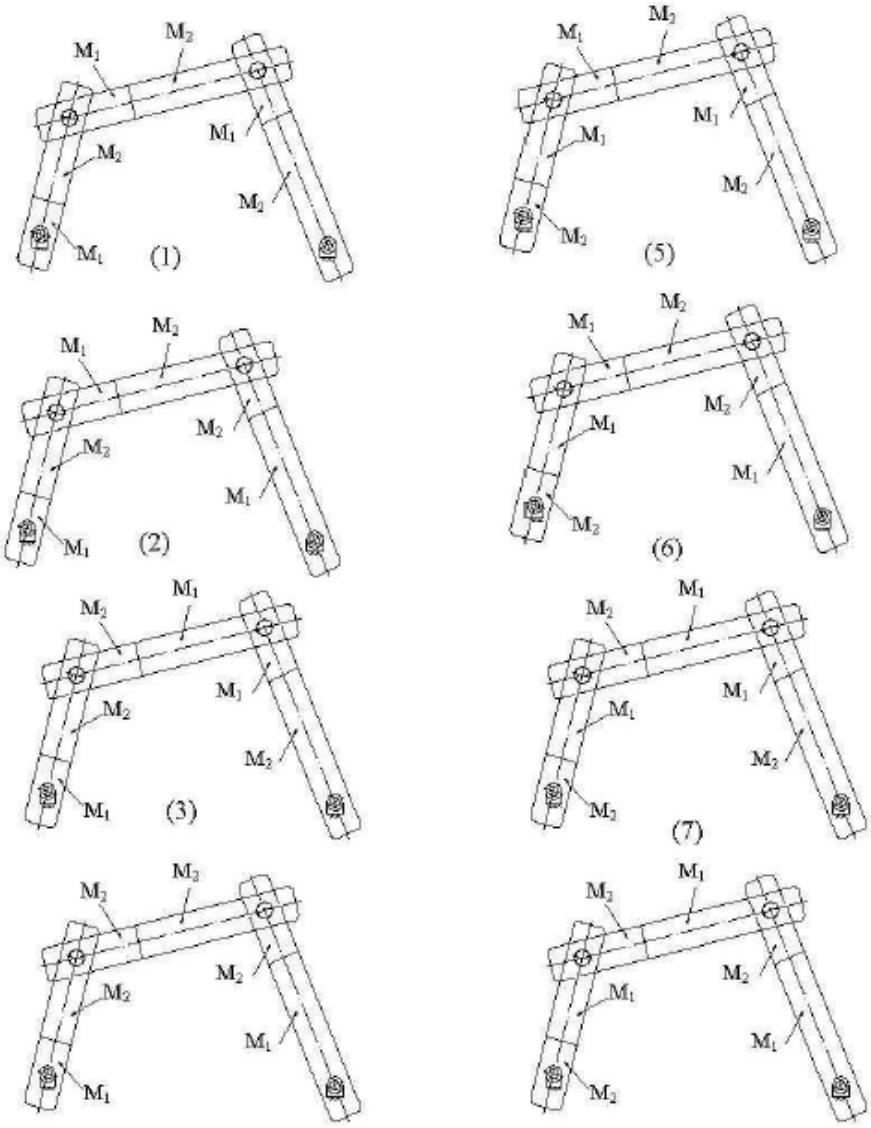

M_1 and M_2 represent two different materials

Fig. 2.11 *Balancing of four-bar mechanism by designing bi-material moving links (Soong and Hsu, 2007)*

In another method, Erkaya (2013) formulated the objective function by adding the sub-components of shaking force and moment and analysed the sensitivity of the optimum result to weighting factors used in the objective function. The kinematic and

dynamic parameters such as link length, structural angle, mass, inertia and center of mass location are defined as the design variables.

In addition to the methods discussed above the forces and moments transmitting to the engine mounts due to reciprocating parts and gas pressure in a four-stroke seven-cylinder marine engine are reduced by optimizing the crank angles (Park et al., 2007). The steepest decent method with golden section search was used for the optimization.

2.4 Methods for Link Shape Synthesis

After obtaining optimum inertial properties for the balanced mechanism, links shapes are to be decided to carry various loads acting on them. Several methods are suggested in the literature to find the mechanism link shapes for specified inertial properties that require an initial design domain to start with. The methods for link shape synthesis available in the literature may be categorised as:

2.4.1 Small element superposing method

Feng et al. (2002) developed a Small Element Superposing Method (SESM) to find link shapes which discretize the initial assumed shape into small mass elements and locate them systematically along the link length (Fig. 2.12). The design equations corresponding to the optimized mass, center of mass location and inertia are satisfied to form the link by superposing these small mass elements.

2.4.2 Voxel-based discretization

In the convex optimization method developed by Demeulenaere (2004a, b, 2006, 2010) designing point-mass counterweights and minimum-inertia counterweights was reformulated as a convex nonlinear optimization problem. This method was used to optimally design the counterweights used for the balancing purpose.

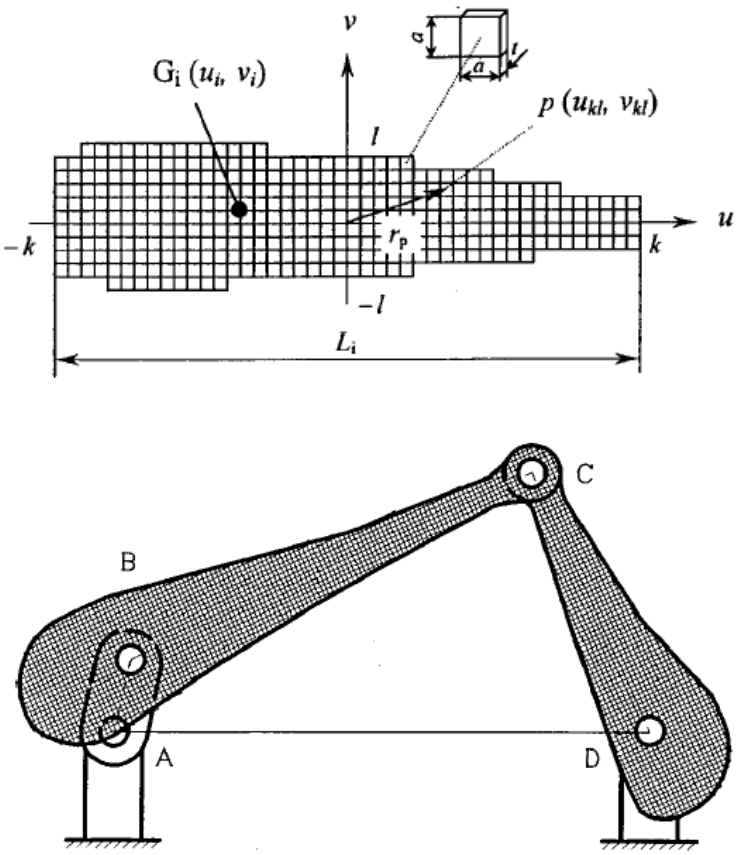

Fig. 2.12 *Small element superposing method for finding link shape (Feng et al., 2002)*

For planar mechanisms, a particular counterweight shape is enforced through the additional constraints. The counterweight shapes considered were point-mass, minimum-inertia counterweights and sector-type counterweights. Based on this approach Verschuure (2008a, b, 2009) used a voxel-based discretization to describe the final counterweight shape, inspired by the typical discretizations used in the area of topology optimization.

2.4.3 Evolutionary structural optimization method

The Evolutionary Structural Optimization (ESO) method is used to optimize the rotating machinery shaft's shape by gradually removing ineffective material from the design domain (Xie and Steven, 1993, 1996; Kim et. al., 2002). This method executes the Finite Element Analysis (FEA) with finite size elements in each iteration to find the optimum shape.

2.4.4 Gradient-based method

In this method, the link shapes are synthesized by maximizing external work done by a given external force considering total volume of all links as the constraint function (Azegami et al., 2013). The external work done for the mechanism defined as the objective function satisfies the requirement of the kinetic energy of the mechanism for an assigned time interval. The initial design domain for the link is considered as the design variable and is optimized to get optimum link shape (Fig. 2.13).

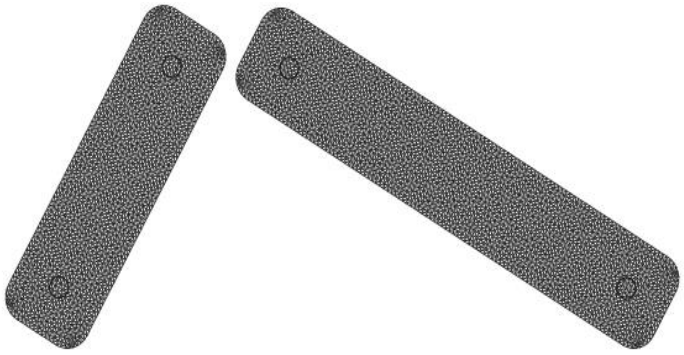

(a) Initial shapes

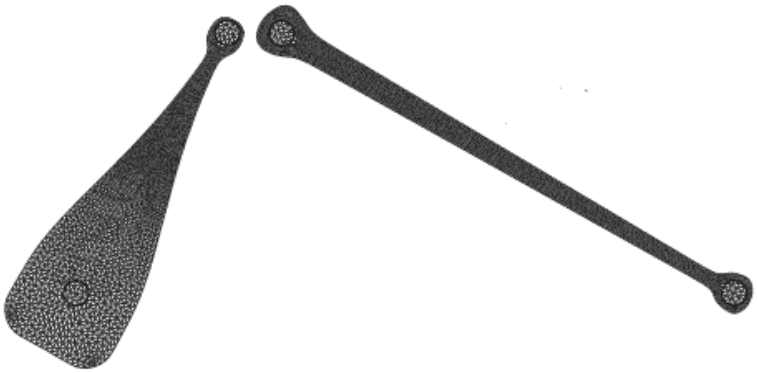

(b) Optimum shapes

Fig. 2.13 *Optimum shape for piston-crank mechanism using gradient-based method (Azegami et al., 2013)*

2.4.5 Topology optimization method

The link shapes are also found through the topology optimization based on parametric curves (Xu and Ananthasuresh, 2003) and non-intersecting closed polygons

(Yoganand and Sen, 2011). In this approach, the vertices of the control polygon that define parametric curves for links are used to identify the design space. Based on FEA, this formulation considers the constraints to avoid self-intersections and intersections with other segments. It also ensures the optimum utilization of the available space and material. The required inertial properties of the design domain are achieved through optimizing the vertices of the control polygon as shown in Fig. 2.14.

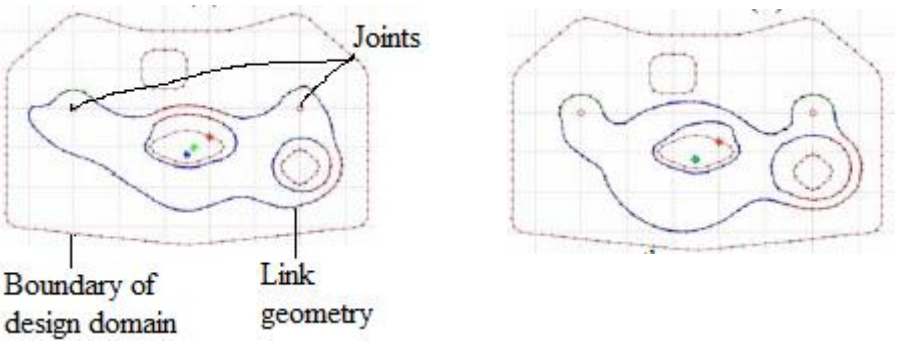

Fig. 2.14 *Geometry synthesis through topology optimization (Yoganand and Sen, 2011)*

2.4.6 Shapes for specific path and motion

The link shapes for the interference-free motion are found by identifying feasible material domain associated with the link geometries (Sen et al., 2004). Similarly, the mechanism's dimensional synthesis to generate specified path or motion based on graphical and analytical techniques can also be used for shape optimization (Sandor and Erdman, 1984; Freudenstein, 2010).

2.5 Optimization Techniques

The limitation of these methods for finding link shapes is that they require a pre-defined design domain to start with and do not consider the dynamic balance for the mechanisms during formulation. Thus, the optimization methods available in the literature are used separately (1) for the dynamic balancing of the planar mechanisms and (2) for synthesizing their link shapes. It is found that the formulation of dynamic balancing problem as an optimization problem is the crucial step in mechanism

design. It is also found that an equimomental system of point-masses can be effectively used for the problem formulation. Its use can be further explored for multiloop mechanisms having both fundamental joints, i.e., revolute joint and prismatic joint. In this dissertation, the use of the equimomental system of point-masses is explored in terms of problem-solving strategies. Modern optimization algorithms are applied to solve the problems. These algorithms are explored from the view of computation aspect and convergence basis.

2.6 Summary

Techniques of shaking force balancing and its effect on other dynamic quantities are reviewed in Section 2.1. It was found that only shaking force balancing is not useful as it increases shaking moment and driving torque in the mechanism. Review on the literature regarding the complete balancing of the shaking force and the shaking moment in Section 2.2 states that there will be no clear-cut method for static and dynamic balancing. Several works of literature are very specific and applicable to the specific mechanism. A generalised methodology is not available which can be applied to all types of mechanisms, particularly multiloop mechanisms. Therefore, optimal balancing methods are explored. The literature based on the methods developed for optimal balancing of force and moment is reviewed in Section 2.3 including the various optimization methods for simultaneous minimization of the shaking force and the shaking moment. However, the methods used for balancing the flexible mechanisms are excluded in these sections.

In Section 2.4, the methods used for the link shape synthesis are reviewed and it is concluded that these methods require an initial design domain to start the procedure and don’t relate the final link shapes with the dynamic balance of the

mechanisms. The limitations of all these methods are also discussed which justifies the research gap.

Chapter 3

Optimization Techniques

This chapter discusses the popular evolutionary optimization technique, Genetic Algorithm (GA) and Teaching-learning-based Optimization (TLBO) algorithm. It also covers the definitions of various parameters used by these algorithms.

Most of the engineering design problems are competing multi-objective problems for which the optimal values of the design variables are searched that optimize several objectives for a given set of constraints. The different methods available to formulate a multi-objective problem as a single objective problem are weighted global criterion method, weighted sum method, lexicographic method, weighted min-max method, exponential weighted criterion, weighted product method, goal programming methods, bounded objective function method, and physical programming (Marler and Arora, 2004). The weighted sum approach is more widely used in which a normalized objective function is formulated by assigning proper weighting factors to all the objectives. By selecting different values of the weighting factors to objectives, the results are obtained as a set of optimum solutions and each solution in this set is a trade-off between the different objectives (Marler and Arora, 2010).

A constrained optimization problem is considered more complex than that of an unconstrained problem. It finds a feasible solution that optimizes one or more mathematical functions in a constrained search space. The constrained optimization problem is transformed into an unconstrained optimization problem by modifying the objective function on the basis of the constraint violations. The constraint violations are used to penalize infeasible solutions to favor the feasible solutions. The constraints are normally treated as penalty functions such as static, dynamic or

adaptive penalty to the objective function. The various constraint handling techniques are suggested such as superiority of feasible solutions (SF) (Deb, 2000), stochastic ranking technique (SR) (Runarsson and Yao, 2005), ε-constraint technique (EC) (Takahama and Sakai, 2006), self-adaptive penalty approach (SP) (Tessema and Yen, 2006) and ensemble of constraint handling techniques (Montes and Coello, 2005; Mallipeddi and Suganthan, 2010).

After formulating the optimization problem, it can be solved by using either traditional or evolutionary optimization algorithms. The traditional or classical optimization algorithms are based on deterministic approach, i.e., they use gradient information of objective function with respect to the design variables and move from one solution to other following the specific rules. Depending on the starting solution these algorithms may end up with a local optimum solution. Therefore, one has to explore all local solutions; one of them is the global optimum solution. To improve the chances of getting the global optimum solution, a large set of randomly generated initial solutions is required for these algorithms. The global optimum solution is then found as the best of all local optimum solution provided by different instances of the algorithm. The popular methods in this category are quadratic programming, steepest descent method, linear programming, nonlinear programming, dynamic programming and geometric programming, etc. For the complex optimization problem having a large number of design variables and multiple local minimum solutions, these methods converge on the optimum solution near to the initial solution provided and thus produce local optimum solution (Marler and Arora, 2004; Mariappan and Krishnamurty, 1996). These techniques are generally not suitable for the optimization problems with (1) large number of constraints (2) large number of design variables (3) multi-objective function (4) multi-modality and (5) differentiability. A function is

multimodal if it has two or more local optimum solutions in the design space. A function is regular if it is differentiable at each point of its domain. The traditional optimization methods require the gradient information and thus not useful in case of the non-differentiable functions.

Evolutionary or advanced optimization techniques are stochastic in nature, and the optimum solution is searched following the probabilistic transition rules. These algorithms mimic the natural evolutionary principles and start with a set of solutions known as the population to search the optimum solution through parallel computing. Thus, it is advantageous to use these techniques to find the global optimum solution with less computational efforts for large and difficult optimization problems. The popular techniques in this category are: Genetic algorithm (GA), Simulated Annealing (SA), Particle Swarm Optimization (PSO), Biogeography-based optimization (BBO), Ant Colony Optimization (ACO), Differential Evolution (DE), Grey Wolf Optimizer (GWO), Fireworks Algorithm (FA), Directed Bee Colony Optimization (DBC), Harmony Elements Algorithm (HEA), Artificial Bee Colony (ABC), Artificial Immune Algorithm (AIA), Shuffled Frog Leaping Algorithm (SFLA), Grenade Explosion Algorithm (GEA) etc. These techniques provide a near-global optimum solution for an optimization problem complex in nature having a large number of variables and constraints. The performance of these algorithms is dependent on the values of algorithm controlling parameters and chosen strategy for the initialization of population. Hence, these algorithms are sensitive to parameter tuning. The choice of the common parameters like population size and number of iterations is based upon the experience as there is no specific rule to select their values. The total function evaluations for an optimization algorithm is defined as the product of population size

and number of iterations, and different combination of these parameters are tried to improve the performance of the algorithm.

3.1 Definitions of Different Terms Used In Optimization Techniques

The following terms define the working of an optimization technique.

Problem dimension: Defined by number of design variables for the optimization problem.

Search space: An area searched to find the optimum solution. It is defined by range or bounding limits of the design variables.

Exploration: Exploring the entire search space to find the best solution.

Exploitation: Intensive search in a specific region to get solution near to the global optimum solution.

Feasible solution: The solutions in entire search space that satisfy all the constraints and for which all the design variables are within the defined bounding limits.

Efficiency: Percentage of times an algorithm finds result close to best result for different runs.

Convergence: Process of moving from initial solution to the optimum solution through successive iterations until the termination criterion is satisfied.

Accuracy: Defines the quality of the best solution. For different runs, solutions should be close to each other.

Diversity: It reduces the chances of the local trapping. With increased diversity, an algorithm provides a variety of solutions.

Local trapping: When the solution obtained is local optimum for a specific region, and global optimum is not known.

Search space reduction: Prominent values of the design variables are chosen for which optimum value can be obtained. It improves the accuracy and reduces CPU time.

Computation burden: Time taken to solve an optimization problem. It depends on population size along with number of iterations, design variables, and constraints.

Solution quality: It depends upon best, worst and mean values of the objective function. Quality is also checked by standard deviation and coefficient of variation.

Coefficient of variance: Ratio of standard deviation and mean value of objective function.

Termination criterion: An algorithm can be stopped after a specific time or number of iterations known as the termination criterion.

The balancing of exploration and exploitation is important for an optimization technique. Through efficient reduction of the search space without missing global optimum solution, the accuracy is improved, and algorithm requires less computational time to solve the optimization problem. For the benchmark problems, two common criteria considered for comparison of different optimization algorithms are success rate and mean function evaluations required. The success rate shows the consistency of the algorithm for finding an optimum solution in different runs while number of function evaluations indicates the computational efficiency. The results are found for different runs for which the mean solution shows the average ability of the algorithm to find the global optimum solution and standard deviation describes the variations in the solution from the mean solution. The best and worst solutions are also used to compare the performance of the different optimization algorithms.

3.2 Genetic Algorithm

Genetic algorithm (GA) works on the principle of the Darwinian theory of the survival of the fittest and evolution of the living beings (Holland, 1992). It's a nature inspired population-based optimization algorithm and guides the search through the solution space by using the natural selection and genetic operators such as crossover, mutation and the selection (Deb, 2010; Gao et al., 2000). The population means a group or a set of solutions. The design variables are encoded into the solution strings of a finite length, and the search starts with a population of the encoded solutions created at random instead of the single point in the solution space. Based on the solutions in the current population, it uses the genetic operators to replace the old population with the new population of solutions till the termination criteria are satisfied. Thus, this algorithm evaluates only the objective function, and genetic operators - selection, crossover, and mutation are used for exploring the search space. One can specify the bounds and constraints for the variables in this algorithm. The optimization process takes place in the following manner:

Initialization of population of solutions

In basic GA, the randomly generated design variables are coded in binary strings having 1's and 0's representing their values whereas some variants of GA directly use them. The string length is decided on the basis of the desired solution accuracy.

Fitness function

GA is suitable for the maximization problem as it works on the principle of the survival of the fittest. The fitness function is same as that of the objective function in the case of the maximization problem. Moreover, a minimization problem is solved by transforming it into the maximization problem where the fitness function as:

$$\text{fitness function} = 1/(1 + \text{objective function})$$

Selection or reproduction

The survival of the fittest principle is implemented in this step. It selects the good solutions or strings out of the current population for generating the next population according to the assigned fitness. The good solutions are chosen from the current population, and their multiple copies are included in the new population in a probabilistic manner. The different selection schemes available are roulette-wheel selection, tournament selection and stochastic selection, etc. The commonly used selection scheme is the roulette-wheel selection that selects a solution with a probability corresponding to its fitness value. The solution having better fitness value will have more number of copies in the new population. Thus, this stage increases the number of more fit solutions satisfying the condition of survival of the fittest. This operator doesn't generate new strings as done by the other two operators, crossover and mutation. After selection, crossover and mutation operators recombine and alter parts of solutions to generate the new population of solutions.

Crossover or recombination

Crossover is also known as the recombination operator that exchanges parts of the solutions from two or more randomly selected solutions called parents and combines these parts to generate new solutions, called children, with a defined crossover probability. More solutions may get a chance to go for the crossover procedure with a high crossover probability. There are different ways to implement a recombination operator. The simplest crossover operator is single point crossover in which the crossover site is selected randomly from where the exchange of bits takes place.

Parents						**Children**				
	1	0	0	1	0		1	0	0	0	1
Crossover site →											
	1	1	0	0	1		1	1	0	1	0

This results in better or worse solutions which will be copied more or less, respectively, in next reproduction. From the entire population, this operator works on a percentage of strings same as that of the crossover probability.

Mutation

After crossover, the solutions are altered to generate the new solutions in this step. Crossover works with two solutions while Mutation operates on an individual solution in the population. The popular mutation operator is the bitwise mutation in which a random site is selected from the string of the solutions and changed from 1 to 0 or vice versa to generate a new solution according to the mutation probability.

1	0	0	1	0

$\downarrow$

1	0	1	1	0

The mutation probability is kept low so that the algorithm doesn't get unstable. This operator is required to create a solution in the neighborhood of the current solution to achieve a local search around it. It is also important to maintain the diversity in the search procedure and to improve the variety in the new population.

One cycle of these operations completes an iteration in GA. In the next iteration, the good strings are copied whereas the bad strings are eliminated, and the best obtained solutions are saved using elitism. The crossover and mutation operators do not modify the elite solutions but can replace them if better solutions are obtained in any iteration. The flow chart for the genetic algorithm is shown in Fig. 3.1.

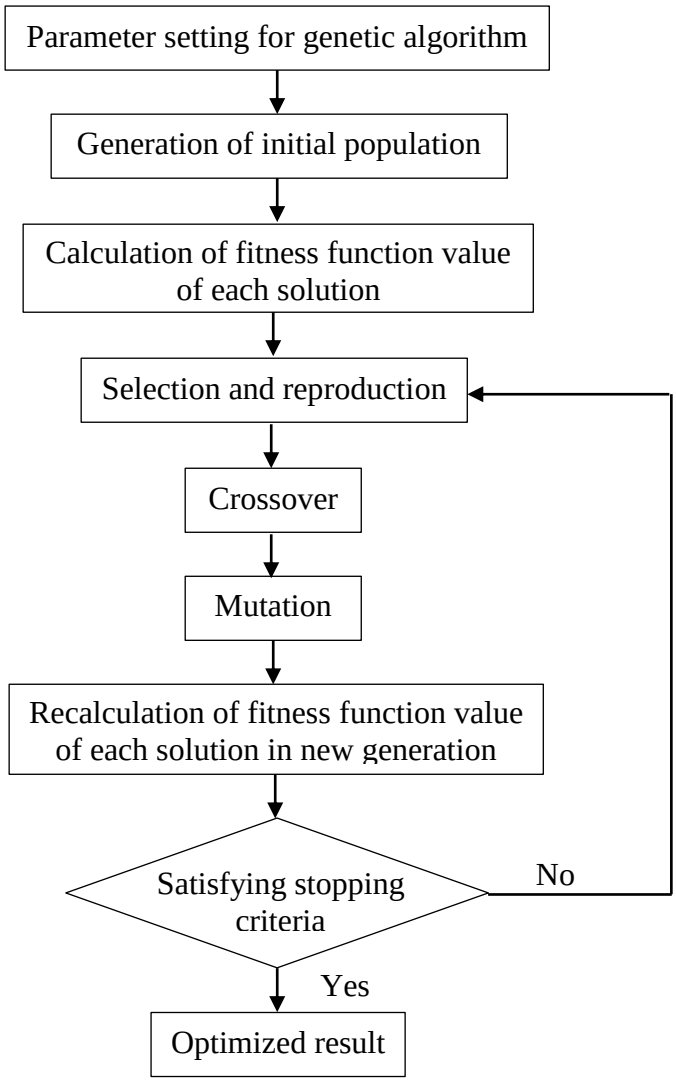

Fig. 3.1 *Flow chart of the genetic algorithm*

The working of GA is now demonstrated by the following example:

$$\text{Maximize } Z = x^2 - y^2 + 2xy - x^2 y + xy^2$$

$$\text{for } 0 \le x \le 5, 0 \le y \le 5$$

1. The initial population of solutions, i.e., sets of design variables within the bounding limits is generated at random. In Table 3.1, column 2 contains the randomly generated solutions and binary coded strings representing them are given in column 3.

Table 3.1 *Initial population for genetic algorithm example*

Solution	(x, y)	String
1	(2,4)	0 1 0 1 0 0
2	(5,1)	1 0 1 0 0 1
3	(2,0)	0 1 0 0 0 0
4	(3,1)	0 1 1 0 0 1
5	(4,2)	1 0 0 0 1 0
6	(2,3)	0 1 0 0 1 1

2. Next, the objective function values, Z, corresponding to these solutions are calculated, given in Table 3.2.

3. The probability of selection of good solutions is now calculated as:

$$\frac{Z_i}{\sum_{i=1}^{6} Z_i}$$

The probability and cumulative probability for each solution are given in columns 5 and 6 of in Table 3.2, respectively.

Table 3.2 *Selection of solutions to generate new generation*

Solution	(x,y)	String generated	f(x,y)	Probability	Cumulative probability	Random number	String copied
1	(2,4)	0 1 0 1 0 0	20	0.2817	0.2817	0.7734	1 0 0 0 1 0
2	(5,1)	1 0 1 0 0 1	14	0.1972	0.4789	0.1536	0 1 0 1 0 0
3	(2,0)	0 1 0 0 0 0	4	0.0563	0.5352	0.4123	1 0 1 0 0 1
4	(3,1)	0 1 1 0 0 1	8	0.1127	0.6479	0.9734	0 1 0 0 1 1
5	(4,2)	1 0 0 0 1 0	12	0.1690	0.8169	0.7657	1 0 0 0 1 0
6	(2,3)	0 1 0 0 1 1	13	0.1831	1.0000	0.9342	0 1 0 0 1 1

Using roulette-wheel selection scheme that assigns a probability proportional to the fitness or objective function value, the good solutions are selected. The random numbers corresponding to the probability are shown in seventh column of Table 3.2.

The solutions are copied according to the cumulative probability range in which these random numbers fall. This represents a new population with multiple copies of the good solutions as given in column 7 of the Table 3.2.

4. Now, single point crossover operator is used to generate new solutions. Crossover site from where the exchange of bits takes place is selected randomly as shown below. For a random number generated, the corresponding bit is selected for crossover. In this example, the random number generated was 0.6529. As it falls in the range of 0.52-0.68, the fourth bit is selected for crossover between parents to generate children.

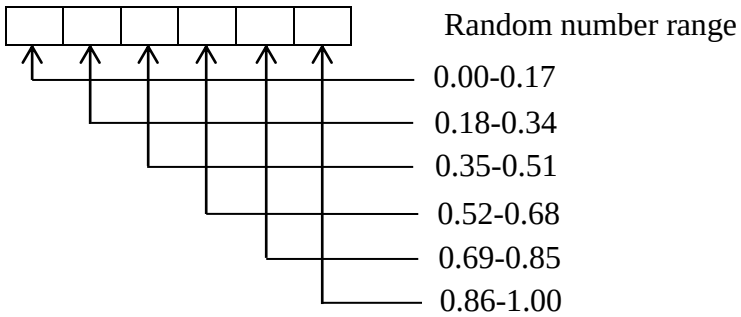

Fig. 3.2 *Crossover site selection*

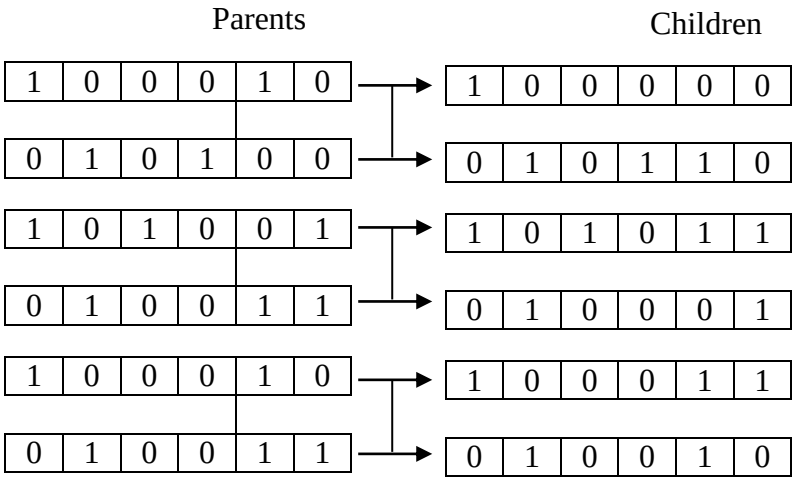

Fig. 3.3 *Parent's crossover to produce children*

The selected crossover site may be same or different for different pairs of parents.

5. Next, the bitwise mutation takes place for this new set of solutions to further explore the search space. A particular bit of the strings is selected for which value is

changed from 1 to 0 or vice versa. For the problem considered, it is decided that mutation takes place for the third bit of the string. A criterion is also set that mutation operator will be used for a particular string only if the random number generated is greater than 0.8. Using this criterion for the problem considered, a random number is generated for each string representing solutions. The random number generated for fourth and six strings was above 0.8, and hence mutation operator was used for them.

1	0	0	0	0	0
0	1	0	1	1	0
1	0	1	0	1	1
0	1	**0**	0	0	1
1	0	0	0	1	1
0	1	**0**	0	1	0

1	0	0	0	0	0
0	1	0	1	1	0
1	0	1	0	1	1
0	1	**1**	0	0	1
1	0	0	0	1	1
0	1	**1**	0	1	0

Fig. 3.4 *Bitwise mutation*

The final set of solutions after mutation is in Table 3.3:

Table 3.3 *Final population at the end of one iteration of genetic algorithm*

String generated	(x,y)	f(x,y)
1 0 0 0 0 0	(4,0)	16
0 1 0 1 0 0	(2,4)	20
1 0 1 0 1 1	(5,3)	16
0 1 1 0 0 1	(3,1)	8
1 0 0 0 1 1	(4,3)	19
0 1 1 0 1 0	(3,2)	11

Though the maximum value of the objective function for these solutions, i.e., 20 is same as those of the initially generated population of solutions but the average value is increased to 15 from 11.84. This completes an iteration of GA that improves the

maximum and average value of the objective function by using genetic operators. This final set of solutions is used as the initial population for the next iteration. Thus, the parameters required to start GA are: population size indicating number of solutions, number of iterations necessary for the termination criterion, crossover probability, mutation probability, number of design variables, range of design variables and string length for binary version. The limitations of GA are that (1) it requires a large amount of computational work and (2) there is no absolute guarantee that a global solution is obtained. These drawbacks may be overcome by using parallel computers and by executing the algorithm several times or allowing it to run longer (Arora, 1989). *These drawbacks motivate us to explore other optimization techniques which are suitable for the mechanism design*.

3.3 Teaching-learning-based Optimization Algorithm

The teaching-learning-based optimization (TLBO) algorithm is also a population-based optimization method that converges to the optimum solution by using a population of the solutions. TLBO is known as a parameter-less optimization algorithm as no algorithm-specific parameters are required to be handled to implement it (Rao and Savsani, 2012). Whereas, in GA, the parameters like crossover rate and mutation rate are to be optimally controlled to solve the optimization problem. Thus, the main limitation of the available evolutionary optimization algorithms including GA is the optimum setting or tuning of the algorithm-specific parameters for the proper working of the algorithms. The improper selection of these control parameters may results in local optimum solution along with the requirement of more computational efforts. The difficulty further increases with the modification and hybridization of the algorithms. The hybridization of the algorithms means combining the properties of the different optimization algorithms to improve the

effectiveness of the algorithm. The modification in a particular optimization method suits well to a specific problem and may not work for the other applications. Furthermore, for any modification in an optimization algorithm, it is required to check that algorithm for a wide variety of the problems before drawing any general conclusions for the modifications incorporated. The control parameters required by the popular evolutionary and swarm intelligence based optimization algorithms other than population size and numbers of iterations are listed in Table 3.4 (Rao and Savsani, 2012).

Table 3.4 *Controlling parameters for different evolutionary optimization algorithms*

Algorithm	Control parameters
Genetic Algorithm (GA)	Mutation and crossover rates
Particle Swarm Optimization (PSO)	Inertia weight, social and cognitive parameters
Artificial Bee Colony (ABC)	Number of bees and limit
Harmony Search (HS)	Number of improvisation, pitch adjusting rate and harmony memory consideration rate
Ant Colony Optimization (ACO)	Exponent parameters, pheromone evaporation rate, reward factor

In TLBO, a group of learners is considered as the population and different subjects offered to the learners is considered as design variables. The learners' result is analogous to the objective function value of the optimization problem. TLBO works in two successive phases in each iteration explained as follows.

Teacher phase – learning from the teacher

In this phase, the learners learn from the teacher. The teacher should be the most experienced and knowledgeable person for a subject. Thus, the learner with the best result is identified as the teacher. The teacher increases the mean result of the population and outcome depends on the quality of teacher as well as learners. In this phase, subject marks of all learners are updated on the basis of subject marks of the learner with the best solution, i.e., teacher.

Each learner's results corresponding to initial and updated marks are compared, and the subject marks corresponding to the better result are kept for the learner who becomes part of the new population. The Teacher phase ends with the creation of new population. This population of the Teacher phase is treated as the initial population in the second phase, i.e., Learner phase of the algorithm.

Learner phase – learning through interaction

In this phase, the learners gain knowledge through discussion and interaction among themselves. The Learner phase starts with the final population obtained in the Teacher phase. To improve the marks, each learner interacts randomly with at least one other learner in the population. The learner improves his/her subject marks if another learner has more marks in corresponding subjects.

Similar to Teacher phase, each learner's result corresponding to initial and updated marks in this phase is compared, and the subject marks corresponding to the better result are retained for the final population. It ends the Learner phase of the algorithm.

The flow chart for the TLBO algorithm is shown in Fig. 3.5. The various parameters of TLBO algorithm are defined as:

p = Population size, i.e., number of learners

s = Design variables, i.e., subjects offered to learners

LL_k, UL_k = Lower and upper limits for kth subject marks

n = Number of iterations

i = ith Iteration, i.e., a teaching-learning cycle

Z_j = Objective function value of jth learner

M_k = Mean of marks kth subject for the population

B_k = Marks of kth subject of best learner whose objective

function value, Z_j, is minimum

R= random number

Algorithm begin

% Initialization of marks for each subject for the whole population

for j=1,…,p

for k=1,…,s

% Marks of kth subject of jth learner, m_{jk}^{0}

$$m_{jk}^{0} = LL_k + \left(\left(UL_k - LL_k\right) \times R\right) \tag{3.1}$$

end

end

% Mean marks of kth subject for the population

$$M_k = \frac{\sum_{j=1}^{p} m_{jk}^{0}}{p} \tag{3.2}$$

% Updating the subject marks of all learners

for i=1,…,n

$$m_{jk,i}^{1} = m_{jk}^{0} + \left(\left(B_k - M_k\right) \times R\right) \tag{3.3}$$

% Compute and compare the updated value of Z_j^1 with previous one, Z_j^0

If $Z_j^0 < Z_j^1$

% Updating marks

$m_{jk,i}^{2} = m_{jk}^{0}$

else

$m_{jk,i}^{2} = m_{jk}^{1}$

% End of Teacher phase

% Start of Learner phase

% Result comparison of two learners *j* and *l* in population, $m^{2}_{jk,i}$

for *j*=1,…,*l*,…,*p* and if $l \neq j$

If $Z^{2}_{j} < Z^{2}_{l}$

for *k*=1,…,*s*

$$m^{3}_{jk,i} = m^{2}_{jk} + \left(\left(m^{2}_{jk} - m^{2}_{lk}\right) \times R\right) \tag{3.4}$$

else

$$m^{3}_{jk,i} = m^{2}_{jk} + \left(\left(m^{2}_{lk} - m^{2}_{jk}\right) \times R\right) \tag{3.5}$$

end

end

% Comparison of updated value of Z^{3}_{j} with the previous one, Z^{2}_{j}

If $Z^{2}_{j} < Z^{3}_{j}$

% Updating marks

$m^{4}_{jk,i} = m^{2}_{jk}$

else

$m^{4}_{jk,i} = m^{3}_{jk}$

% Conditions to check limits of subject marks

$$m^{4}_{jk,i} = \max\left(m^{4}_{jk,i}, LL_{k}\right) \tag{3.6}$$

$$m^{4}_{jk,i} = \min\left(m^{4}_{jk,i}, UL_{k}\right) \tag{3.7}$$

end

% End of *i*th iteration

Algorithm end

The parameter R represents a random number within a range of 0 and 1 which may have a different value for different equations. The population obtained at the end of Learner phase is treated as the final population of the current iteration, and this is used as the initial population for Teacher phase in the next iteration. From the final population of the last iteration, the best solution is obtained as the optimum solution. To handle the constraints, the heuristic constrained handling method (Deb, 2000) is used in which the tournament selection operator selects and compares two solutions by following specific heuristic rules. These rules are implemented at the end of the Teacher phase and the Learner phase.

The example solved in the previous section is used now to demonstrate the working of TLBO algorithm.

$$\text{Minimize } Z = x^2 - y^2 + 2xy - x^2y + xy^2$$

$$\text{for } 0 \le x \le 5, 0 \le y \le 5$$

Let the population size is the same as used in genetic algorithm.

1. At first in Teacher phase, the marks for each subject for initial population of six learners, i.e., sets of design variables within the bounding limits are generated at random using Eq. (3.1). In Table 3.5, columns 2 and 3 contain the randomly generated marks of two subjects, x and y. Column 4 presents the value of objective function, i.e., the result of learners.

2. The mean of marks in each subject for all learners is calculated using Eq. (3.2) and shown in the last row of the Table 3.5.

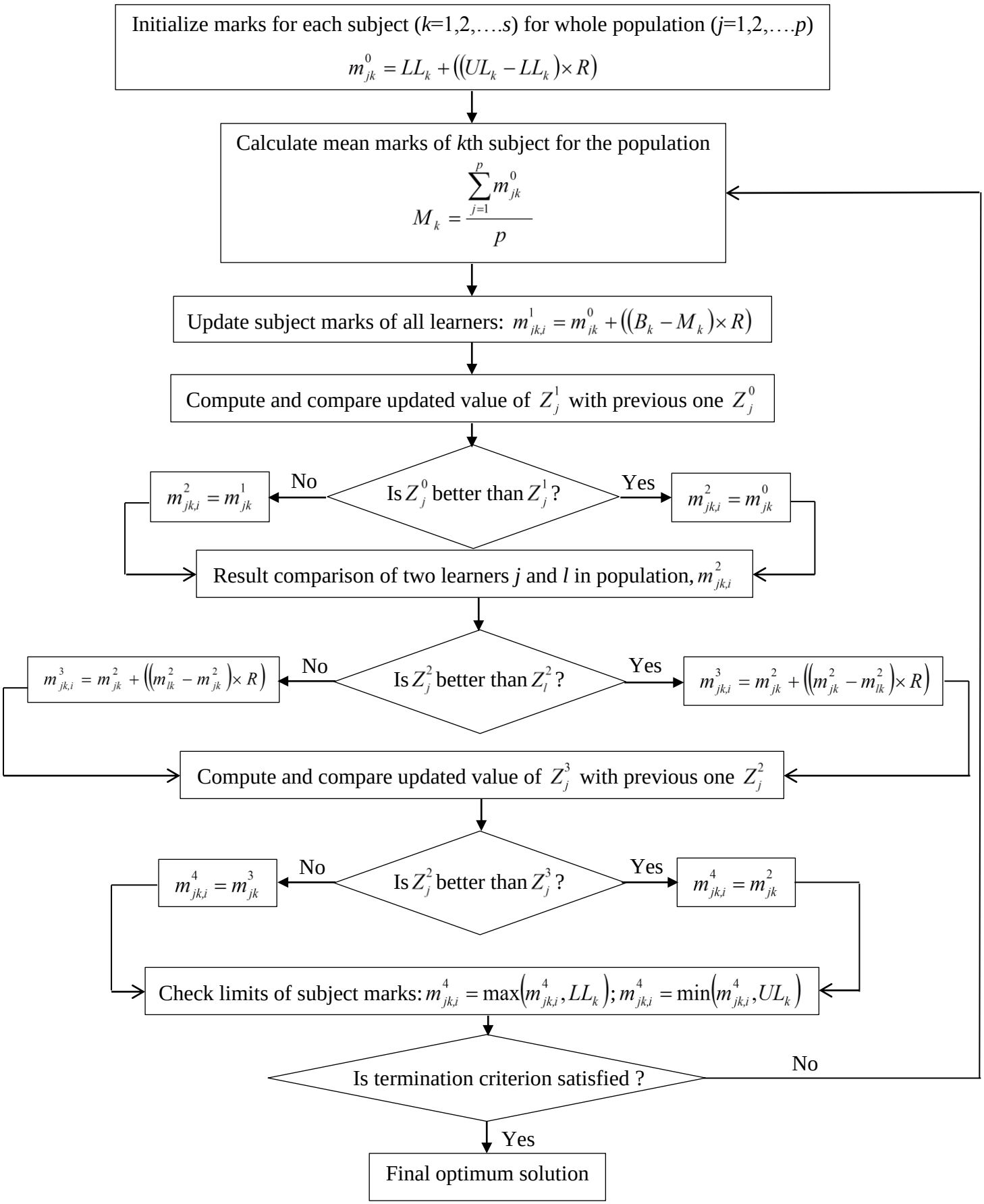

Fig. 3.5 Flow chart of the TLBO algorithm

Table 3.5 Initial population generation for TLBO example

Learner	Subjects		Result Z
	x	y	
1	2	4	20
2	5	1	14
3	2	0	4
4	3	1	8
5	4	2	12
6	2	3	13
Mean $\longrightarrow$	3	1.83	

3. The learner with the best result, i.e., minimum value of Z is treated as the teacher. Hence, learner 3 becomes teacher and the subject marks of all learners are now updated on the basis of teacher's marks using Eq. (3.3). The updated values of subject marks and result of all learners are shown in the Table 3.6.

Table 3.6 *Modified population in Teacher phase*

Learner	Subjects		
	x	y	Result Z
1	1.1853	2.9992	5.9680
2	4.8730	0.7116	15.7448
3	1.0866	-0.2597	0.9288
4	2.3676	0.6867	5.6528
5	3.9025	0.7079	11.4282
6	1.7215	2.9417	10.6175

4. Now, the updated result of each learner is compared with his/her previous result, and the better value is kept along with the respective subject marks as the new set of

solutions, given in Table 3.7. This completes the Teacher phase of the TLBO algorithm.

5. In Learner phase, each learner's result is compared with at least one another learner randomly chosen in the population and subject marks are updated accordingly using Eq. (3.4) or Eq. (3.5).

6. Next, the updated result of each learner is compared with his/her previous result, and the better value is kept along with the respective subject marks as the new set of solutions. This completes the Learner phase of the TLBO algorithm (Table 3.8).

Table 3.7 *Modified population at the end of Teacher phase*

Learner	Subjects		
	x	y	Result Z
1	1.1853	2.9992	5.9680
2	5	1	14
3	1.0866	-0.2597	0.9288
4	2.3676	0.6867	5.6528
5	3.9025	0.7079	11.4282
6	1.7215	2.9417	10.6175

7. Finally, the subject marks obtained are checked to confirm within the bounding limits (Table 3.9).

The minimum value of the objective function for these solutions is 0.3140 which is clearly better than the minimum value of the objective function for initially generated solutions, i.e., 4. Also, the average value is reduced from 11.84 to 5.30.

Table 3.8 *Modified population in Learner phase*

Learner	Subjects		Pair	Result Z
	x_1	x_2		
1	1.1580	2.6827	1, 3	5.0938
2	2.3003	2.4864	2, 6	11.6125
3	0.5604	-0.5268	3, 5	-0.2329
4	0.5784	0.4815	4, 2	0.6327
5	3.4607	0.9806	5, 1	9.3856
6	2.0435	0.7775	6, 4	4.7376

Table 3.9 *Modified population at the end of Learner phase*

Learner	Subjects		Pair	Result Z
	x_1	x_2		
1	1.1580	2.6827	1, 3	5.0938
2	2.3003	2.4864	2, 6	11.6125
3	0.5604	0	3, 5	0.3140
4	0.5784	0.4815	4, 2	0.6327
5	3.4607	0.9806	5, 1	9.3856
6	2.0435	0.7775	6, 4	4.7376

3.4 Applications

Guo et al. (2000) used GA to solve an optimization problem formulated to balance planar mechanism based on three different approaches – (1) mass redistribution, (2) counterweight addition and (3) mixed mass redistribution. The results obtained using genetic algorithm was found better as compared to the traditional nonlinear optimization technique. A hybrid genetic algorithm (HGA) was used by Yang et al. (2005) for the vibration optimum design for the low-pressure steam-turbine rotor of a 1007-MW nuclear power plant. This hybridized algorithm (HGA) combines a genetic algorithm and a local concentration search algorithm using a modified simplex

method. The shaft diameter, bearing length and clearance were chosen as the design variables to minimize the resonance response of the second occurring mode in the excessive vibration. It was proved that the HGA reduces the excessive response at the critical speed and also improves the stability. Erkaya and Uzmay (2009, 2013) used GA to investigate the effect of joint clearances on the dynamic properties of the planar mechanism. Using the concepts of physical pendulum and inertia counterweights, the optimization problem formulated for balancing of a planar four-bar mechanism is solved using multiobjective particle swarm optimization, and non-dominated sorting genetic algorithm II (Farmani et al., 2011).

The teaching-learning-based optimization (TLBO) algorithm was used for the optimization of mechanical design problems such as springs, bearings, pulleys and gear train by Rao et al. (2011). This algorithm was also used to optimally design the heat exchanger and the two-stage thermoelectric cooler through multi-objective optimization problem formulation by Rao and Patel (2013a, b). For different multi-objective unconstrained and constrained benchmark functions, TLBO was found more efficient than GA and other popular optimization techniques (Rao and Waghmare, 2014).

3.5 Summary

This chapter discusses various classical and evolutionary optimization techniques followed by the terms defining their working. The popular evolutionary optimization techniques, genetic algorithm (GA), and teaching-learning-based optimization (TLBO) algorithm are presented in details and explained by solving a numerical example. The application of these optimization techniques in different areas including the mechanical design are also highlighted.

Chapter 4

Optimal Dynamic Balancing

This chapter presents the optimization problem formulation for dynamic balancing of the simple and multiloop planar mechanisms having revolute and/or prismatic joints. The equations of motion are presented to determine the shaking force and shaking moment in the planar mechanisms. This formulation is simplified by representing the inertial properties of the mechanism links in terms of the equimomental point-mass parameters. The point-mass parameters are used as the design variables for the proposed optimization problem formulation. The numerical problems to achieve optimal dynamic balancing for widely used planar mechanisms are solved using Genetic algorithm (GA) and Teaching-learning-based optimization algorithm (TLBO).

4.1 Equations of Motion of Rigid Link Moving In a Plane

Consider an *i*th rigid link having motion in XY plane for which a local frame, $X_i\,Y_i$, is fixed at O_i and X_i axis is aligned along O_i to O_{i+1} as shown in Fig. 4.1. Generally, points O_i and O_{i+1} are chosen as joints used to connect $(i\text{-}1)_{st}$ and $(i\text{+}1)_{st}$ rigid links. The XOY is the global inertial frame. The Newton-Euler (NE) equations of motion for the link are written as (Chaudhary and Saha, 2009):

$$\mathbf{f}_i^c = m_i \dot{\mathbf{v}}_i^c \tag{4.1}$$

$$\mathbf{n}_i^c = \mathbf{I}_i^c \dot{\boldsymbol{\omega}}_i + \boldsymbol{\omega}_i \times \mathbf{I}_i^c \boldsymbol{\omega}_i \tag{4.2}$$

where $\mathbf{f}_i^c$ is the resultant force acting on the link at center of mass C_i, $\mathbf{n}_i^c$ is the resultant of the pure moment and the moment of forces about C_i, and $\mathbf{I}_i^c$ is the centroidal inertia tensor with respect to C_i.

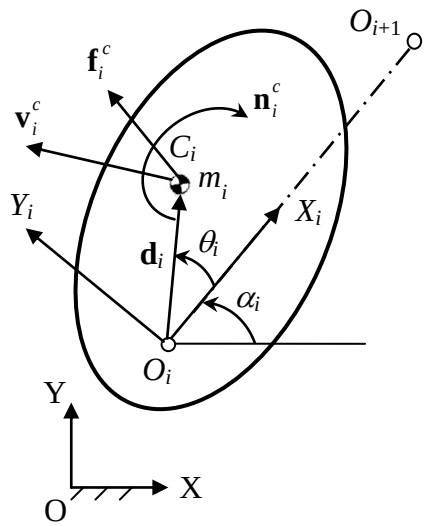

Fig. 4.1 *The ith rigid link moving in XY plane*

The notations, m_i, $\boldsymbol{\omega}_i$ and $\dot{\boldsymbol{\omega}}_i$ represent mass, angular velocity and angular acceleration of the *i*th link whereas $\dot{\mathbf{v}}_i^c$ denotes the linear acceleration of C_i, of the *i*th link. All particles of the rigid link move in planes which are parallel to a fixed plane XOY. Therefore, the rigid link has a parallel-plane motion, i.e.., $v_z^c = 0$, $\omega_x = \omega_y = 0$ and $\omega_z \neq 0$. Hence, for parallel-plane motion, Eqs. (4.1) – (4.2) can be presented in scalar form as:

$$f_{ix} = m_i \dot{v}_{ix}^c \tag{4.3}$$

$$f_{iy} = m_i \dot{v}_{iy}^c \tag{4.4}$$

$$f_{iz} = 0 \tag{4.5}$$

$$n_{ix}^c = -I_{ixz}^c \dot{\omega}_{iz} + I_{iyz}^c \omega_{iz}^2 \tag{4.6}$$

$$n_{iy}^c = -I_{iyz}^c \dot{\omega}_{iz} - I_{ixz}^c \omega_{iz}^2 \tag{4.7}$$

$$n_{iz}^c = I_{izz}^c \dot{\omega}_{iz} \tag{4.8}$$

In the right-hand side of Eq. (4.2), the first term is inertia torque about center of mass of the *i*th rigid link. This term takes very simple form in the case of planar motion if inertia tensor is determined about local principal frame at center of mass. In this condition, the products of inertias terms vanish. Hence, Eq. (4.2) is represented by Eq. (4.8) only.

If velocity and acceleration of the *i*th link are represented at point O_i instead of C_i then:

$$\mathbf{v}_i = \mathbf{v}_i^c + \boldsymbol{\omega}_i \times \mathbf{d}_i \tag{4.9}$$

$$\dot{\mathbf{v}}_i = \dot{\mathbf{v}}_i^c + \dot{\boldsymbol{\omega}}_i \times \mathbf{d}_i + \boldsymbol{\omega}_i \times \left(\boldsymbol{\omega}_i \times \mathbf{d}_i\right) \tag{4.10}$$

and in scalar form for planar motion:

$$v_{ix} = v_{ix}^c - \omega_{iz} d_{iy} \tag{4.11}$$

$$v_{iy} = v_{iy}^c + \omega_{iz} d_{ix} \tag{4.12}$$

$$\dot{v}_{ix} = \dot{v}_{ix}^c - \dot{\omega}_{iz} d_{iy} - \omega_{iz}^2 d_{ix} \tag{4.13}$$

$$\dot{v}_{iy} = \dot{v}_{iy}^c + \dot{\omega}_{iz} d_{ix} - \omega_{iz}^2 d_{iy} \tag{4.14}$$

where v_{ix} and v_{iy} are components of linear origin O_i. Note that $d_{ix} = d_i \cos\left(\theta_i + \alpha_i\right)$ and $d_{iy} = d_i \sin\left(\theta_i + \alpha_i\right)$ and ω_{iz} is angular velocity perpendicular to the plane of motion. Here, d_i and θ_i are polar coordinates of the mass center C_i in the local frame, $X_i\, O_i Y_i$. the angular position of the link, α_i, is given by angle between X_i-axis and X-axis. For planar motion, we drop the subscript z and use $\omega_{iz} \equiv \omega_i$ and $I_{izz} \equiv I_i$ throughout the

thesis. Substituting Eqs. (4.13) – (4.14) in Eqs. (4.3) – (4.5) and Eq. (4.8), the resultant forces and moment are given by:

$$f_{ix} = m_i \dot{v}_{ix} - \dot{\omega}_i m_i d_i \sin\left(\theta_i + \alpha_i\right) - \omega_i^2 m_i d_i \cos\left(\theta_i + \alpha_i\right) \tag{4.15}$$

$$f_{iy} = m_i \dot{v}_{iy} + \dot{\omega}_i m_i d_i \cos\left(\theta_i + \alpha_i\right) - \omega_i^2 m_i d_i \sin\left(\theta_i + \alpha_i\right) \tag{4.16}$$

$$n_i = \dot{\omega}_i I_i - \dot{v}_{ix} m_i d_i \sin\left(\theta_i + \alpha_i\right) + \dot{v}_{iy} m_i d_i \cos\left(\theta_i + \alpha_i\right) \tag{4.17}$$

where n_i is resultant moment about O_i, and f_{ix} and f_{iy} are the components of the resultant force at O_i, respectively. I_i is the mass moment of inertia of the ith rigid link about z-axis passing through O_i.

4.2 Equimomental System of Point-masses

A system of rigidly connected point-masses moving in a plane is explored in this section. The rigid links of a mechanism can be modeled as a dynamically equivalent system of point-masses known as equimomental systems (Routh, 1905; Sherwood and Hockey, 1968; Haung, 1983; Chaudhary and Saha, 2008). This simplifies the mechanism dynamics through the simpler mass distribution represented by dynamically equivalent point-mass system for the rigid links. Routh (1905) presented the general requirements for the dynamic equivalence between a rigid body and the point-masses. For a general three-dimensional motion, minimum four particles are needed to represent the rigid body. Wenglarz et al. (1969) and Haung (1983) suggested the sets of two and four point-masses for planar and spatial motion, respectively. Sherwood and Hockey (1968) presented the method of optimization of mass distribution in mechanisms using the concept of equimomental system of point-masses. In this approach, each rigid link of the mechanism is treated as a dynamically equivalent system of point-masses and the link masses are optimally distributed for

the dynamic balancing. This concept is also applied for the kinematic and dynamic analyses of mechanisms (Attia H. A., 2003; Molian, S., 1973).

The rigid link and the system of point-masses will be dynamically equivalent (equimomental) if they have same mass, same center of mass and same inertia with respect to the same coordinate frame (Chaudhary and Saha, 2009). Hence, for the *i*th rigid link shown in Fig. 4.1, a set of rigidly connected *k* point-masses, m_{ij}, located at (l_{ij}, θ_{ij}), where j=1,…,k must satisfy the following conditions:

$$\sum_{j=1}^{k} m_{ij} = m_i \tag{4.18}$$

$$\sum_{j=1}^{k} m_{ij} l_{ij} \cos\theta_{ij} = m_i d_i \cos\theta_i \tag{4.19}$$

$$\sum_{j=1}^{k} m_{ij} l_{ij} \sin\theta_{ij} = m_i d_i \sin\theta_i \tag{4.20}$$

$$\sum_{j=1}^{k} m_{ij} l_{ij}^2 = I_i^c + m_i d_i^2 \tag{4.21}$$

Where l_{ij} and θ_{ij} are polar coordinates of point-mass m_{ij} in the local frame. Note that Eqs. (4.18) – (4.21) are written in local body fixed frame $O_iX_iY_i$. The first subscript *i* denotes link number and the second subscript *j* represents the point-mass belong to the link (Fig. 4.2).

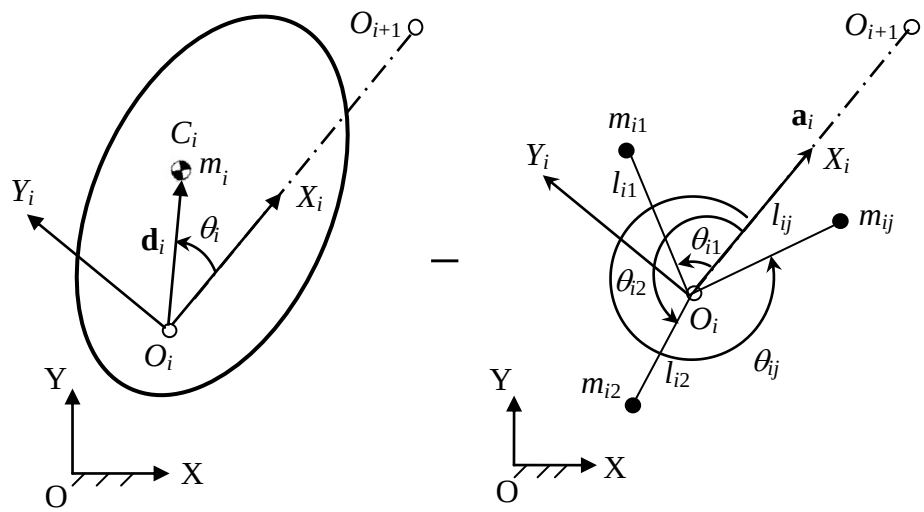

Fig. 4.2 *Equimomental system of point-masses for ith rigid link*

As each point-mass needs three parameters, (m_{ij}, l_{ij}, θ_{ij}), to identify it, a total of 3k parameters are required to define an equimomental system of k point-masses. Furthermore, this system should also satisfy the four constraints presented by Eqs. (4.18) – (4.21). The equimomental system of point-masses for $k \geq 2$ presents an infinite number of solutions because it makes the resultant system of equations underdeterminate for which the number of unknowns is more than number of constraints, Eqs. (4.18) – (4.21). Note that a single point-mass cannot represent rigid link as the three parameters of it must satisfy the four constraint equations. This makes the resulting system of equations overdeterminate in which the number of unknowns is less than the number of equations need to be satisfied. Thus, an equimomental system for a rigid link moving in a plane cannot be represented using single point-mass. At least two point-masses with six unknown parameters are required to represents rigid bodies in which two parameters need to be assigned arbitrarily. Similarly, for three point-mass representation, five parameters need to be assigned arbitrarily to satisfy the equimomental conditions. In general, for an equimomental system of k point-masses, (3k-4) parameters need to be assigned arbitrarily so that the remaining four are determinate.

For an equimomental system of three point-masses, the conditions for the dynamic equivalence are given as:

$$\sum_{j=1}^{3} m_{ij} = m_i \tag{4.22}$$

$$\sum_{j=1}^{3} m_{ij} l_{ij} \cos\theta_{ij} = m_i d_i \cos\theta_i \tag{4.23}$$

$$\sum_{j=1}^{3} m_{ij} l_{ij} \sin\theta_{ij} = m_i d_i \sin\theta_i \tag{4.24}$$

$$\sum_{j=1}^{3} m_{ij} l_{ij}^2 = m_i k_i^2 \tag{4.25}$$

where $m_i k_i^2 = I_i^c + m_i d_i^2$ and k_i is the radius of gyration of ith link about the point, O_i. Hence, this system has nine unknowns, m_{ij}, l_{ij}, and θ_{ij}, for j=1, 2, 3, and four constraint equations, Eqs. (4.22) – (4.25). The dynamic equivalence conditions, Eqs. (4.22) – (4.25), can be presented in the linear form in point-masses by assigning some suitable values to l_{ij} and θ_{ij}. Assuming, $l_{i2} = l_{i3} = l_{i1}$, and substituting them in Eq. (4.25) gives:

$$\sum_{j=1}^{3} m_{ij} l_{i1}^2 = m_i k_i^2 \tag{4.26}$$

which gives $l_{i1} = \pm k_i$. Taking the positive value for l_{i1}, the three point-masses are then solved from Eqs. (4.22) – (4.24) by substituting $l_{i1} = k_i$. Equations (4.22) – (4.24) are written in matrix form as:

$$\begin{bmatrix} 1 & 1 & 1 \\ k_i \cos\theta_{i1} & k_i \cos\theta_{i2} & k_i \cos\theta_{i3} \\ k_i \sin\theta_{i1} & k_i \sin\theta_{i2} & k_i \sin\theta_{i3} \end{bmatrix} \begin{bmatrix} m_{i1} \\ m_{i2} \\ m_{i3} \end{bmatrix} = \begin{bmatrix} m_i \\ m_i d_i \cos\theta_i \\ m_i d_i \sin\theta_i \end{bmatrix} \tag{4.27}$$

The masses m_{i1}, m_{i2} and m_{i3} can be found by solving Eq. (4.27). It further establishes that any two point-masses should not lie on the same radial line starting from the origin, O_i. The solution for masses is obtained as:

$$\begin{bmatrix} m_{i1} \\ m_{i2} \\ m_{i3} \end{bmatrix} = \frac{k_i}{\mathrm{S}} \begin{bmatrix} k_i \sin(\theta_{i3} - \theta_{i2}) & (\sin\theta_{i2} - \sin\theta_{i3}) & (\cos\theta_{i3} - \cos\theta_{i2}) \\ -k_i \sin(\theta_{i3} - \theta_{i1}) & (\sin\theta_{i3} - \sin\theta_{i1}) & (\cos\theta_{i1} - \cos\theta_{i3}) \\ -k_i \sin(\theta_{i1} - \theta_{i2}) & (\sin\theta_{i1} - \sin\theta_{i2}) & (\cos\theta_{i2} - \cos\theta_{i1}) \end{bmatrix} \begin{bmatrix} m_i \\ m_i d_i \cos\theta_i \\ m_i d_i \sin\theta_i \end{bmatrix}$$

(4.28)

in which, $\mathrm{S} = k_i^2[\sin(\theta_{i3} - \theta_{i2}) + \sin(\theta_{i2} - \theta_{i1}) + \sin(\theta_{i1} - \theta_{i3})]$. For example, if $\theta_{i1} = 0$, $\theta_{i2} = 2\pi/3$, and $\theta_{i3} = 4\pi/3$, the point masses are calculated as

$$m_{i1} = \frac{m_i}{3}\left(1 + \frac{2d_i \cos\theta_i}{k_i}\right) \tag{4.29}$$

$$m_{i2} = \frac{m_i}{3}\left(1 - \frac{d_i \cos\theta_i}{k_i} + \frac{\sqrt{3} d_i \sin\theta_i}{k_i}\right) \tag{4.30}$$

$$m_{i3} = \frac{m_i}{3}\left(1 - \frac{d_i \cos\theta_i}{k_i} - \frac{\sqrt{3} d_i \sin\theta_i}{k_i}\right) \tag{4.31}$$

Eqs. (4.29) – (4.31) take simpler form if the origin, O_i, coincides with the mass center of the link, C_i, i.e., $d_i = 0$. Substitution of $d_i = 0$ in Eqs. (4.29) – (4.31) gives $m_{i1} = m_{i2} = m_{i3} = m_i/3$. Thus, the point-masses of the link are distributed equally, and located on the circumference of a circle having radius k_i. Using equimomental

conditions, Eqs. (4.18) – (4.21), the Newton-Euler equations of motion for *i*th rigid link, Eqs. (4.15) – (4.17), are rewritten in terms of point-mass parameters as:

$$f_{ix} = \sum_{j=1}^{k} \left[m_{ij}\dot{v}_{ix} - \dot{\omega}_i m_{ij} l_{ij} \sin(\theta_{ij} + \alpha_i) - \omega_i^2 m_{ij} l_{ij} \cos(\theta_{ij} + \alpha_i) \right] \tag{4.32}$$

$$f_{iy} = \sum_{j=1}^{k} \left[m_{ij}\dot{v}_{iy} + \dot{\omega}_i m_{ij} l_{ij} \cos(\theta_{ij} + \alpha_i) - \omega_i^2 m_{ij} l_{ij} \sin(\theta_{ij} + \alpha_i) \right] \tag{4.33}$$

$$n_i = \dot{\omega}_i \sum_{j=1}^{k} \left[m_{ij} l_{ij}^2 - \dot{v}_{ix} m_{ij} l_{ij} \sin(\theta_{ij} + \alpha_i) + \dot{v}_{iy} m_{ij} l_{ij} \cos(\theta_{ij} + \alpha_i) \right] \tag{4.34}$$

Equations (4.32) – (4.34) define the force and moment for the *i*th rigid link of a mechanism represented by an equimomental system of *k* point-masses.

4.3 Shaking Force and Shaking Moment

In this section, the shaking force and shaking moment in planar mechanism is defined and presented using the concept of equimomental point-mass system described in the previous section. The shaking force and shaking moment in a mechanism depend on the mass and inertia of each link, and their mass centre location. Figure 4.3 shows a six-link multiloop mechanism where the fixed link is detached from the moving links to show reactions.

The shaking force defined as the reaction of the vector sum of all the inertia forces in the mechanism is given as:

$$\mathbf{f}_{\mathrm{sh}} = -\sum_{i=1}^{5} m_i \dot{\mathbf{v}}_i \tag{4.35}$$

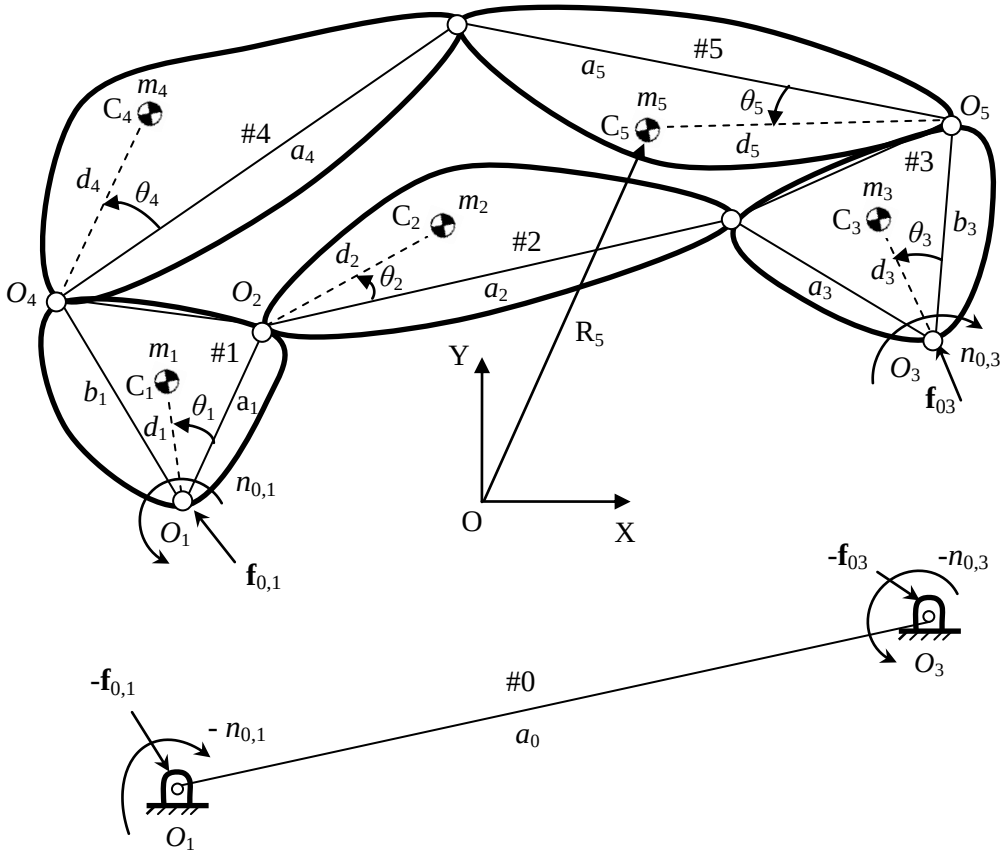

Fig. 4.3 *Definitions of various parameters for a multiloop mechanism*

The two components of the shaking force in point-mass parameters using Eqs. (4.32) – (4.33) are obtained as:

$$f_{shx} = -\sum_{i=1}^{5}\sum_{j=1}^{k}\left[m_{ij}\dot{v}_{ix} - \dot{\omega}_i m_{ij} l_{ij}\sin(\theta_{ij}+\alpha_i) - \omega_i^2 m_{ij} l_{ij}\cos(\theta_{ij}+\alpha_i)\right] \tag{4.36}$$

$$f_{shy} = -\sum_{i=1}^{5}\sum_{j=1}^{k}\left[m_{ij}\dot{v}_{iy} + \dot{\omega}_i m_{ij} l_{ij}\cos(\theta_{ij}+\alpha_i) - \omega_i^2 m_{ij} l_{ij}\sin(\theta_{ij}+\alpha_i)\right] \tag{4.37}$$

Similarly, the shaking moment is the reaction of the resultant of the inertia moment and the moment of the inertia forces about stationary point O and is given by:

$$\mathbf{n}_{\mathrm{sh}} = -\sum_{i=1}^{5}\left[\left(\mathbf{I}_i\dot{\boldsymbol{\omega}}_i + \boldsymbol{\omega}_i \times \mathbf{I}_i\boldsymbol{\omega}_i\right) + \mathbf{R}_i \times m_i\dot{\mathbf{v}}_i\right] \tag{4.38}$$

where $\mathbf{R}_i$ represents the vector from O to mass centre of the ith link, C_i. Eq. (4.38) is further simplified using point-mass parameters as:

$$\begin{aligned} n_{\text{sh}} = -\sum_{i=1}^{5}\sum_{j=1}^{k}\Big[& \left(\dot{\omega}_i m_{ij} l_{ij}^2 - \dot{v}_{ix} m_{ij} l_{ij} \sin(\theta_{ij}+\alpha_i) + \dot{v}_{iy} m_{ij} l_{ij} \cos(\theta_{ij}+\alpha_i)\right) \\ & + R_{iy}\left(m_{ij}\dot{v}_{ix} - \dot{\omega}_i m_{ij} l_{ij} \sin(\theta_{ij}+\alpha_i) - \omega_i^2 m_{ij} l_{ij} \cos(\theta_{ij}+\alpha_i)\right) \\ & + R_{ix}\left(m_{ij}\dot{v}_{iy} + \dot{\omega}_i m_{ij} l_{ij} \cos(\theta_{ij}+\alpha_i) - \omega_i^2 m_{ij} l_{ij} \sin(\theta_{ij}+\alpha_i)\right)\Big] \end{aligned} \tag{4.39}$$

here, m_{ij} is jth point mass of ith link, and l_{ij} and θ_{ij} are polar coordinates in the link fixed frame (Fig. 4.2).

4.4 Optimization Problem Formulation

To formulate the optimization problem to achieve the optimal dynamic balancing in the planar mechanism, each link is converted into a system of k equimomental point-masses and the point-mass parameters are taken as the design variables. As each point mass needs three parameters (m_{ij}, l_{ij}, θ_{ij}) to identify it, a 3k-vector, $\mathbf{x}_i$, of design variables for ith link is defined as:

$$\mathbf{x}_i = [m_{i1} \quad l_{i1} \quad \theta_{i1} \quad m_{i2} \quad l_{i2} \quad \theta_{i2} \quad \ldots \quad m_{ik} \quad l_{ik} \quad \theta_{ik}]^{\mathrm{T}} \tag{4.40}$$

Hence, the 3kn-design-vector, $\mathbf{x}$, for the mechanism having n moving links is given by:

$$\mathbf{x} = [\mathbf{x}_1^{\mathrm{T}} \quad \mathbf{x}_2^{\mathrm{T}} \quad \ldots \quad \mathbf{x}_n^{\mathrm{T}}]^{\mathrm{T}} \tag{4.41}$$

As the shaking force and shaking moment have different units, they are normalized with respect to a reference link of the mechanism as (Conte et al., 1975):

$$\bar{f} = \frac{|\mathbf{f}|}{ma\omega^2} \tag{4.42}$$

$$\bar{n} = \frac{n}{ma^2\omega^2} \tag{4.43}$$

where a and m are the length and mass of the reference link whereas ω is its angular velocity. Considering the RMS values of the magnitude of shaking force, $f_{\text{sh,rms}}$ and shaking moment, $n_{\text{sh,rms}}$ defined in Eqs. (4.36) – (4.39), the optimization problem is posed as weighted sum of the shaking force and shaking moment as:

$$\text{Minimize } Z = w_1 f_{\text{sh,rms}} + w_2 n_{\text{sh,rms}} \tag{4.44}$$

$$\text{Subject to } m_{i,\min} \le \sum_j m_{ij} \le m_{i,\max};\ I_{i,\min} \le \sum_j m_{ij} l_{ij}^2$$

$$\sum_j m_{ij} l_{ij} \sin\left(\theta_{ij} + \alpha_i\right) = 0 \left(\text{for symmetry about } \mathrm{X}_i \text{ axis}\right)$$

$$\text{for } i = 1, 2, \ldots, n \text{ and } j = 1, 2, \ldots, k \tag{4.45}$$

where w_1 and w_2 are the weighting factors used to assign weightage to shaking force and shaking moment, respectively, in the objective function (Eq. 4.44). The different approaches can be adopted to select weighting factors (Marler and Arora, 2004, 2010). The weights represent the relative importance given to various conflicting functions in the objective. These weights transform the number of objective functions into a single function. In this study, there are two objectives, i.e. shaking force and shaking moment. They are normalised with respect to parameters of driving link of the mechanism to avoid domination of one objective over other. For the normalised objective functions, it becomes easy to set the weights between 0 and 1 depending upon the application. When equal importance is given to both the normalised objective functions, the weights would be w_1=0.5 and w_2=0.5. Similarly, weights for different objectives may be chosen by the mechanism designer as per the requirement

in real problems. For example, for complete shaking force balance and complete shaking moment balance, these values are taken as (w_1=1, w_2=0) and (w_1=0, w_2=1), respectively. The constraints on design variables depend on the allowable minimum and maximum values of mass and inertia of the links. The minimum mass, $m_{i,\min}$, of the ith link and its mass distribution can be decided by load bearing capability of its material. Furthermore, the maximum mass, $m_{i,\max}$, can be taken into account according to what extent the shaking force and shaking moment are eliminated. Similarly, the limits on parameters, l_{ij}, can be determined based on the limiting values of the moment of inertia. The solution of this optimization problem finds the optimum values of design variables, i.e., the point-mass parameters, for minimizing the objective function (Eq. 4.44).

4.5 Planar Mechanisms

The effectiveness of the proposed optimization method is shown by applying it to four most popular and basic mechanisms used in machines. The balancing problems can be framed as single objective or multi-objective optimization problems to simultaneously minimize shaking force and shaking moment. As shaking force and shaking moment are of different units, these quantities need to be made dimensionless for adding them in a single objective function. For this, the mechanism parameters are made dimensionless with respect to the parameters of the driving link of the mechanism. In this study, three-point mass model is used to achieve better mass distribution. The equimomental point-mass systems with more number of point-masses may be used but will increase the overall computational time to evaluate the objective function and constraints. Further the dimension of the problem can be reduced by assigning five parameters for each link as:

$$\theta_{i1}=0;\ \theta_{i2}=2\pi/3;\ \theta_{i3}=4\pi/3 \text{ and } l_{i2}=l_{i3}=l_{i1} \tag{4.46}$$

Out of nine variables, m_{ij}, l_{ij}, θ_{ij}, for j=1, 2, 3, for ith link, the other four point-mass parameters, m_{i1}, m_{i2}, m_{i3} and l_{i1} are brought into the optimization scheme as the design variables. To solve these problems, Genetic algorithm (GA) and Teaching-learning-based optimization (TLBO) algorithm are used in MATLAB 2008 and run on a laptop machine having Intel Core i3 processor with 2.27 GHz and 4 GB RAM. Considering $\mathrm{m}_{i,\min} = 0.25m_i^{\mathrm{o}}$, $\mathrm{m}_{i,\max} = 5m_i^{\mathrm{o}}$ and $\mathrm{I}_{i,\min} = 0.25I_i^{\mathrm{o}}$ for ith link, the optimization problem as explained in Eqs. (4.44) – (4.45) is solved using both optimization techniques. The superscript 'o' represents parameters for original mechanism. The simultaneous minimization of shaking force and shaking moment is considered taking the weighting factors, w_1 and w_2, as 0.5. With the default values of genetic operators, i.e., crossover rate 0.8 and mutation rate 0.2, GA was run for 100 iterations with population size of 20. With the same population size, the performance of GA and TLBO is compared in terms of number of function evaluations needed to reach the optimum solution. For both optimization techniques, the best values of objective function and corresponding design variables are found for 30 independent runs. The convergence plots are presented to compare the computational efficiency of both the techniques for different examples. An algorithm is more efficient if it requires less function evaluations or number of iterations to find the optimum solution. In convergence plots, the objective function values are shown against the function evaluations for both the algorithms. The kinematic and dynamic calculations are verified using Altair HyperWorks software.

4.5.1 Four-bar mechanism

A numerical problem of planar four-bar mechanism (Berkof, 1973; Farmani et al., 2011) as shown in Fig. 4.4 is solved using the method proposed in this chapter. The link length, mass and other geometric parameters of the original mechanism are given

in Table 4.1. Three equimomental point-masses for each link are considered and their parameters are given in Table 4.2. For this example, the driving link, i.e., link #1, rotates with a constant speed of 100 rad/sec.

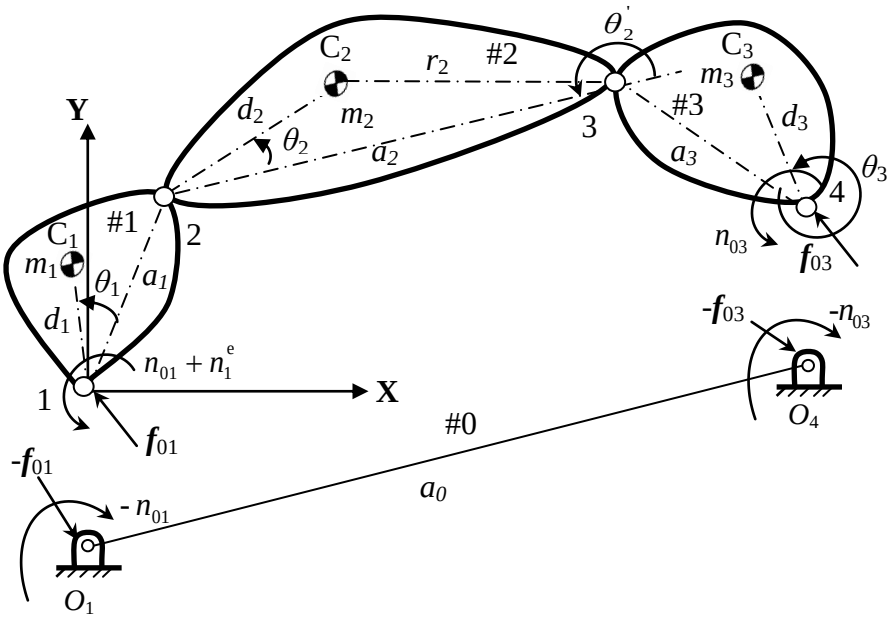

Fig. 4.4 *Four-bar mechanism detached from its frame*

Table 4.1 *Original parameters of four-bar mechanism*

Link i	Length a_i (m)	Mass m_i (kg)	Moment of inertia I_i^c (kg-m^2)	d_i (m)	θ_i (deg)
1	0.1	0.3925	0.0004	0.05	0
2	0.4	1.5700	0.0213	0.20	0
3	0.3	1.1775	0.0091	0.15	0
0	0.3	$\sum m_i^o = 3.139$	-		

Link #1 is the driving link

Table 4.2 *Equimomental point-mass parameters for normalised four-bar mechanism links*

Link	m_{i1}	m_{i2}	m_{i3}	l_{i1}
1	0.8952	0.0524	0.0524	0.5932
2	3.6377	0.1812	0.1812	2.3145
3	2.7255	0.1373	0.1373	1.7386

Six different cases are investigated to balance this mechanism:

In case (1), full force balancing is considered in which the weighting factors, w_1 and w_2, are 1 and 0, respectively, in Eq. (4.44). Also, rotating links #1 and #3 are considered for mass redistribution keeping link #2 intact. In case (2), the simultaneous minimization of force and moment is considered where the weighting factors, w_1 and w_2, as 0.5. In this case, the point-masses of all three links are chosen to find their optimum mass distribution.

Particularly, four-bar mechanism is also balanced by converting coupler into physical pendulum (Berkof, 1973; Farmani et al., 2011). To investigate the effect of this conversion, the cases (1) and (2) are repeated after making link #2 as the physical pendulum and reported as cases (3) and (4), respectively. In case (5), the mechanism is balanced without changing the original link masses while balancing using links with non-symmetry about X_i axis, i.e., $\sum_j m_{ij} l_{ij} \sin\left(\theta_{ij} + \alpha_i\right) \neq 0$, is presented as case (6).

To solve this optimization problem using GA, "*ga*" function in *Genetic Algorithm and Direct Search Toolbox* of MATLAB was used. The comparison of original RMS and peak values of shaking force, shaking moment and driving torque with those of optimum values are provided in Table 4.3. Figures 4.5, 4.6 and 4.7 show the variations in the shaking force, shaking moment and driving torque, respectively, over the complete crank cycle. The case (2) most effectively minimizes the shaking force, shaking moment and driving torque. The link parameters for the optimally balanced mechanism, i.e., case (2), are then found by using the equimomental conditions and given in Table 4.4.

Table 4.3 *Values of dynamic quantities in the original and optimally balanced four-bar mechanism*

Case	Type of balancing	Normalised shaking force		Normalised shaking moment		Normalised driving torque	
		RMS	Peak	RMS	Peak	RMS	Peak
	Original mechanism	5.9604	11.8837	10.7250	12.3939	3.0588	5.0480
Case 1: w_1=1, w_2=0; keeping link #2 intact	Force balance	0.0087 (-99.85%)	0.3395 (-97.14%)	16.1133 (+50.24%)	16.3722 (+32.10%)	5.4359 (+77.71%)	9.4000 (+86.21%)
Case 2: w_1=0.5,w_2=0.5; all links are considered	Force and moment balance	2.3451 (-60.65%)	4.4830 (-62.27%)	3.6977 (-65.52%)	5.1770 (-58.23%)	0.8769 (-71.33%)	1.6990 (-66.34%)
Case 3: w_1=1, w_2=0; link #2 is made as physical pendulum and then kept intact	Force balance	0.0688 (-99.85%)	0.1861 (-98.43%)	27.1472 (+153.12%)	30.6055 (+146.94%)	8.7761 (+186.91%)	15.7899 (+212.79%)
Case 4: w_1=0.5, w_2=0.5; link #2 is made as physical pendulum and then all links are considered	Force and moment balance	4.0330 (-37.34%)	6.3998 (-46.15%)	5.9502 (-44.52%)	8.5520 (-30.99%)	1.5747 (-48.52%)	3.0076 (-40.42%)
Case 5: w_1=0.5, w_2=0.5; Keeping link masses unchanged	Force and moment balance	4.3761 (-27.66%)	7.2856 (-38.69%)	5.5974 (-48.12%)	6.7374 (-45.64%)	1.5819 (-48.49%)	2.7111 (-46.29%)
Case 6: w_1=0.5, w_2=0.5; Non-symmetrical shapes	Force and moment balance	4.0172 (-32.95%)	7.4941 (-36.94%)	6.3747 (-40.59%)	7.4163 (-40.16%)	1.7958 (-41.30%)	2.9809 (-40.95%)

Table 4.4 *Link parameters of the optimally balanced four-bar mechanism*

Case	Link I	Mass m_i (kg)	Total mass (kg)	Moment of inertia I_i^c (kg-m^2)	d_i (m)	θ_i (deg)
Case 1	1	1.8572	7.5060	0.0131	0.0453	180
	2	1.5705		0.0841	0.2000	0
	3	4.0783		0.1112	0.0540	180
Case 2	1	0.2458	1.9651	0.0005	0.0222	0
	2	1.0442		0.0299	0.0594	0
	3	0.6751		0.0115	0.0702	0
Case 3	1	2.4368	10.7788	0.0208	0.0463	180
	2	2.3107		0.1577	0.2000	0
	3	6.0313		0.1781	0.0566	180
Case 4	1	0.3555	2.8784	0.0008	0.0180	0
	2	1.4582		0.0545	0.0824	0
	3	1.0647		0.0196	0.0541	0
Case 5	1	0.3909	3.1400	0.0007	0.0134	0
	2	1.5703		0.0468	0.0962	0
	3	1.1788		0.0192	0.0601	0
Case 6	1	0.2895	2.4405	0.0008	0.0314	006.72
	2	1.2536		0.0488	0.1417	358.15
	3	0.8974		0.0225	0.1087	001.42

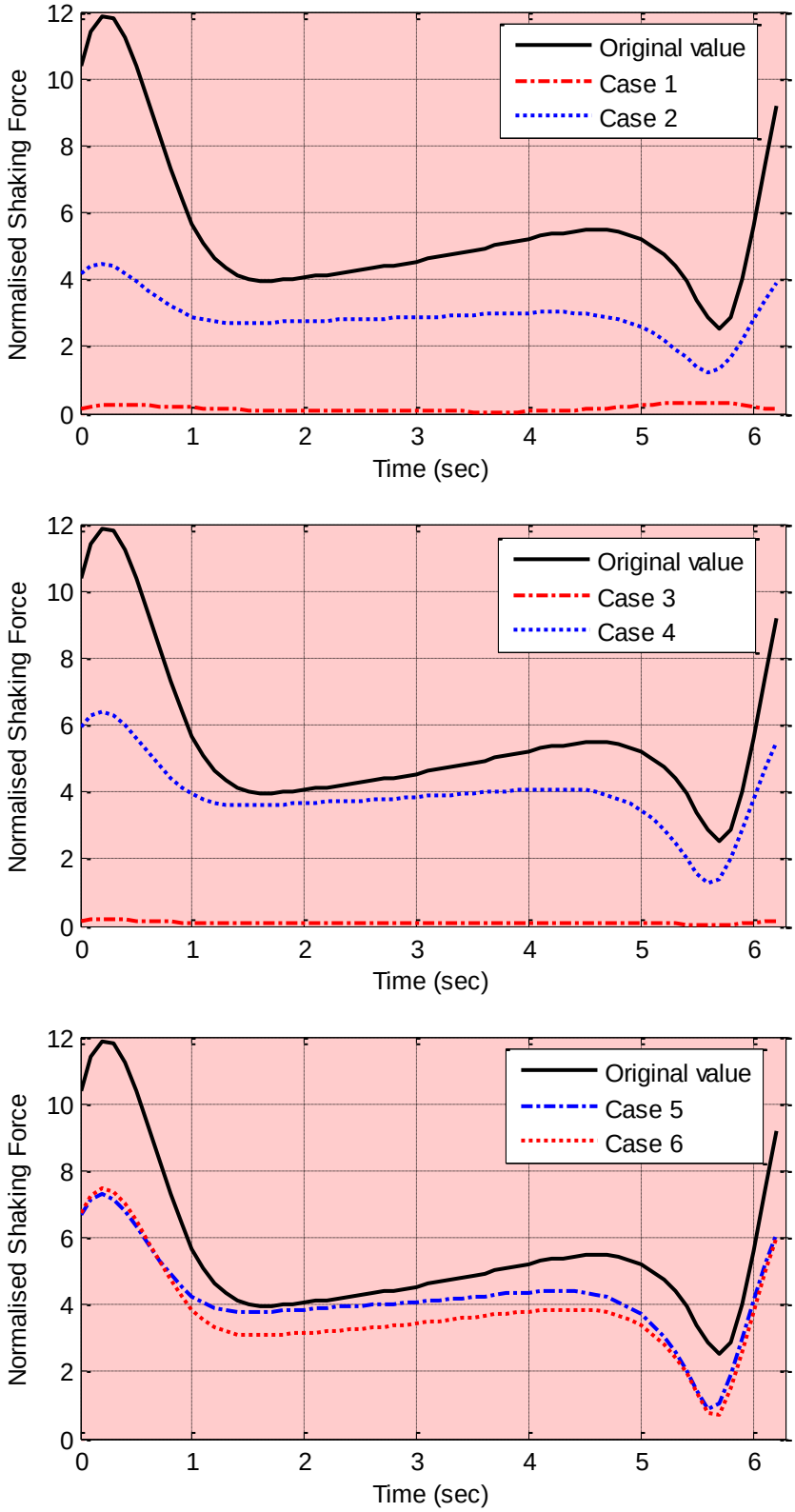

Fig. 4.5 *Variation in shaking force with time for one complete crank cycle. Case (1), (2), (5) and (6) without converting link #2 into physical pendulum; Case (3) and (4) with link #2 as physical pendulum in four-bar mechanism*

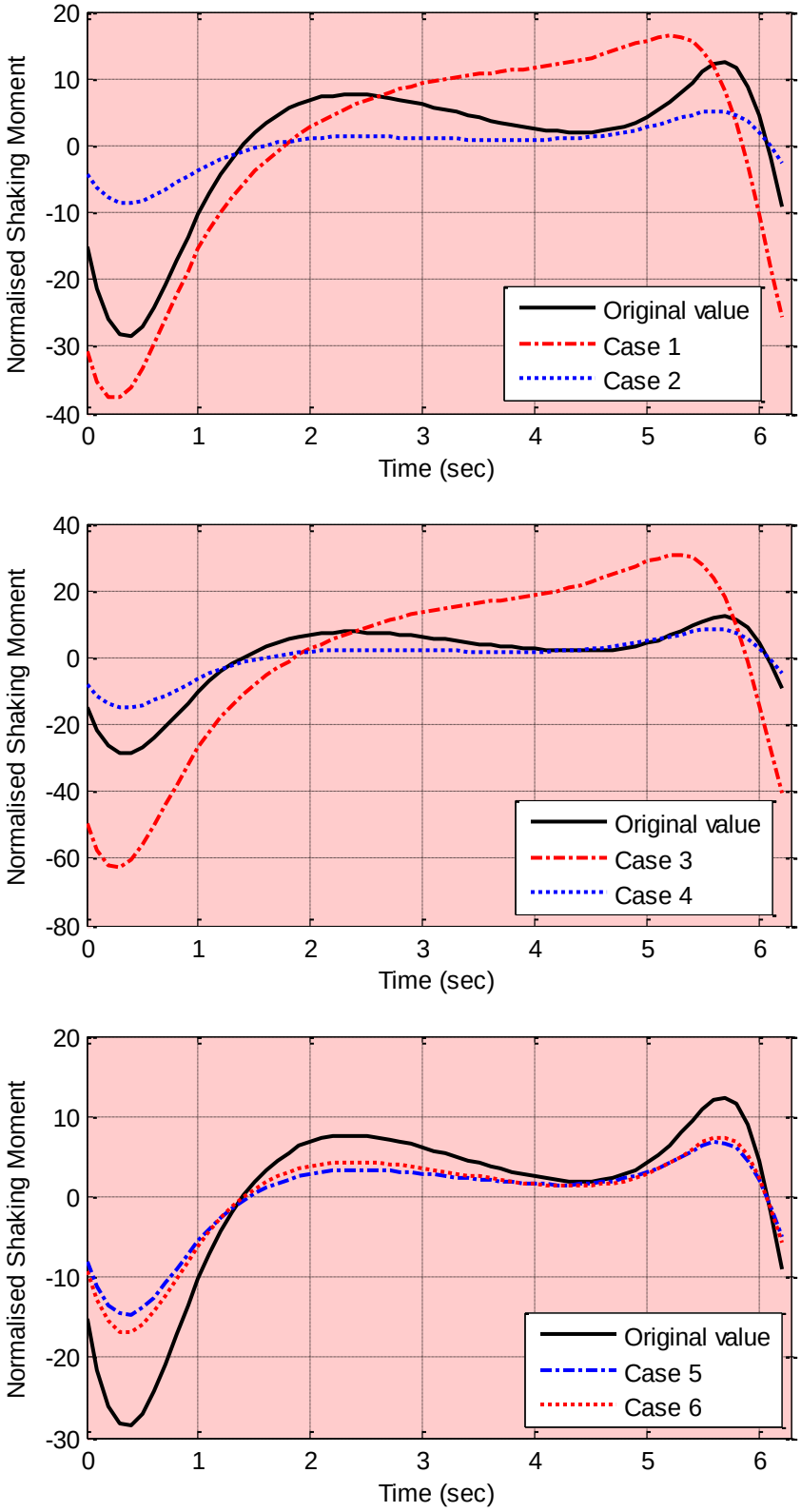

Fig. 4.6 *Variation in shaking moment with time for one complete crank cycle. Case (1), (2), (5) and (6) without converting link #2 into physical pendulum; Case (3) and (4) with link #2 as physical pendulum in four-bar mechanism*

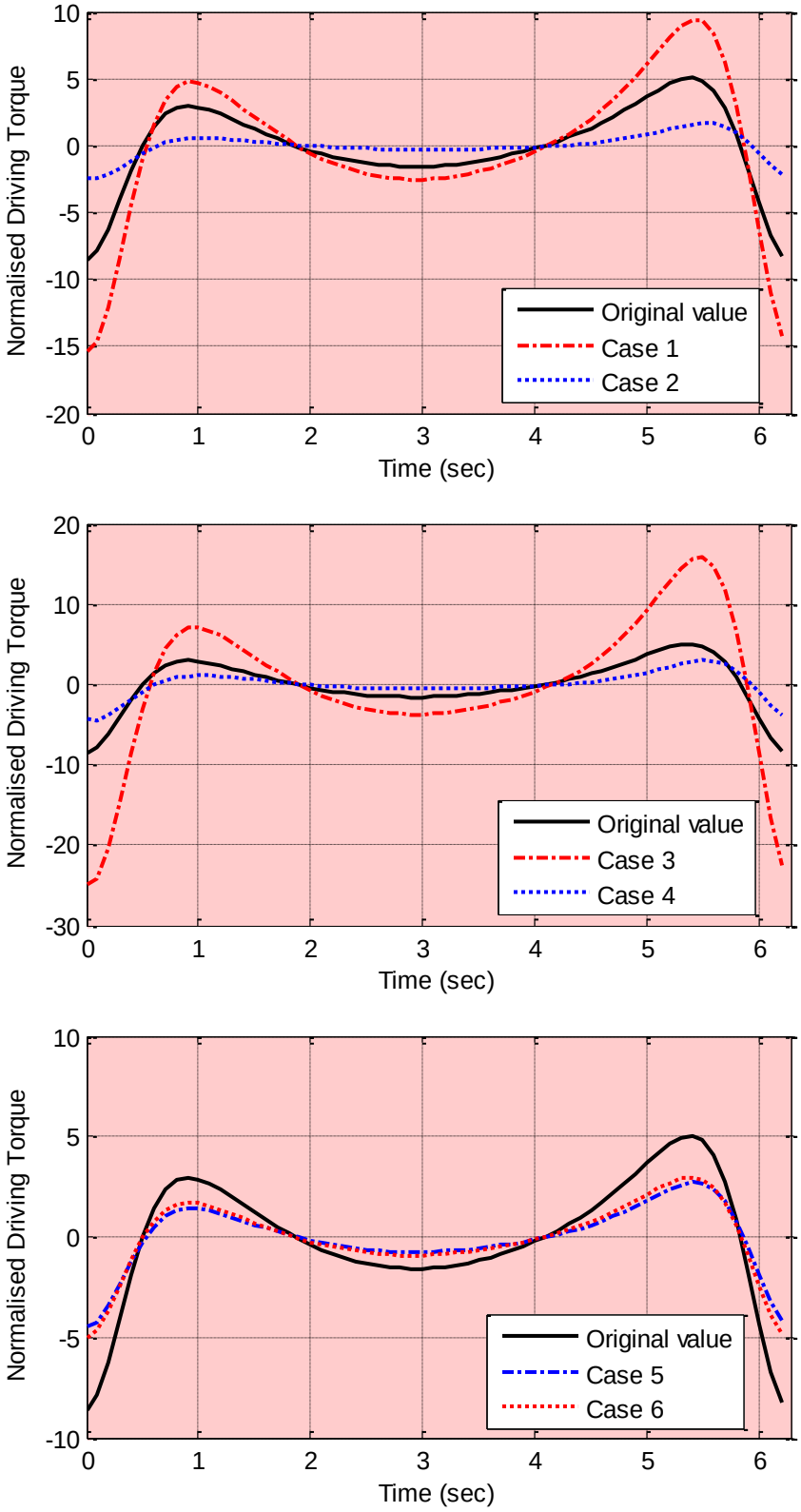

Fig. 4.7 *Variation in driving torque with time for one complete crank cycle. Case (1), (2), (5) and (6) without converting link #2 into physical pendulum; Case (3) and (4) with link #2 as physical pendulum in four-bar mechanism*

The complete shaking force balancing is achieved numerically by redistribution of link masses in case (1). The result obtained using the proposed optimization methodology is compared with the analytical full force balancing conditions (Berkof and Lowen, 1969) which are as follow:

$$m_1 d_1 = m_2 r_2 \frac{a_1}{a_2}, \text{ and } \theta_1 = \theta_2^{'}; \; m_3 d_3 = m_2 d_2 \frac{a_3}{a_2}, \text{ and } \theta_3 = \theta_2 + \pi \tag{4.47}$$

where all the parameters are defined in Fig. 4.4.

These conditions of full force balancing are satisfied for the complete force balanced mechanism achieved for cases (1) and (3). Note that this is achieved by redistributing masses of link #1 and #3. Conventionally this is done by adding counterweights to link #1 and #3 which is not useful from the mechanical design point of view. However, the total mass is increased to 7.505 kg and 10.777 kg from the total mass of 3.139 kg of the original mechanism, respectively in both approaches. As shown in Table 4.3, the RMS values of the shaking moment and the driving torque are increased by 50.24% and 77.71%, respectively for the complete force balancing (case 1). This confirms that both the shaking moment and driving torque are increased in a force balanced mechanism (Lowen et al., 1974). In case (3), the force balancing is achieved after converting link #2 into the physical pendulum. It requires more mass to be added for balancing in comparison of case (1) as given in Table 4.4. Moreover, the shaking moment and the driving torque increments over original are 153.12% and 186.91%, respectively. *Hence, the conversion of coupler into physical pendulum has adverse effect on the shaking moment and the driving torque*.

The best solution is found as case (2) which reduces the RMS values of shaking force, shaking moment and driving torque by 60.65%, 65.52% and 71.33%, respectively. Now, the computational efficiency of GA is compared with TLBO for case (2). The

comparison of the RMS values of shaking force, shaking moment and driving torque of original mechanism with those of optimally balanced mechanism found using GA and TLBO are provided in Table 4.5. Figure 4.8 shows the variations in the shaking force, shaking moment and driving torque over the complete crank cycle for the original as well as for the optimally balanced mechanisms while Pareto front is shown in Fig. 4.9. The performance of GA and TLBO is compared and is shown in Fig. 4.10 as the convergence plot. Table 4.6 presents the optimum values of the design variables, i.e., the point-mass parameters for the balanced mechanism.

Table 4.5 *Normalized RMS values of dynamic quantities in the original and optimally balanced four-bar mechanism using GA and TLBO (case 2)*

	Normalised shaking force	Normalised shaking moment	Normalised driving torque	No. of function evaluations
Original mechanism	5.9604	10.7253	3.0588	
Optimally balanced using GA	2.3451 (-60.65%)	3.6977 (-65.52%)	0.8769 (-71.33%)	42000
Optimally balanced using TLBO	2.0682 (-65.30%)	2.8576 (-73.36%)	0.7564 (-75.27%)	24000

Table 4.6 *Normalised optimum equimomental point-mass parameters for balanced four-bar mechanism (case 2)*

	Link	m_{i1}	m_{i2}	m_{i3}	l_{i1}
Optimally balanced using GA	1	0.3389	0.0557	0.0557	0.5363
	2	1.5078	0.1771	0.1771	2.0391
	3	1.0681	0.1443	0.1443	1.5058
Optimally balanced using TLBO	1	0.3084	0.0507	0.0507	0.4880
	2	1.3721	0.1612	0.1612	1.8556
	3	0.9720	0.1313	0.1313	1.3703

The traditional approach (Berkof, 1973; Farmani et al., 2011) suggests the use of physical pendulum concept, the force and inertia counterweights to balance a planar

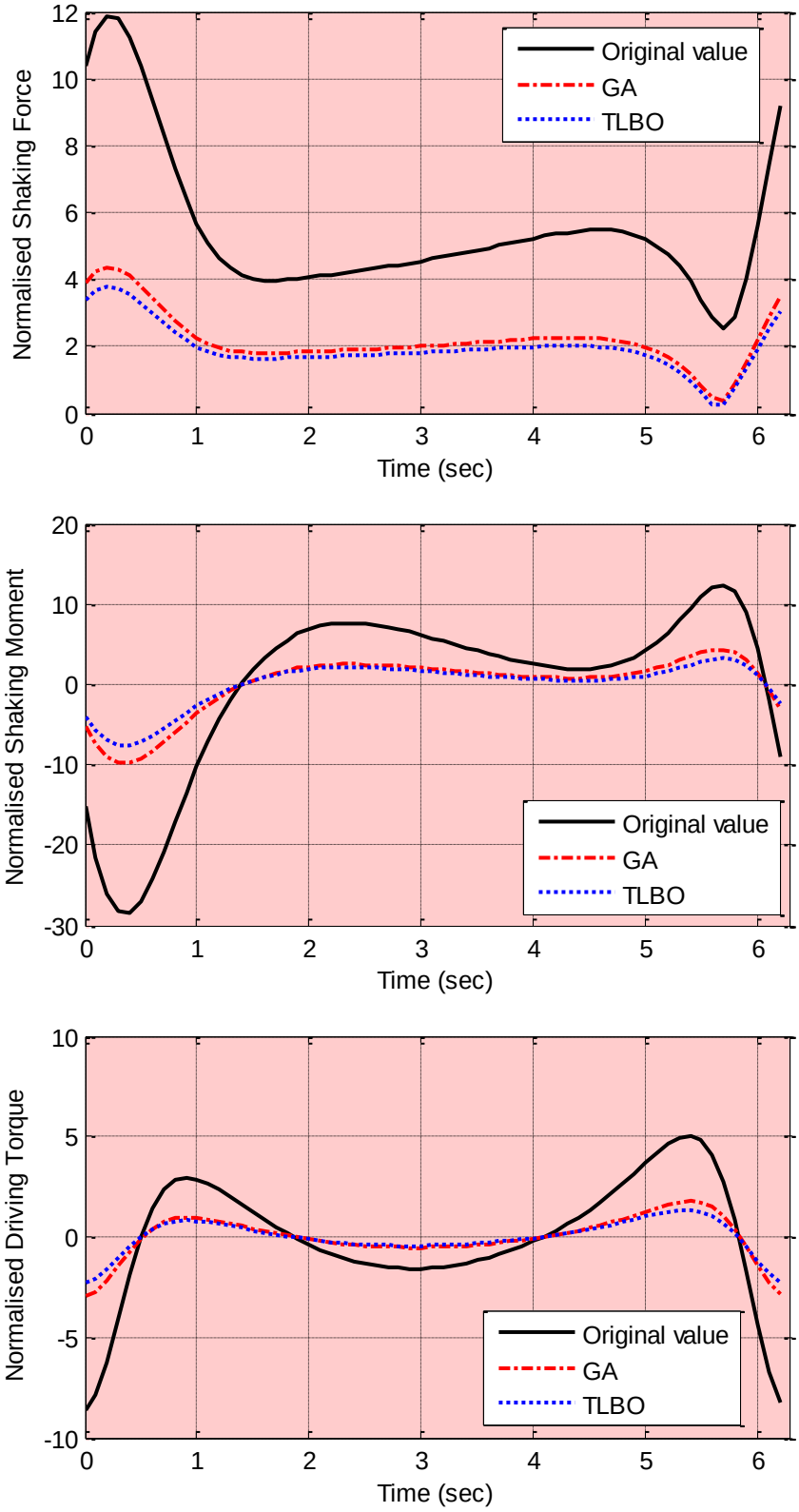

Fig. 4.8 *Variations in the dynamic quantities of original and optimally balanced four-bar mechanism using GA and TLBO for complete cycle of operation*

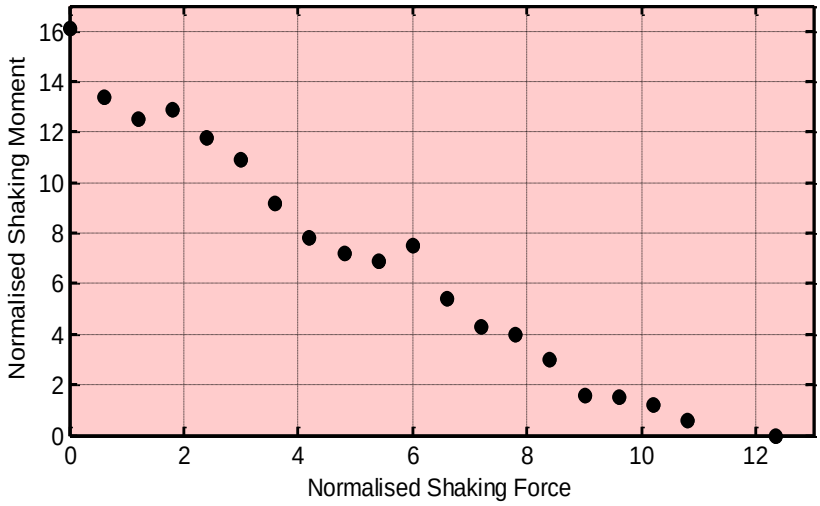

Fig. 4.9 *Pareto front for four-bar mechanism*

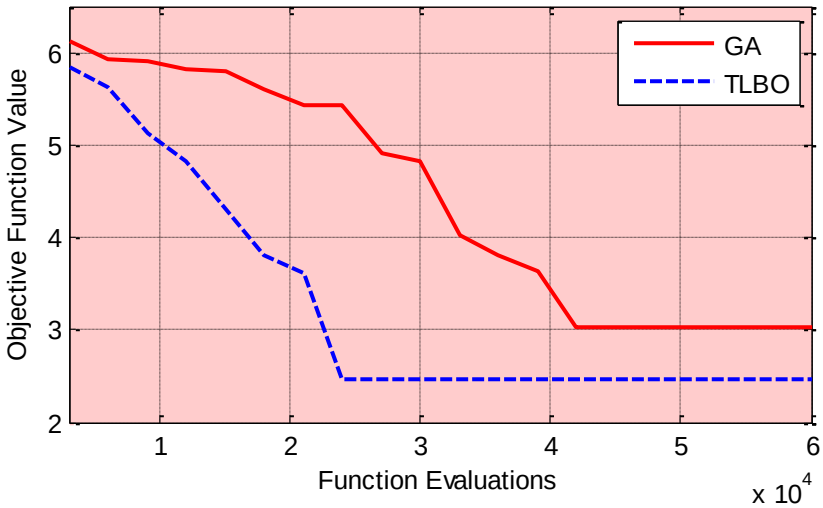

Fig. 4.10 *Convergence plot comparing GA and TLBO values for four-bar mechanism*

four-bar mechanism. Alternatively, here reductions in the shaking force, shaking moment and driving torque are achieved by optimally redistributing the link masses. The reductions of about 65%, 73% and 75% in RMS values of shaking force, shaking moment and driving torque, respectively, are achieved using TLBO with 43% less function evaluations than that of GA as shown in Table 4.5. The parameters of optimally balanced mechanism are obtained from the optimal design variables using equimomental conditions and given in Table 4.7.

Table 4.7 *Parameters of original and optimally balanced four-bar mechanism*

Link i	Length a_i (m)	Original mechanism				Optimally balanced mechanism			
		Mass m_i (kg)	Moment of inertia I_i^c (kg-m^2)	d_i (m)	θ_i (deg)	Mass m_i (kg)	Moment of inertia I_i^c (kg-m^2)	d_i (m)	θ_i (deg)
1	0.1	0.3925	0.0014	0.05	0	0.1608	3.83e-4	0.0307	0
2	0.4	1.5700	0.0841	0.20	0	0.6651	0.0229	0.1326	0
3	0.3	1.1775	0.0356	0.15	0	0.4846	0.0091	0.0933	0
0	0.3	$\sum m$ =3.1400				$\sum m$ =1.3105			

4.5.2 Five-bar Mechanism

The method proposed in this chapter is used to solve the balancing problem of a planar five-bar mechanism, Fig. 4.11, reported by Ilia and Sinatra (2009). The parameters of original mechanism as reported in (Ilia and Sinatra, 2009) are given in Table 4.8 where the input motions of links #1 and #4 are considered as the cycloidal motion and the harmonic motion, respectively.

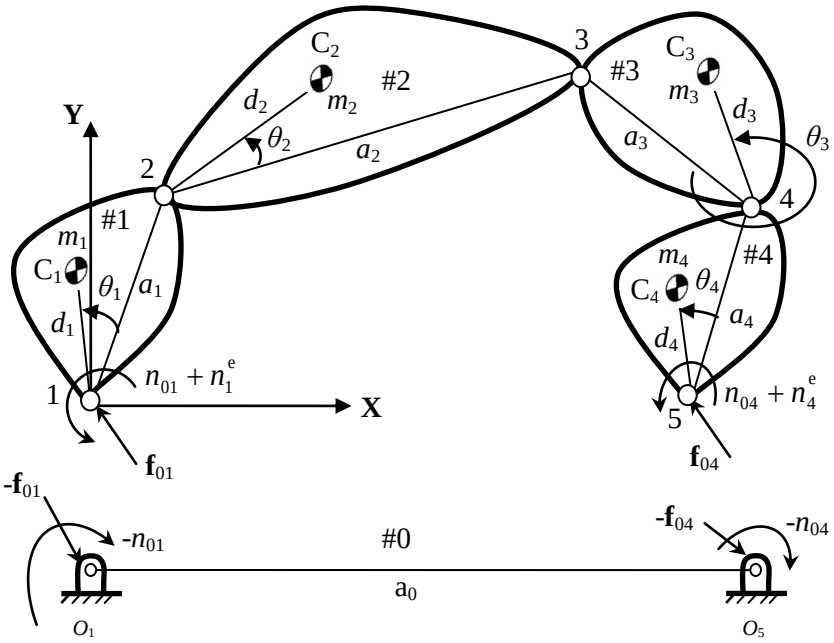

Fig. 4.11 *Planar five-bar mechanism detached from its frame*

Ilia and Sinatra (2009) presented a method for only shaking force balancing of the mechanism using natural orthogonal complement dynamic modeling and is solved by conventional optimization method. It uses non-linear constraint optimization in which the center of mass parameters of moving links are chosen as the design variables. However, the resulting effect on shaking moment and driving torque was not considered. For the same numerical problem, both shaking force and shaking moment are simultaneously minimized here using proposed methodology taking weighting factors, w_1 and w_2, as 0.5.

Table 4.8 *Parameters of original and optimally balanced planar five-bar mechanism*

Link i	Length a_i (m)	Original mechanism				Optimally balanced mechanism			
		Mass m_i (kg)	Moment of inertia I_i^c (kg-m^2)	d_i (m)	θ_i (deg)	Mass m_i (kg)	Moment of inertia I_i^c (kg-m^2)	d_i (m)	θ_i (deg)
1	0.02	0.03	1.00e-6	0.01	0	0.015	2.93e-6	0.0017	180
2	0.10	0.15	1.25e-4	0.05	0	0.052	1.07e-4	0.0146	0
3	0.10	0.15	1.25e-4	0.05	0	0.038	8.72e-5	0.0312	0
4	0.04	0.06	8.00e-6	0.02	0	0.021	8.05e-6	0.0061	0
0	0.04	$\sum m = 3.9000$				$\sum m = 0.1260$			

Note that we consider all moving links in optimization for mass redistribution. Figure 4.12 shows the variations in the shaking force, shaking moment and driving torque over the complete crank cycle. The optimized link parameters are then found by using the equimomental conditions and given in Table 4.8. The comparison of the RMS values of shaking force, shaking moment and driving torque of original mechanism with those of optimally balanced mechanism are provided in Table 4.9.

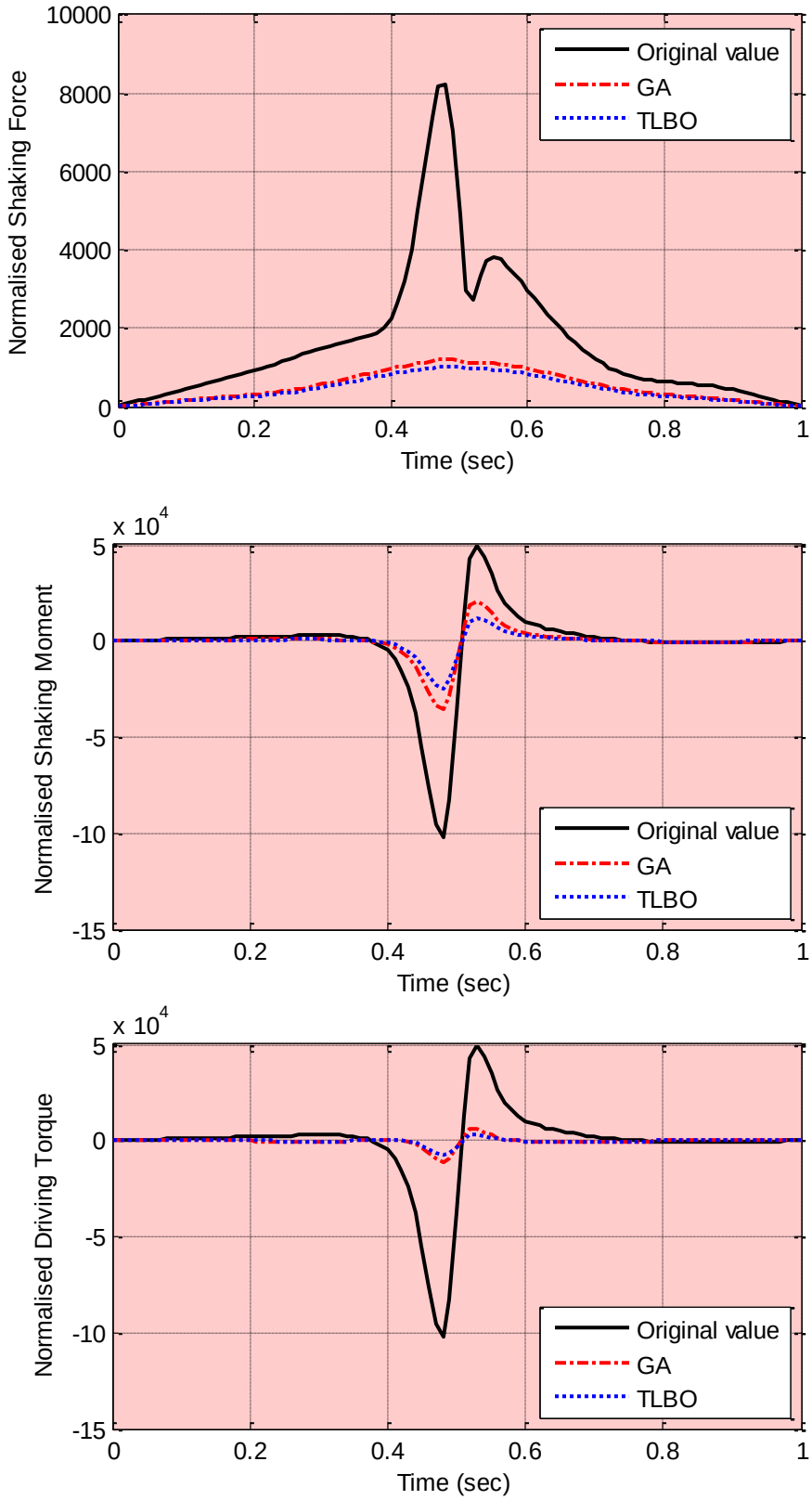

Fig. 4.12 *Variations in the dynamic quantities of original and optimally balanced five-bar mechanism using GA and TLBO for complete cycle of operation*

Table 4.9 *Normalized RMS values of dynamic quantities in the original and optimally balanced five-bar mechanism using GA and TLBO*

	Normalised shaking force	Normalised shaking moment	Normalised driving torque	No. of function evaluations
Original mechanism	2388	21913	6111	
Optimally balanced using GA	641.00 (-73.15%)	7934.00 (-63.79%)	2183.7 (-64.26%)	68000
Optimally balanced using TLBO	549.30 (-77.00%)	5248.10 (-76.05%)	1457.4 (-76.15%)	36000

Figure 4.13 shows Pareto front while Fig. 4.14 presents the convergence plot for the performance comparison of both the optimization techniques. The optimum values of the design variables, i.e., the point-mass parameters are given in Table 4.10. The reduction of about 77%, 76% and 76% in the RMS values of shaking force, shaking moment and driving torque, respectively, are achieved using TLBO with 47% less function evaluations than that of GA.

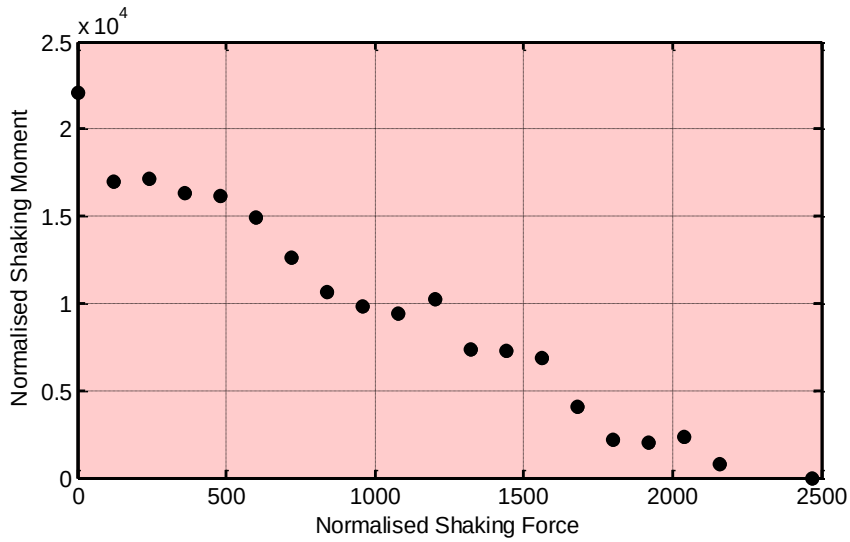

Fig. 4.13 *Pareto front for five-bar mechanism*

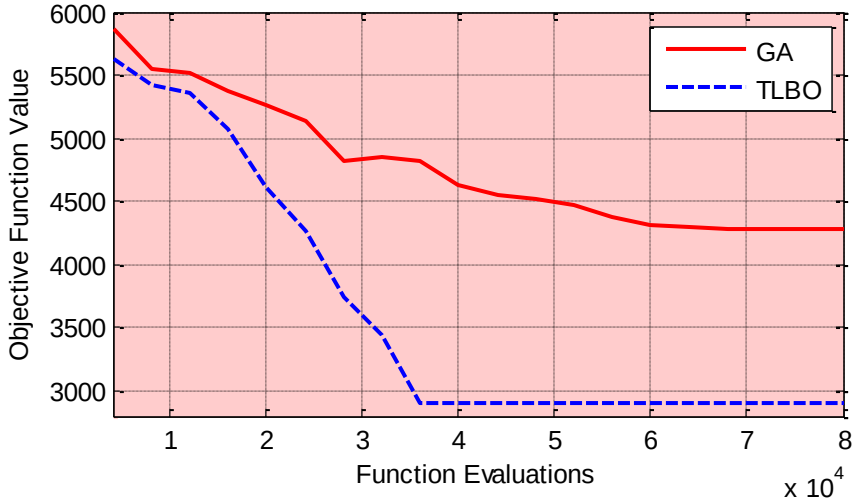

Fig. 4.14 *Convergence plot comparing GA and TLBO values for five-bar mechanism*

Table 4.10 *Normalised optimum equimomental point-mass parameters for balanced five-bar mechanism*

	Link	m_{i1}	m_{i2}	m_{i3}	l_{i1}
Original mechanism	1	0.9107	0.0447	0.0447	0.5774
	2	4.5534	0.2233	0.2233	2.8868
	3	4.5534	0.2233	0.2233	2.8868
	4	1.8214	0.0893	0.0893	1.1547
Optimally balanced using GA	1	0.1669	0.1639	0.1639	0.6822
	2	0.8698	0.8368	0.8368	3.2733
	3	0.8243	0.7988	0.7988	3.3033
	4	0.2730	0.2695	0.2695	1.3657
Optimally balanced using TLBO	1	0.1430	0.1405	0.1405	0.5848
	2	0.7456	0.7172	0.7172	2.8057
	3	0.7066	0.6847	0.6847	2.8314
	4	0.2340	0.2310	0.2310	1.1706

4.5.3 Stephenson Six-bar Mechanism

The analytical conditions are presented by Berkof and Lowen (1969) for only shaking force balancing of planar six-bar mechanism in which counterweight methodology is used. In another method (Verschuure et al., 2007), a convex optimization technique is used in determining the optimal shape, position and mass of the counterweights.The method proposed in this chapter is used to solve the balancing problem of a planar Stephenson six-bar mechanism as reported by Verschuure et al.(2007) shown in Fig.

4.3 for which parameters of original mechanism are given in Table 4.11. For the constant angular velocity of 2π rad/sec for link #3, both the shaking force and the shaking moment are minimized by redistributing the link masses as against the addition of counterweights as suggested in (Berkof and Lowen, 1969; Verschuure et al., 2007).

Table 4.11 *Parameters of original and optimally balanced planar Stephenson six-bar mechanism*

Link i	Length a_i (m)	Original mechanism				Optimally balanced mechanism			
		Mass m_i (kg)	Moment of inertia I_i^c (kg-m^2)	d_i (m)	θ_i (deg)	Mass m_i (kg)	Moment of inertia I_i^c (kg-m^2)	d_i (m)	θ_i (deg)
1	0.0559	0.060	4.98e-5	0.0286	3	0.031	3.72e-5	0.0249	0
2	0.1206	0.082	3.27e-4	0.0630	0	0.060	2.00e-4	0.0409	0
3	0.0032	0.075	7.27e-7	0.0031	5	0.019	2.27e-6	0.0057	180
4	0.1397	0.173	1.21e-3	0.0836	19	0.058	2.88e-4	0.0566	0
5	0.0444	0.039	1.53e-5	0.0197	0	0.018	8.12e-6	0.0566	0
0	0.1238	$\sum m = 0.4290$				$\sum m = 0.1860$			

The variations in the shaking force, shaking moment and driving torque over the complete crank cycle are shown in Fig. 4.15 whereas Fig. 4.16 shows Pareto front. The optimized link parameters for the balanced mechanism are given in Table 4.11 while Table 4.12 presents original and optimized values of shaking force, shaking moment and driving torque. The reduction of about 70%, 73% and 58% were found in the RMS values of shaking force, shaking moment and driving torque, respectively using TLBO with 31% less function evaluations than that of GA (Fig. 4.17).

Table 4.12 *Normalized RMS values of dynamic quantities in the original and optimally balanced Stephenson six-bar mechanism using GA and TLBO*

	Normalised shaking force	Normalised shaking moment	Normalised driving torque	No. of function evaluations
Original mechanism	14.8371	11.3617	0.3295	
Optimally balanced using GA	5.3241 (-64.12%)	4.2023 (-63.01%)	0.1705 (-48.25%)	78000
Optimally balanced using TLBO	4.5064 (-69.63%)	3.0534 (-73.12%)	0.1394 (-57.69%)	54000

The optimum values of the design variables, i.e., the point-mass parameters are given in Table 4.13.

Table 4.13 *Normalised optimum equimomental point-mass parameters for balanced Stephenson six-bar mechanism*

	Link	m_{i1}	m_{i2}	m_{i3}	l_{i1}
Original mechanism	1	0.8039	0.1194	0.0767	0.7238
	2	1.0907	0.1331	0.1331	1.5969
	3	1.2034	0.0806	-0.0389	0.0581
	4	2.2220	0.6928	-0.0661	2.1104
	5	0.5230	0.0633	0.0633	0.4981
Optimally balanced using GA	1	0.5541	0.0797	0.0469	0.7963
	2	1.0403	0.1245	0.1245	1.3394
	3	-0.0057	0.1963	0.2178	0.2535
	4	1.0530	0.2886	-0.0907	1.6318
	5	0.3059	0.0395	0.0395	0.4940
Optimally balanced using TLBO	1	0.4688	0.0649	0.0397	0.6738
	2	0.8802	0.1054	0.1054	1.1333
	3	-0.0048	0.1661	0.1843	0.2145
	4	0.8910	0.2442	-0.0768	1.3807
	5	0.2588	0.0334	0.0334	0.4180

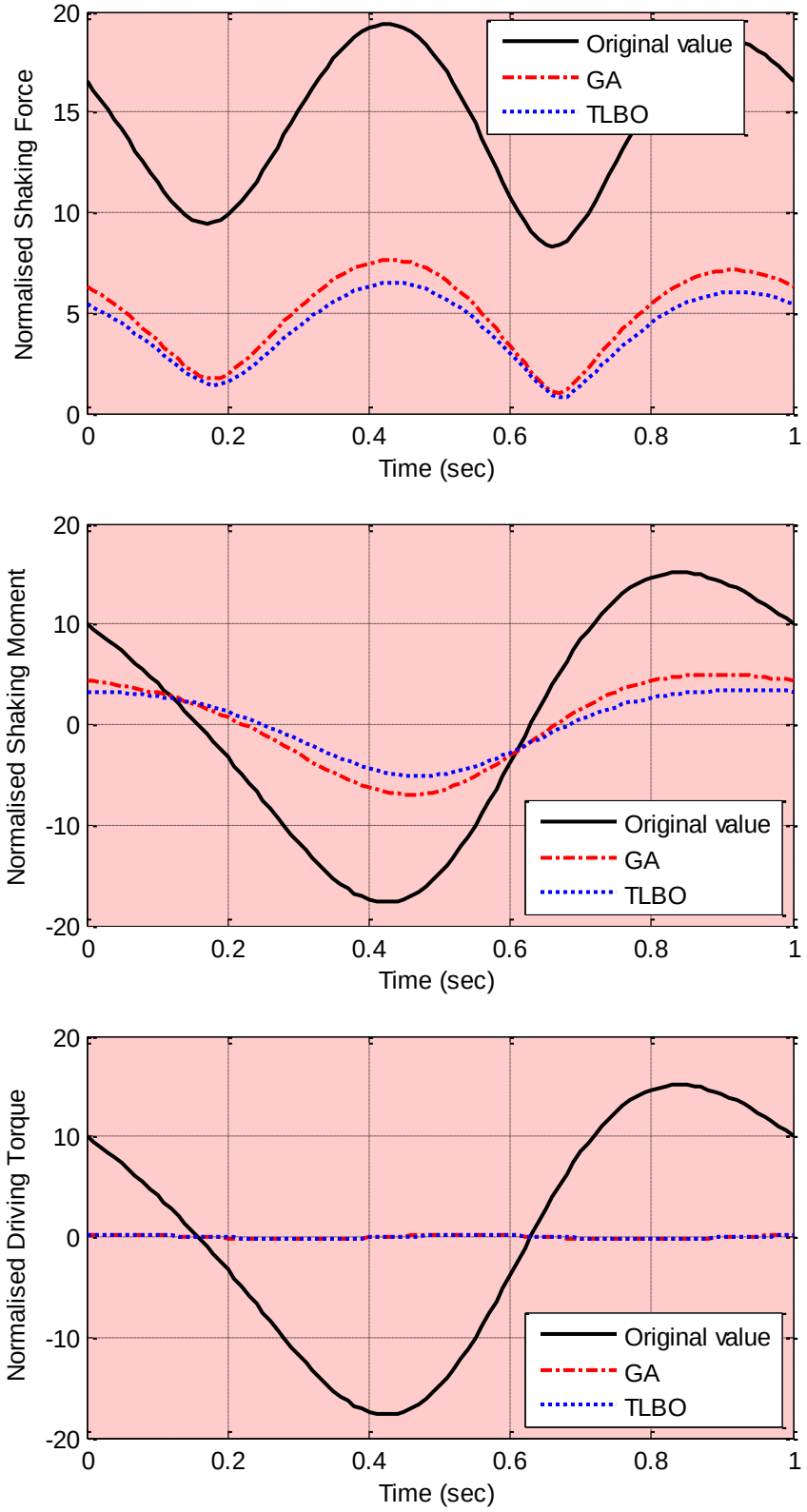

Fig. 4.15 *Variations in the dynamic quantities of original and optimally balanced Stephenson six-bar mechanism using GA and TLBO for complete cycle of operation*

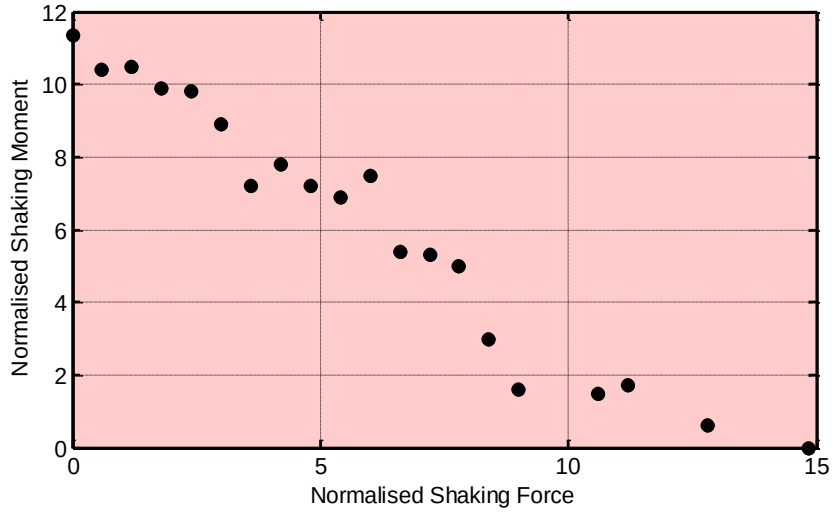

Fig. 4.16 *Pareto front for Stephenson six-bar mechanism*

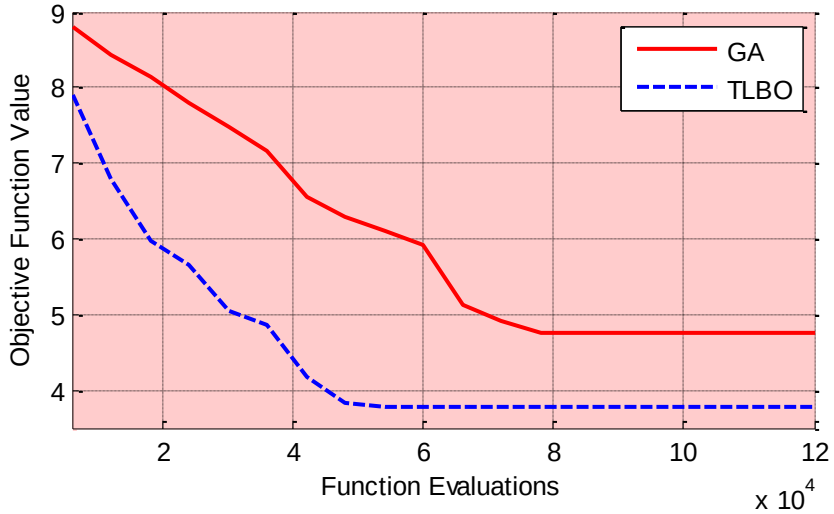

Fig. 4.17 *Convergence of objective function in GA and TLBO for Stephenson six-bar mechanism*

4.5.4 Slider-crank Mechanism

A slider-crank mechanism consists of crankshaft, connecting rod and piston. It is the fundamental mechanism in vehicle engines, compressors and piston pumps. The slider-crank mechanism needs to be dynamically balanced to reduce vibrations and noise in the engine and to improve the vehicle performance. For an unbalanced mechanism, the shaking force and shaking moment are transmitted to the frame which

worsen the dynamic performance of vehicle engine and generate vibrations, wear and noise. It leads to expensive repairs and replacement of crankshaft and connecting rod and their reverse effects on the other parts such as cylinder block and piston.

Figure 4.18 shows a planar slider-crank mechanism where the fixed link is detached from the moving links to show the reactions. The slider moves parallel to x-axis and O_4 is the projection of piston center of mass on the frame. The parameters for original (Arakelian and Briot, 2010) and optimally balanced mechanism are given in Table 4.14.

Table 4.14 *Original and optimum parameters of statically and dynamically balanced planar slider-crank mechanism*

	Link i	Length a_i (m)	Mass m_i (kg)	Moment of inertia I_i^c (kg-m^2)	d_i (m)	θ_i (deg)
Original mechanism	1	0.292	2	0.03	0.1460	0
	2	0.427	3	0.14	0.2135	0
			$\sum m = 5$			
Force balance mechanism	1	0.292	64.2219	3.2176	0.1398	180
	2	0.427	26.7551	1.1119	0.0638	180
			$\sum m = 90.9770$			
Force and moment balance mechanism [TLBO] result	1	0.292	4.2481	0.0700	0.0030	180
	2	0.427	1.7470	0.0990	0.1834	0
			$\sum m = 5.9951$			

The results for full force balance are compared with the analytical full force balancing conditions (Bagci, 1995) which are as follow:

$$m_1 d_1 = a_1(m_2 + m_3)\,;\, m_3 a_2 = m_2 d_2\,;\, \theta_1 = \pi \text{ and } \theta_2 = \pi \tag{4.48}$$

where all the parameters are defined in Fig. 4.18.

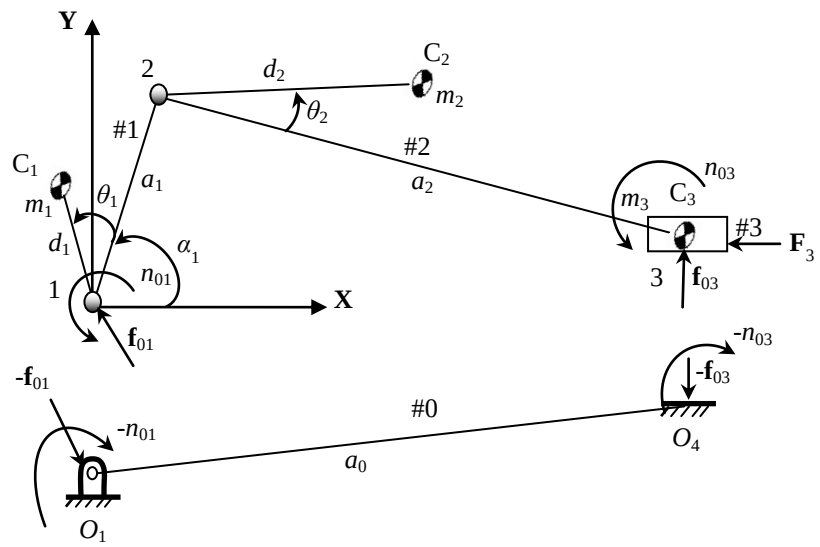

Fig. 4.18 *Planar slider-crank mechanism detached from its frame*

These conditions are satisfied for the complete force balanced mechanism achieved using the optimization method proposed in this chapter. For the optimized mechanism, the shaking force is eliminated while the RMS value of shaking moment is increased by about 563% and driving torque value remains almost same as shown in Table 4.15. This confirms the results found in investigations carried out by Lowen et al. (1974) which shows that the shaking moment is increased for a force balanced mechanism. The variations in the shaking force, shaking moment and driving torque for complete cycle in original and optimally force balanced mechanism are shown in Fig. 4.19 while the parameters of the balanced mechanism are given in Table 4.14. Note that the total mass of mechanism increases excessively from 5 kg to 90.98 kg for the force balanced mechanism.

Simultaneous minimization of the shaking force and shaking moment for slider crank mechanism is now achieved using the proposed optimization methodology. The variations in shaking force, shaking moment and driving torque over the complete crank cycle are shown in Fig. 4.20.

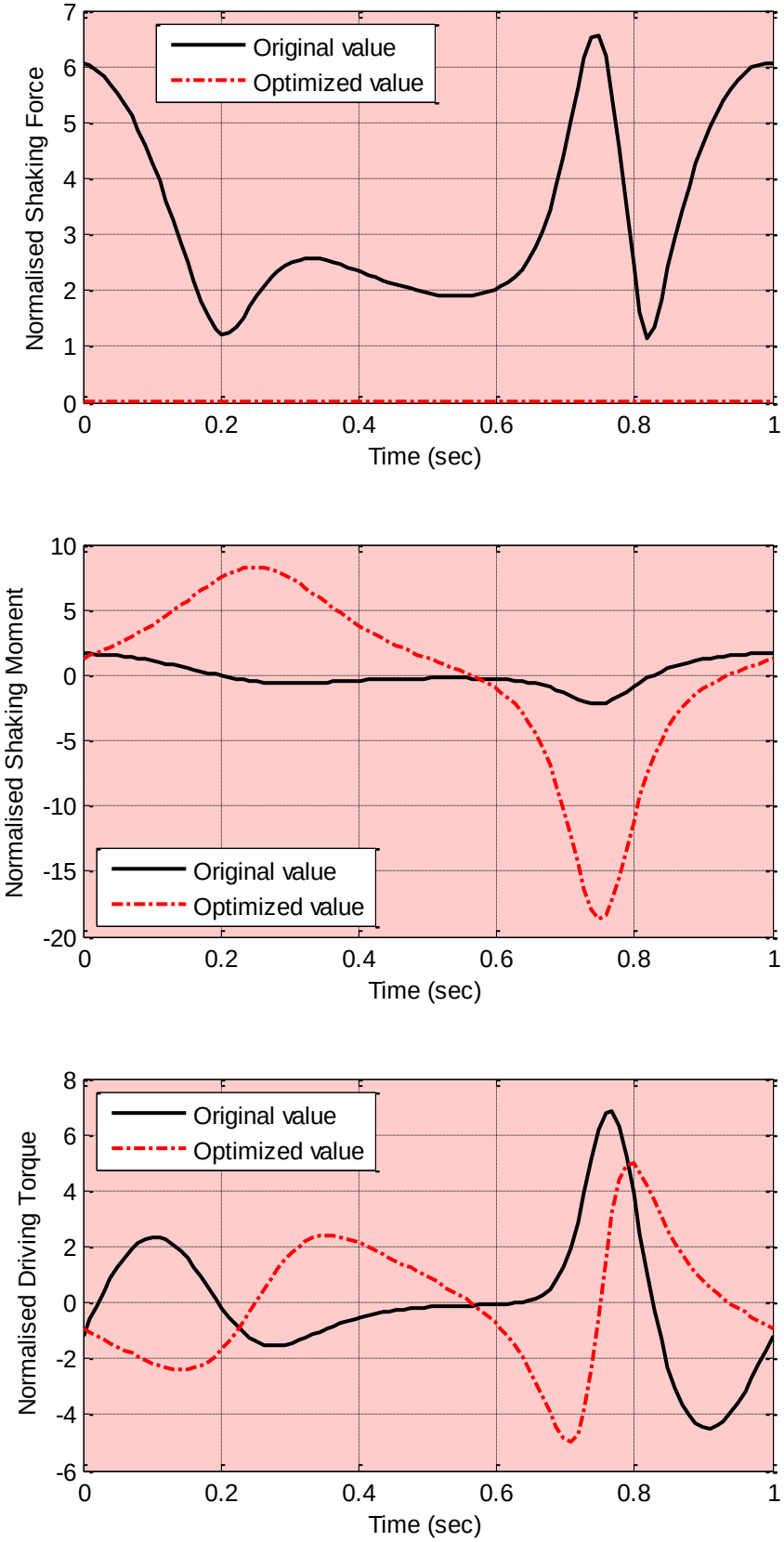

Fig. 4.19 *Variations in the dynamic quantities of original and optimally force balanced slider-crank mechanism for complete cycle of operation*

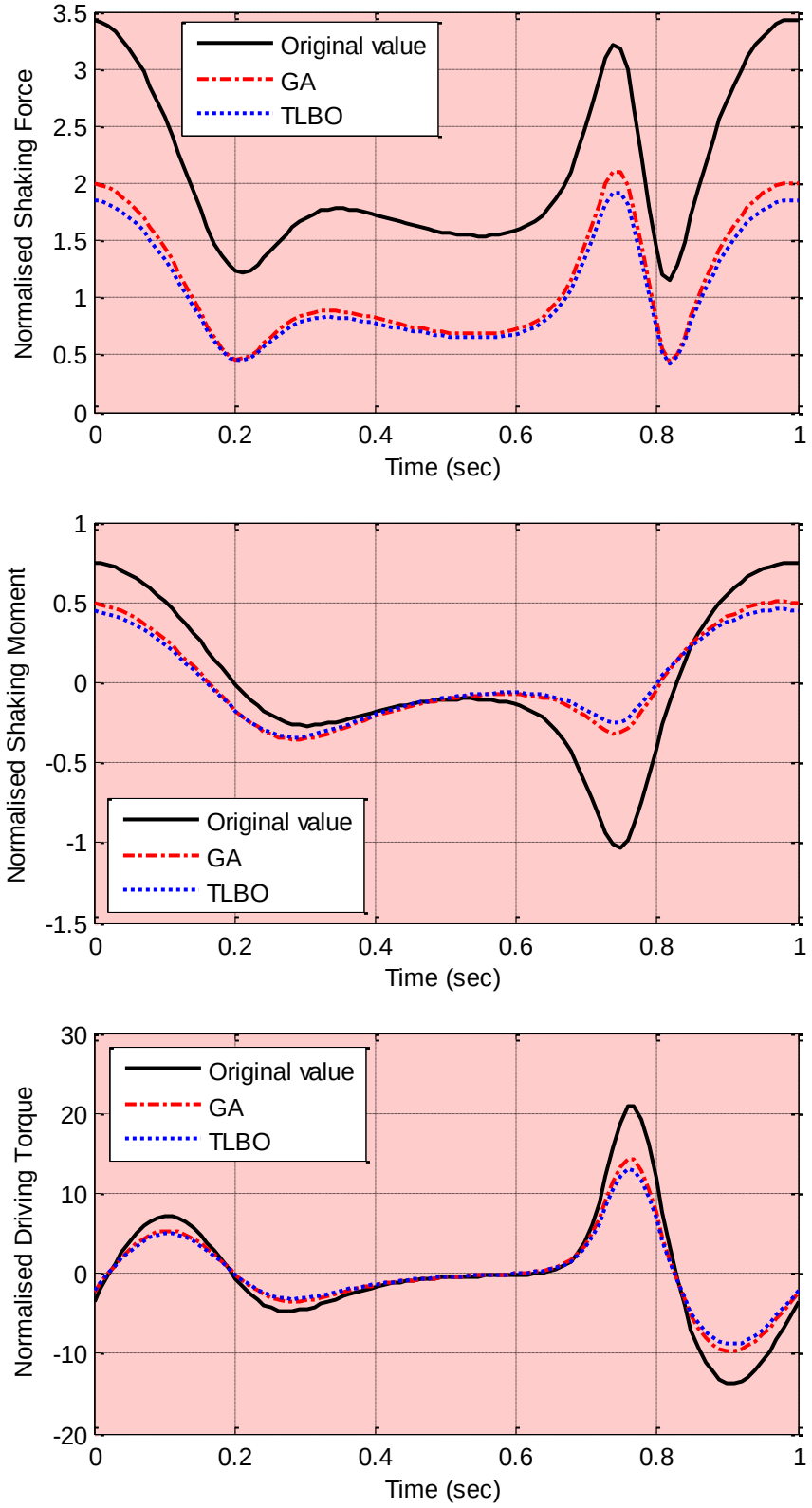

Fig. 4.20 *Variations in the dynamic quantities of original and optimally balanced slider-crank mechanism using GA and TLBO for complete cycle of operation*

The comparison of original RMS values with those of optimum values are provided in Table 4.15 while Table 4.14 gives parameters for the balanced mechanism. Note that the total mass of optimally force and moment balanced mechanism is increased but not as in forced balanced mechanism.

Table 4.15 *Normalized dynamic quantities for planar slider-crank mechanism*

	Normalised shaking force	Normalised shaking moment	Normalised driving torque	No. of function evaluations
Original mechanism	2.2188	0.4597	7.1762	
Force balanced mechanism	0.0035 (-99.84%)	3.0511 (+563.71%)	7.6118 (+06.07%)	
Optimally balanced mechanism using GA	1.2314 (-44.49%)	0.2820 (-38.66%)	5.0746 (-29.28%)	60160
Optimally balanced mechanism using TLBO	1.1438 (-48.45%)	0.2568 (-44.14%)	4.6298 (-35.48%)	32000

Pareto front for this problem is shown in Fig. 4.21. The reduction of about 48%, 44% and 35% in the RMS values of shaking force, shaking moment and driving torque, respectively, are achieved using TLBO with 47% less function evaluations than that of GA (Fig. 4.22). The optimum values of the design variables, i.e., the point-mass parameters are given in Table 4.16. Note here that the reductions in the shaking force and shaking moment are achieved numerically by redistributing masses optimally instead of adding cam mechanisms and counterweights.

Table 4.16 *Optimum equimomental point-mass parameters for balanced slider-crank mechanism*

	Link	m_{i1}	m_{i2}	m_{i3}	l_{i1}
Original mechanism	1	1.6884	0.1558	0.1588	0.1905
	2	2.4060	0.2970	0.2970	0.3037
Optimally balanced using GA	1	1.2011	1.2905	1.2905	0.1143
	2	1.3176	0.1188	0.1188	0.2119
Optimally balanced using TLBO	1	1.3491	1.4495	1.4495	0.1284
	2	1.4800	0.1335	0.1335	0.2380

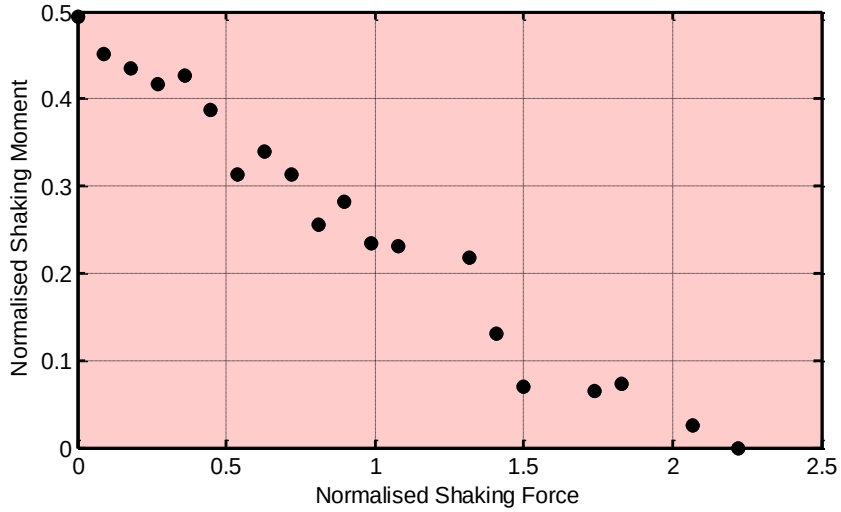

Fig. 4.21 *Pareto front for slider-crank mechanism*

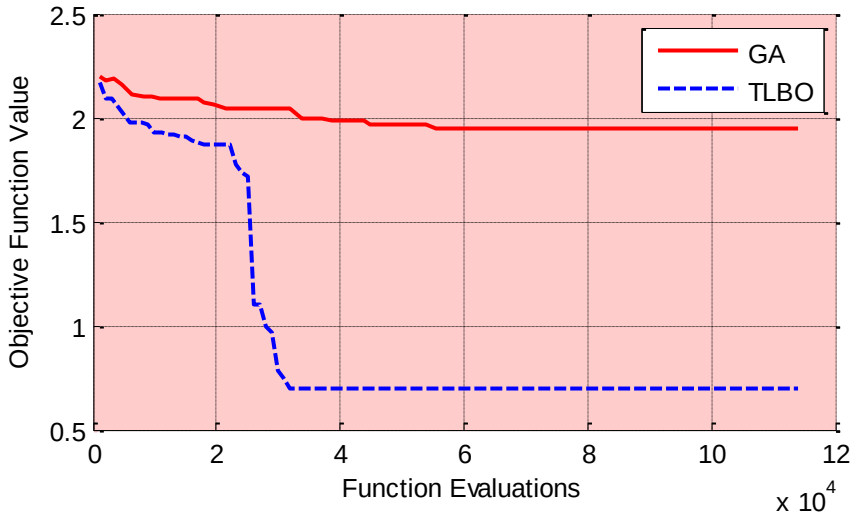

Fig. 4.22 *Convergence of objective function in GA and TLBO for slider-crank mechanism*

The method earlier used to simultaneously reduce the shaking force and shaking moment for the problem considered suggests use of additional members like cam mechanism and counterweight (Arakelian and Briot, 2010). Hence, the optimal dynamic balancing is achieved numerically by redistribution of link masses.

4.6 Multi-cylinder Engine

Multi-cylinder machines such as engines and compressors use multiple slider-crank mechanisms connected to a common crankshaft. The harmonic balancing is recommended for these machines by properly selecting the relative position of the

mechanism planes and the relative orientation of the crank angles (Dresig and Holzweibig, 2010). The complete balancing of shaking force and shaking moment in engines can also be achieved using force and moment balancers (Bagci, 1995). For balancing of shaking force and shaking moment in a four-cylinder inline engine, the crank throws are arranged at 0°,180°,180°,0° on the crankshaft (Fig. 4.23). This arrangement is considered to be the best approach to achieve the primary balance in a multi-cylinder engine.

To balance the secondary forces and moments, two counterrotating balance shafts at twice crankshaft speed with chains and/or gears known as *Lanchester balancer* are used (Garrett et al., 2001; Norton, 2011; Chiou and Davies, 1994; Arakelian and Makhsudyan, 2010). Figure 4.24 shows reaction forces in main bearings in a four-cylinder inline engine having same slider-crank mechanism in each cylinder with arrangement shown in Fig. 4.23. As shown in Fig. 4.24, reaction forces in bearings A, C and E are not vanishing while in bearings B and D, they will vanish. $\mathbf{f}_{01}^{i}$ is the reaction force of the frame on the crank of the slider-crank mechanism of the *i*th cylinder for *i*=1,…,4.

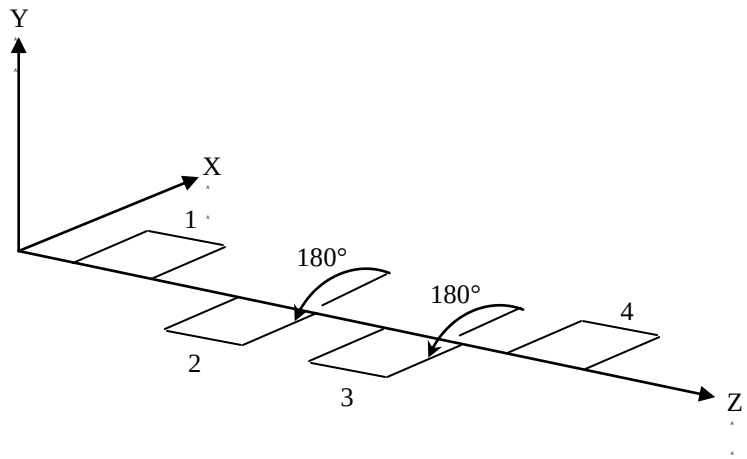

Fig. 4.23 *Crank orientations in four-cylinder inline engine*

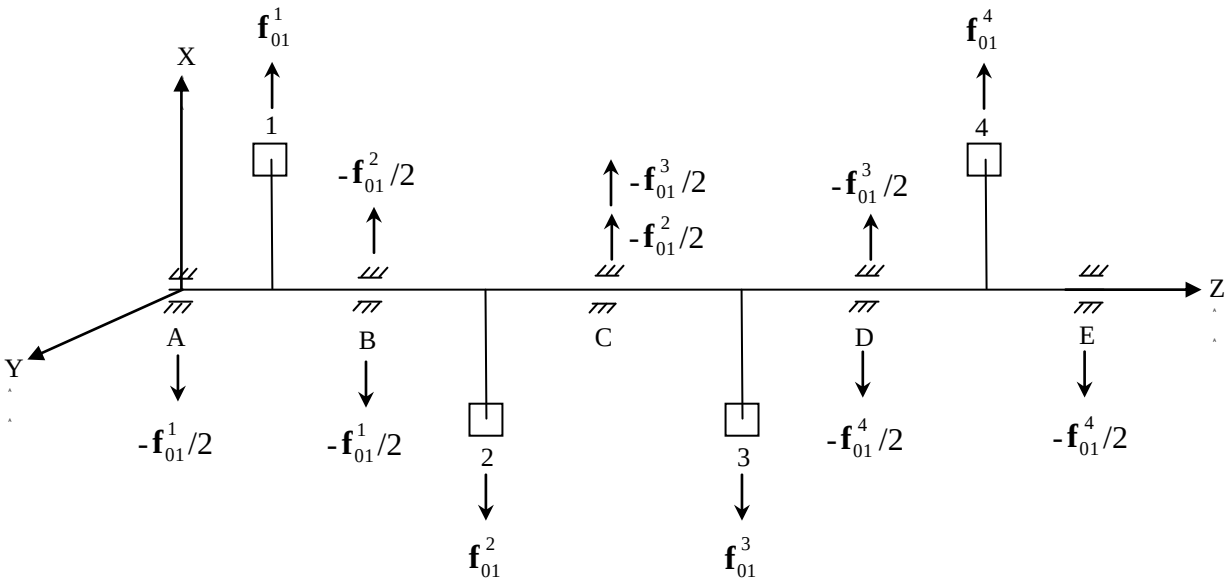

Fig. 4.24 *Bearing forces in four-cylinder inline engine*

Thus, the bearing forces for this arrangement of four-cylinder inline engine are defined as:

$$\mathbf{F}_A = -\mathbf{f}_{01}^1/2;\ \mathbf{F}_B = 0;\ \mathbf{F}_C = -(\mathbf{f}_{01}^2/2 + \mathbf{f}_{01}^3/2);\ \mathbf{F}_D = 0;\ \mathbf{F}_E = -\mathbf{f}_{01}^4/2 \qquad (4.49)$$

The bearing forces can be reduced when optimally balanced slider-crank mechanisms are used in four-cylinder inline engine while the addition of counterweights are suggested in traditional approach (Hoag, 2006) for the same. The RMS and peak values of forces on bearings A, C and E (Fig. 4.24) are calculated using Eq. (4.44) and reduced by about 44% and 71%, respectively, for the optimum mechanism found in previous section. The variation of the bearing force for the complete cycle for heavily loaded bearing C is shown in Fig. 4.25. The original and optimized RMS and peak values of the bearing forces are compared in Table 4.17.

Table 4.17 *Normalized bearing forces in four-cylinder inline engine*

	F_A and F_E		F_C	
	RMS value	Peak value	RMS value	Peak value
Original mechanism	1.5560	8.6715	3.1120	17.3430
Optimized mechanism	0.8663 (-44.32%)	2.4845 (-71.35%)	1.7326 (-44.32%)	4.9690 (-71.35%)

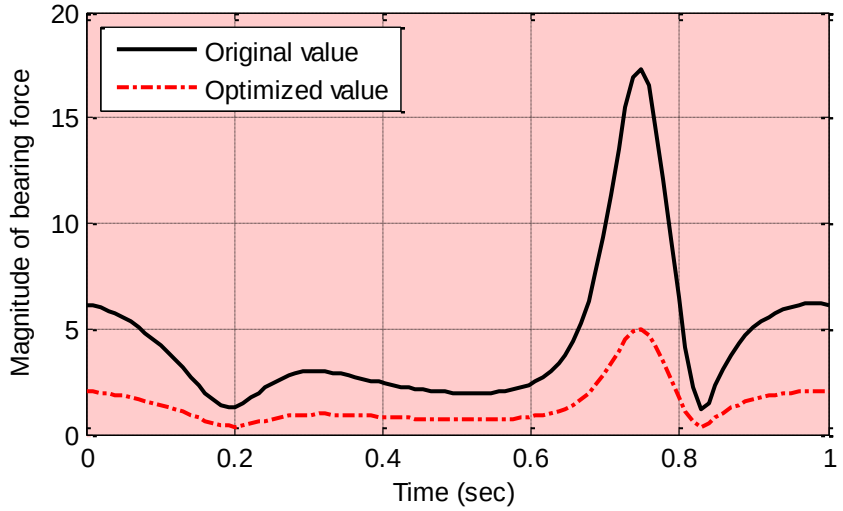

Fig. 4.25 *Force on bearing C in four-cylinder inline engine*

4.7 Summary

The shaking force and shaking moment developed due to inertia forces in the planar mechanisms are minimized by finding the optimal mass distribution of the moving links of the mechanisms. The inertial properties of the mechanism links are represented by the parameters of the equimomental point-mass system to achieve mass distribution. The point-mass parameters are taken as the design variables in the formulation of the optimization problem to minimize the shaking force and shaking moment. The RMS values of normalised shaking force and shaking moment in planar four-bar, five-bar, six-bar and slider-crank mechanism are reduced significantly by (65%, 73%), (77%, 76%), (70%, 73%) and (48%, 44%), respectively. The proposed optimization method also demonstrates GA and TLBO as solvers in mechanism balancing. It is found that TLBO is more computationally efficient and effective for mechanism balancing than that of GA.

Chapter 5

Optimal Link Shape Synthesis

In this chapter, the link shapes are synthesized for optimally balanced mechanism for the given motion. The link shapes satisfying kinematic and dynamic requirements are very crucial for the design of a mechanism and its performance. The shape synthesis using parametric curves like Hermite, Bezier and B-spline curves leads to computer-aided design (CAD) and manufacturing of the mechanism links. Through CAD modeling of the links using these curves; the design, production and functional details can be easily transmitted between engineering and manufacturing operations. The CAD modeling of the links is also useful in analyzing the static and dynamic response of the designed mechanism. The real-time behavior of the mechanism is evaluated through computer simulation and thus it eliminates the need of the experimental tests for the actual mechanism. Therefore, the cost and time are saved to a great extent and any possible error is realized before manufacturing of the mechanism links.

The optimization problem formulation for link shape synthesis for the optimally balanced simple and multiloop planar mechanisms is presented in this chapter. The closed parametric curve is used to represent the link shape and its geometric and inertial properties are calculated using well known Green's theorem. The proposed optimization problem includes the equality constraints to keep the resulting inertial properties same as the inertial properties of the optimally balanced mechanisms obtained in the chapter 4.

5.1 Link Shape

The link shape is represented by the parametric curve, i.e., closed cubic B-spline curve as shown in Fig. 5.1. If the curve interpolates or approximates a set of n+1 control points,

$P_0, P_1, \ldots, P_n$ (Zeid and Sivasubramanian, 2009; Mortenson, 2006) then the position of any point on the curve is defined as:

$$\mathbf{P}(u) = \sum_{i=0}^{n} \mathbf{P}_i N_{i,k}(u), \quad 0 \le u \le u_{\max} \tag{5.1}$$

For a curve of degree (k-1), the B-spline function $N_{i,k}(u)$ is computed iteratively as:

$$N_{i,k}(u) = (u - u_i)\frac{N_{i,k-1}(u)}{u_{i+k-1} - u_i} + (u_{i+k} - u)\frac{N_{i+1,k-1}(u)}{u_{i+k} - u_{i+1}} \tag{5.2}$$

where

$$N_{i,1} = \begin{cases} 1, & u_i \le u \le u_{i+1} \\ 0, & \text{otherwise} \end{cases} \tag{5.3}$$

In Eq. (5.3), $N_{i,1}$ is a unit step function and u_i are known as parametric knots or knot values. These values form a sequence of nondecreasing integers called the knot vector. The parametric equation of ith curve segment of a cubic B-spline curve having control points P_{i-1}, P_i, P_{i+1} and P_{i+2} for $u \in [u_{i-1}, u_i]$ is given as:

$$P_i(u) = \frac{\alpha_1 P_{i-1} + \alpha_2 P_i + \alpha_3 P_{i+1} + \alpha_4 P_{i+2}}{6} \tag{5.4}$$

where

$$\alpha_1 = -u^3 + 3u^2 i - 3ui^2 + i^3 \tag{5.5}$$

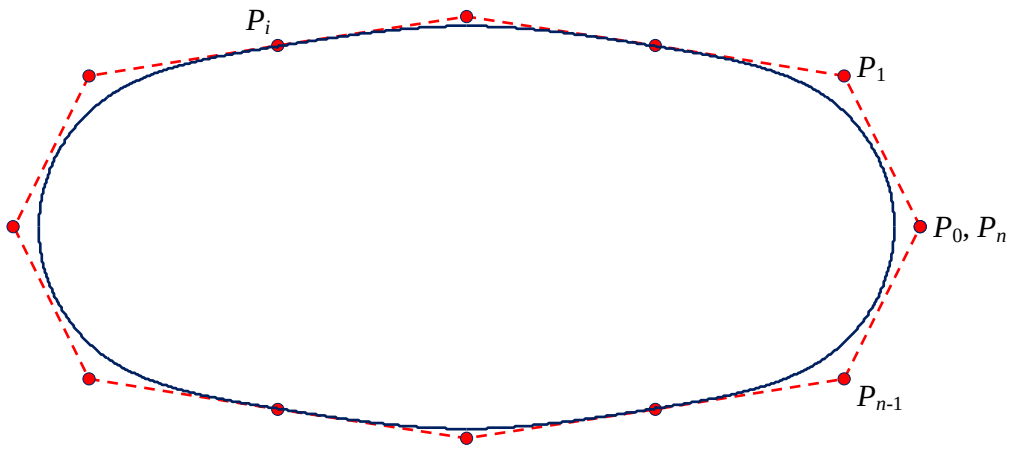

Fig. 5.1 *Closed cubic B-spline curve and its control points*

$$\alpha_2 = 3u^3 + u^2(3-9i) + u(-3+9i^2-6i) - 3i^3 + 3i^2 + 3i + 1 \tag{5.6}$$

$$\alpha_3 = -3u^3 + u^2(-6+9i) + u(-9i^2+12i) + 3i^3 - 6i^2 + 4 \tag{5.7}$$

$$\alpha_4 = u^3 + u^2(3-3i) + u(3+3i^2-6i) - i^3 + 3i^2 - 3i + 4 \tag{5.8}$$

The control points form the vertices of the characteristic polygon of the B-spline curve as shown in Fig. 5.1. Note that the cubic B-spline curve is a composite sequence of curve segments connected with C^2 continuity which blends two curve segments with same curvature. The coordinates of any point on the *i*th segment of the curve are given by Eq. (5.4) as:

$$x_i(u) = \frac{\alpha_1 x_{i-1} + \alpha_2 x_i + \alpha_3 x_{i+1} + \alpha_4 x_{i+2}}{6} \tag{5.9}$$

$$y_i(u) = \frac{\alpha_1 y_{i-1} + \alpha_2 y_i + \alpha_3 y_{i+1} + \alpha_4 y_{i+2}}{6} \tag{5.10}$$

where the terms α_1, α_2, α_3 and α_4 are defined in Eqs. (5.5) – (5.8), and (x_{i-1}, y_{i-1}), (x_i, y_i), etc. are the coordinates of points P_{i-1}, P_i, etc. respectively. The mass and inertia of the link that is synthesized using closed cubic B-spline curve can be calculated using

Green's theorem (Crisco et al., 1998; Brlek et al., 2005). For two functions $P(x, y)$ and $Q(x, y)$ over a closed region D in the plane with boundary ∂D, Green's theorem presents:

$$\iint_D \left(\frac{\partial Q}{\partial x} - \frac{\partial P}{\partial y} \right) dxdy = \oint_{\partial D} \left(Pdx + Qdy \right) \tag{5.11}$$

The area of closed region D is calculated as:

$$A = \iint_D dxdy \tag{5.12}$$

This area is calculated using Green's theorem by taking $P(x,y) = 0$ and $Q(x,y) = x$ that gives:

$$A = \iint_D \left(\frac{\partial Q}{\partial x} - \frac{\partial P}{\partial y} \right) dxdy \tag{5.13}$$

$$A = \oint_{\partial D} xdy \tag{5.14}$$

For a plane curve specified parametrically as $(x(u), y(u))$ for $u \in [u_0, u_1]$, Eq. (5.14) becomes:

$$A = \int_{u_0}^{u_1} xy' du \tag{5.15}$$

Similarly, the moment about x-axis and y-axis of plane are computed as:

using $P = -y^2/2$ and $Q = 0$

$$M_x = \iint ydxdy = -\frac{1}{2} \oint y^2 dx = -\frac{1}{2} \int_{u_0}^{u_1} y^2 x' du \tag{5.16}$$

using $P = 0$ and $Q = x^2/2$

$$M_y = \iint x dx dy = \frac{1}{2}\oint x^2 dy = \frac{1}{2}\int_{u_0}^{u_1} x^2 y' du \tag{5.17}$$

The geometric centroid $(\bar{x}, \bar{y})$ of plane curve is given by $\bar{x} = M_y/A$ and $\bar{y} = M_x/A$. Finally, the area moments of inertia can be computed as:

using $P = -y^3/3$ and $Q = 0$

$$I_{xx} = \iint y^2 dx dy = -\frac{1}{3}\oint y^3 dx = -\frac{1}{3}\int_{u_0}^{u_1} y^3 x' du \tag{5.18}$$

using $P = 0$ and $Q = x^3/3$

$$I_{yy} = \iint x^2 dx dy = \frac{1}{3}\oint x^3 dy = \frac{1}{3}\int_{u_0}^{u_1} x^3 y' du \tag{5.19}$$

Hence, the area A, centroid $(\bar{x}, \bar{y})$ and area moment of inertia about centroidal axes $[I_{xx}, I_{yy}, I_{zz}]$ of the closed curve made of n cubic B-spline segments are calculated as:

$$A = \sum_{i=1}^{n} \int_{u_{i-1}}^{u_i} x_i(u) y_i'(u)\, du \tag{5.20}$$

$$\bar{x} = \frac{1}{2A_i} \sum_{i=1}^{n} \int_{u_{i-1}}^{u_i} x_i^2(u) y_i'(u)\, du \tag{5.21}$$

$$\bar{y} = -\frac{1}{2A_i} \sum_{i=1}^{n} \int_{u_{i-1}}^{u_i} y_i^2(u) x_i'(u)\, du \tag{5.22}$$

$$I_{xx} = -\frac{1}{3} \sum_{i=1}^{n} \int_{u_{i-1}}^{u_i} y_i^3(u) x_i'(u)\, du \tag{5.23}$$

$$I_{yy} = \frac{1}{3} \sum_{i=1}^{n} \int_{u_{i-1}}^{u_i} x_i^3(u) y_i'(u)\, du \tag{5.24}$$

$$I_{zz} = I_{xx} + I_{yy} \tag{5.25}$$

The first derivatives $x_i^{'}(u)$ and $y_i^{'}(u)$ of $x_i(u)$ and $y_i(u)$ with respect to *u*, respectively, in Eqs. (5.20) – (5.24) are given by:

$$x_i^{'}(u) = \frac{\beta_1 x_{i\text{-}1} + \beta_2 x_i + \beta_3 x_{i+1} + \beta_4 x_{i+2}}{6} \tag{5.26}$$

$$y_i^{'}(u) = \frac{\beta_1 y_{i\text{-}1} + \beta_2 y_i + \beta_3 y_{i+1} + \beta_4 y_{i+2}}{6} \tag{5.27}$$

where

$$\beta_1 = \text{-}3u^2 + 6ui \text{ - } 3i^2 \tag{5.28}$$

$$\beta_2 = 9u^2 + 2u(3 \text{ - } 9i) \text{ - } 3 + 9i^2 \text{ - } 6i \tag{5.29}$$

$$\beta_3 = \text{-}9u^2 + 2u(\text{-}6 + 9i) - 9i^2 + 12i \tag{5.30}$$

$$\beta_4 = 3u^2 + 2u(3 - 3i) + 3 + 3i^2 - 6i \tag{5.31}$$

For geometric properties defined in Eqs. (5.20) – (5.25), the mass and mass moment of inertia of a link with shape represented by the closed curve are calculated as:

$$m = At\rho \tag{5.32}$$

$$I = I_{zz}t\rho \tag{5.33}$$

where *t* and ρ represent thickness and material density for the link, respectively.

5.2 Optimization Problem Formulation

In this section, an optimization problem is formulated to find the optimum link shapes corresponding to the inertial parameters of the optimally balanced mechanisms obtained in

the chapter 4. To formulate the optimization problem, the Cartesian coordinates of control points of cubic B-spline curve are taken as design variables as shown in Fig. 5.2.

For a binary link, Fig. 5.2 (a), the link length, a_i, between joint origins O_i to O_{i+1} is divided into equal parts. Hence, the x-coordinates of the control points lying between O_i and O_{i+1} are fixed according to the link length. Now, the y-coordinates are taken as the design variables. Furthermore, the extension of link beyond O_i and O_{i+1} is controlled by points P_0, P_1, P_{n-1} at one end and by points $P_{n/2-1}$, $P_{n/2}$, $P_{n/2+1}$ at other end. Hence, x-coordinate of P_0, y-coordinates of P_1 and P_{n-1} are chosen as the design variables at the right end and same is done at left end. Finally, the design vector is proposed as:

$$\mathbf{x} = [x_0 \; y_1 \ldots y_{n/2-1} \; x_{n/2} \; y_{n/2+1} \ldots y_{n-1}]^{\mathrm{T}} \tag{5.34}$$

The conditions for symmetrical and non-symmetrical shapes are imposed by controlling coordinates of the opposite points as $\mathrm{y}_j = -\mathrm{y}_i$ and $\mathrm{y}_j \neq \mathrm{y}_i$, respectively. In addition to manufacturing benefits, the symmetrical shapes have zero products of inertia.

For a ternary link having joint origins as O_i,O_{i+1} and O_{i+2} shown in Fig. 5.2(b), the link length, a_i, can be defined as summation of the distances between joints, i.e., $a_i = a_{i1} + a_{i2} + a_{i3}$. The number of control points between two joints can be decided according to the distance between them.

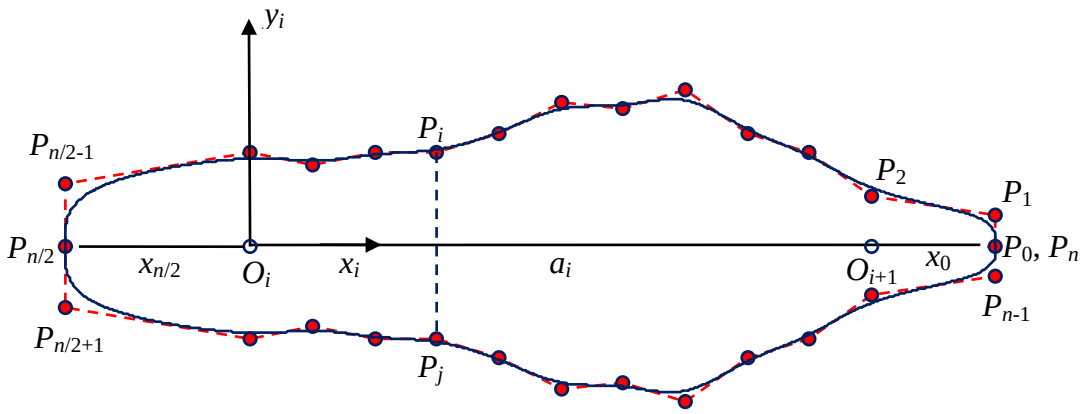

(a) Binary link

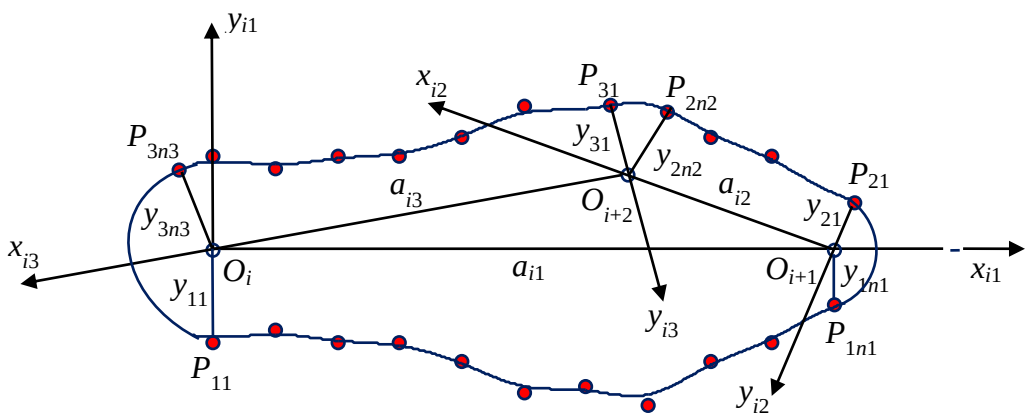

(b) Ternary link

Fig. 5.2 *Closed cubic B-spline curve representing link shape and its control points where P_i and P_j are two opposite points about x-axis*

If n_1, n_2, and n_3 are number of control points for lengths a_{i1}, a_{i2}, and a_{i3}, respectively, then total number of control points is the sum of n_1, n_2, and n_3. At each joint, two points coincide and their y-coordinate can be determined by considering the local coordinate frame in the link as shown in Fig. 5.2 (b). The design vector in this case can be defined as:

$$\mathbf{x} = [y_{11} \dots y_{1n_1}\ y_{21} \dots y_{2n_2}\ y_{31} \dots y_{3n_3}]^{\mathrm{T}} \tag{5.35}$$

Note that for the link having three or more joints, the shapes can be synthesized by selecting *y*-coordinates for each segment of the length between joints. The inertial properties of resulting shapes are constrained by the optimal properties. These constraints ensure that the links with optimum shapes have the same inertial properties as that of the optimally balanced mechanism links. The objective function is formulated to minimize the percentage error in resulting links inertia values as:

$$\text{Minimize Z} = \frac{(I_i^* - I_i)}{I_i^*} \times 100 \tag{5.36}$$

$$\text{Subject to } m_i = m_i^*;\ \bar{x}_i = \bar{x}_i^*;\ \bar{y}_i = \bar{y}_i^* \qquad \text{for } i = 1, 2, \ldots, n \tag{5.37}$$

$\mathrm{y}_j = -\mathrm{y}_i$ (for symmetrical binary link); $\mathrm{y}_j \neq \mathrm{y}_i$ (for non-symmetrical binary link)

here parameters with superscript '*' represent parameters obtained in the chapter 4 for the optimally balanced mechanism and subscript '*i*' is used for *i*th link of mechanism. The teaching-learning-based optimization (TLBO) algorithm is used to solve this optimization problem. It is advantageous to use TLBO as compared to the other evolutionary optimization algorithms, as (1) it doesn't require any algorithm specific parameters to be defined to start the optimization procedure and (2) it converges to the optimum solution faster than other evolutionary optimization algorithms. Also, the initial values of the design variables are not required to start searching the optimum solution and hence no initial shape is required. The thickness of mechanism links is taken as 10 percent of the driving link length and the link material is chosen as the mild steel (density = 7850 kg/m^3) for deciding the density and maximum permissible stress. Furthermore, the thickness of the link is taken uniform normal to the plane of motion and can be different for different link in the mechanism considered. The stress

at the weakest section in each link is calculated for the maximum joint force occurred during the complete cycle of operation. Moreover, the von mises stresses for the peak load is considered to determine minimum cross-section of each link. The inertial properties of links are calculated using Eqs. (5.32) – (5.33) and verified by CAD models developed using Autodesk Inventor software. The flow chart shown in Fig. 5.4 illustrates the two-stage optimization method proposed for the optimum design of the planar mechanisms.

5.3 Planar Mechanisms

In this section, the effectiveness of the proposed optimization method for link shape synthesis is shown by applying it to four optimally balanced planar mechanism obtained in chapter 4. Based on the design variables defined in Fig. 5.2, total 28 design variables, namely, x_0, x_{13}, $y_1 \ldots y_{26}$ are now considered for the optimum link shape synthesis for the planar mechanisms (Fig. 5.3).

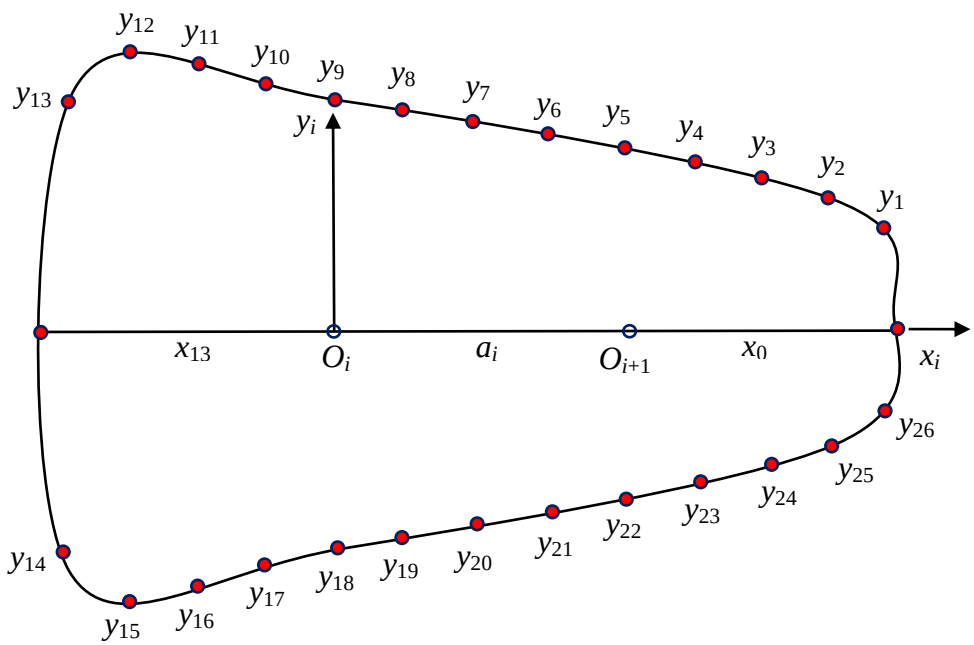

Fig. 5.3 *Design variables to find optimum link shape of planar mechanisms*

Here, a_i represents the link length between joints O_i and O_{i+1}. The design variables x_0 and x_{13} are representing link lengths beyond the joints O_{i+1} and O_i, respectively.

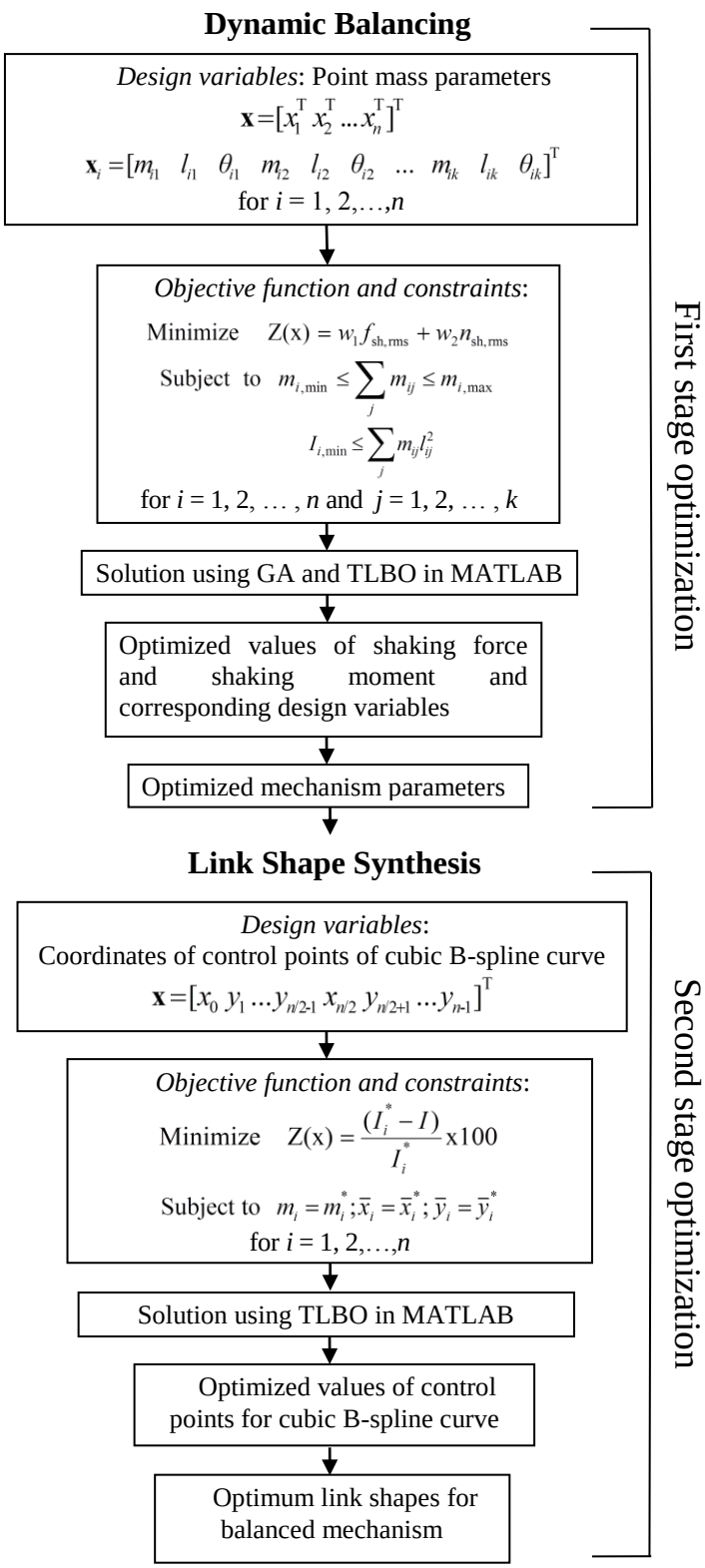

Fig. 5.4 *Two stage optimization scheme to balance mechanism and shape synthesis*

The lengths a_i, x_0 and x_{13} are divided each into equal parts which decide the x-coordinates of control points. So, these x-coordinates are given as follows:

$x_1 = a_i + x_0$; $x_2 = a_i + 0.75x_0$; $x_3 = a_i + 0.50x_0$; $x_4 = a_i + 0.25x_0$; $x_5 = a_i$;

$x_6 = 0.75a_i$; $x_7 = 0.50a_i$; $x_8 = 0.25a_i$; $x_9 = 0$;

$x_{10} = -0.25x_{13}$; $x_{11} = -0.50x_{13}$; $x_{12} = -0.75x_{13}$; $x_{13} = -x_{13}$;

$x_{14} = -x_{13}$; $x_{15} = -0.75x_{13}$; $x_{16} = -0.50x_{13}$; $x_{17} = -0.25x_{13}$;

$x_{18} = 0$; $x_{19} = 0.25a_i$; $x_{20} = 0.50a_i$; $x_{21} = 0.75a_i$;

$x_{22} = a_i$; $x_{23} = a_i + 0.25x_0$; $x_{24} = a_i + 0.50x_0$; $x_{25} = a_i + 0.75x_0$; $x_{26} = a_i + x_0$.

Moreover, the symmetrical link shapes can be obtained by controlling the y-coordinates as:

$$
\begin{array}{llll}
y_{14} = -y_{13} & & y_{21} = -y_6 \\
y_{15} = -y_{12} & & y_{22} = -y_5 \\
y_{16} = -y_{11} & & y_{23} = -y_4 \\
y_{17} = -y_{10} & & y_{24} = -y_3 \\
y_{18} = -y_9 & & y_{25} = -y_2 \\
y_{19} = -y_8 & & y_{26} = -y_1 \\
y_{20} = -y_7 & &
\end{array}
$$

Note that lengths x_0 and x_{13} are variables while a_i is the length of the ith link.

5.3.1 Four-bar Mechanism

The optimization problem of link shape synthesis for a planar four-bar mechanism (Berkof, 1973; Farmani et al., 2011) presented in Eqs. (5.36) – (5.37) is solved and the resulting link shapes are shown in Fig. 5.5.

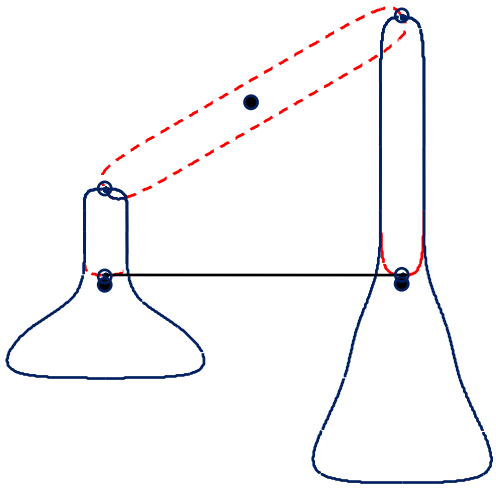

(a) case 1

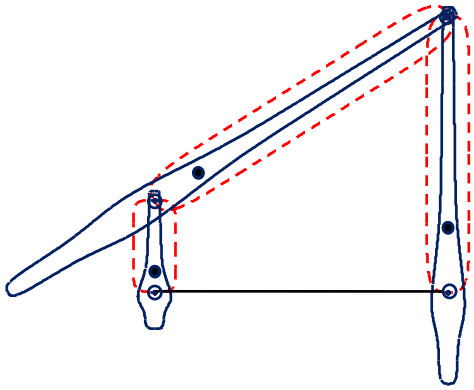

(b) case 2

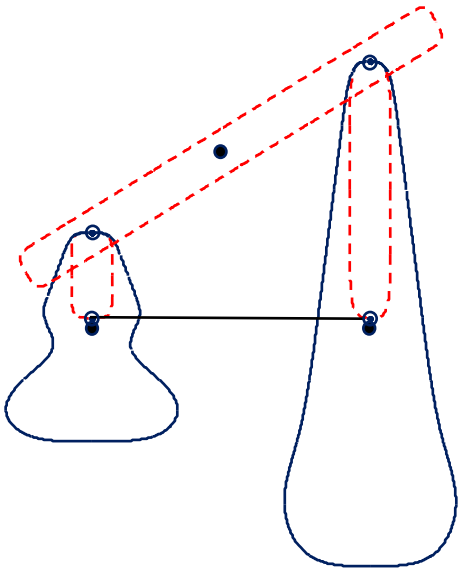

(c) case 3

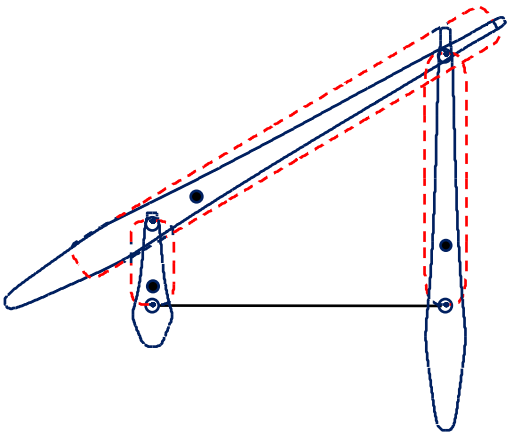

(d) case 4

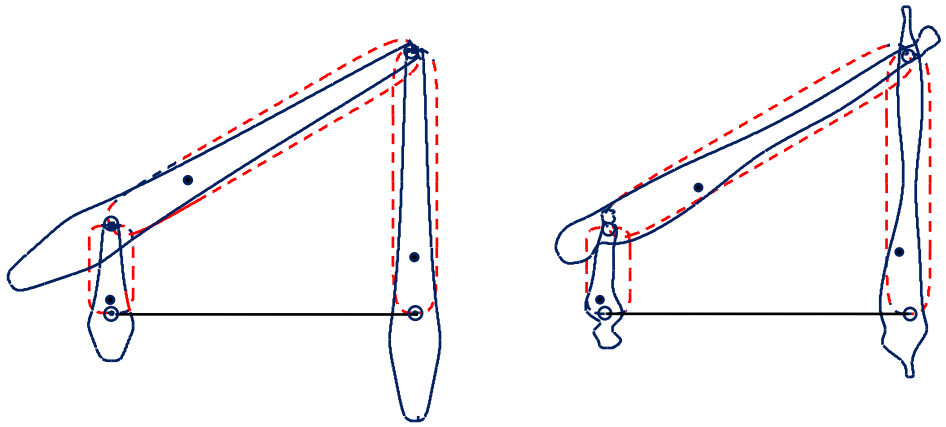

(e) case 5 (f) case 6

- - - - initial mechanism ———— optimized mechanism

○ denotes joint ● denotes mass center

Fig. 5.5 *Original and optimally designed mechanisms corresponding to different cases for four-bar mechanism [all figures drawn on scale]*

The conditions for full force balancing (Eq. 4.42) are satisfied for the complete force balanced mechanism achieved for cases (1) and (3) as shown in Fig. 5.5. Thus the shaking force in a mechanism can be completely eliminated by finding optimum link shapes (Fig. 5.5 (a) and (c)). Note that the complete shaking force balancing is achieved in four-bar mechanism by redistributing the masses of link #1 and #3 instead of adding the counterweights to these links as suggested in the literature. For case (3), as shown in Fig. 5.5 (c), the shaking force is balanced after converting link #2 into the physical pendulum which requires more mass for balancing as compared to case (1). The total mass is increased for a complete force balanced mechanism and also the increments in the RMS values of the shaking moment and the driving torque are found as 50.24% and 77.71%, respectively, in case 1. Similarly, the shapes for different cases considered in chapter 4 are found and shown in Figs. 5.5(b) - 5.5(f) where the non-symmetric link shapes are found as the special case (case 6). The

values of the design variables, defined in Fig. 5.3, for the optimally designed four-bar mechanism are given in Table 5.1 while the CAD model of the mechanism is shown in Fig. 5.6.

Table 5.1 *Design variables for optimally designed four-bar mechanism (all parameters are in meters)*

case 1															
DV / Link	y_1	y_2	y_3	y_4	y_5	y_6	y_7	y_8	y_9	y_{10}	y_{11}	y_{12}	y_{13}	x_0	x_{13}
1	0.000	0.000	0.000	0.000	0.025	0.025	0.025	0.025	0.025	0.035	0.089	0.116	0.117	0.000	0.120
2	0.000	0.000	0.000	0.000	0.025	0.025	0.025	0.025	0.025	0.000	0.000	0.000	0.000	0.000	0.000
3	0.000	0.000	0.000	0.000	0.025	0.025	0.025	0.025	0.025	0.056	0.063	0.095	0.118	0.000	0.242
case 2															
DV / Link	y_1	y_2	y_3	y_4	y_5	y_6	y_7	y_8	y_9	y_{10}	y_{11}	y_{12}	y_{13}	x_0	x_{13}
1	0.011	0.010	0.006	0.007	0.009	0.011	0.013	0.016	0.022	0.027	0.024	0.016	0.011	0.003	0.054
2	0.013	0.012	0.008	0.008	0.011	0.013	0.016	0.020	0.026	0.033	0.027	0.020	0.013	0.005	0.132
3	0.007	0.007	0.007	0.007	0.010	0.012	0.015	0.018	0.025	0.031	0.025	0.018	0.012	0.006	0.123
case 3															
DV / Link	y_1	y_2	y_3	y_4	y_5	y_6	y_7	y_8	y_9	y_{10}	y_{11}	y_{12}	y_{13}	x_0	x_{13}
1	0.000	0.000	0.000	0.000	0.025	0.025	0.032	0.047	0.053	0.035	0.058	0.069	0.082	0.000	0.128
2	0.025	0.025	0.025	0.025	0.025	0.025	0.025	0.025	0.025	0.025	0.025	0.025	0.025	0.082	0.082
3	0.000	0.000	0.000	0.000	0.025	0.032	0.047	0.058	0.063	0.075	0.087	0.095	0.118	0.000	0.261
case 4															
DV / Link	y_1	y_2	y_3	y_4	y_5	y_6	y_7	y_8	y_9	y_{10}	y_{11}	y_{12}	y_{13}	x_0	x_{13}
1	0.006	0.005	0.003	0.003	0.004	0.005	0.007	0.008	0.011	0.014	0.011	0.008	0.005	0.012	0.027
2	0.007	0.006	0.004	0.004	0.005	0.007	0.008	0.010	0.013	0.017	0.013	0.010	0.007	0.005	0.066
3	0.004	0.004	0.004	0.004	0.005	0.006	0.007	0.009	0.012	0.015	0.009	0.006	0.012	0.007	0.062
case 5															
DV / Link	y_1	y_2	y_3	y_4	y_5	y_6	y_7	y_8	y_9	y_{10}	y_{11}	y_{12}	y_{13}	x_0	x_{13}
1	0.011	0.010	0.006	0.006	0.009	0.011	0.013	0.016	0.021	0.027	0.022	0.016	0.011	0.000	0.054

2	0.013	0.012	0.008	0.008	0.011	0.013	0.016	0.020	0.026	0.033	0.027	0.020	0.013	0.000	0.132
3	0.007	0.007	0.007	0.007	0.010	0.012	0.015	0.018	0.025	0.031	0.025	0.018	0.012	0.000	0.123
case 6															
DV / Link	y_1	y_2	y_3	y_4	y_5	y_6	y_7	y_8	y_9	y_{10}	y_{11}	y_{12}	y_{13}	y_{14}	y_{15}
1	0.010	0.03	0.010	0.003	0.013	0.004	0.008	0.002	0.022	0.008	0.002	0.019	0.006	0.011	0.010
2	0.014	0.019	0.010	0.004	0.011	0.005	0.007	0.021	0.023	0.022	0.025	0.024	0.012	0.012	0.018
3	0.003	0.002	0.002	0.007	0.014	0.019	0.005	0.014	0.015	0.026	0.010	0.002	0.009	0.003	0.001
DV / Link	y_{16}	y_{17}	y_{18}	y_{19}	y_{20}	y_{21}	y_{22}	y_{23}	y_{24}	y_{25}	y_{26}	x_0	x_{13}		
1	0.022	0.001	0.032	0.021	0.016	0.014	0.005	0.006	0.006	0.008	0.004	0.020	0.039		
2	0.023	0.004	0.030	0.032	0.009	0.021	0.006	0.011	0.005	0.007	0.005	0.040	0.065		
3	0.038	0.021	0.038	0.023	0.001	0.013	0.011	0.008	0.007	0.003	0.009	0.055	0.073		

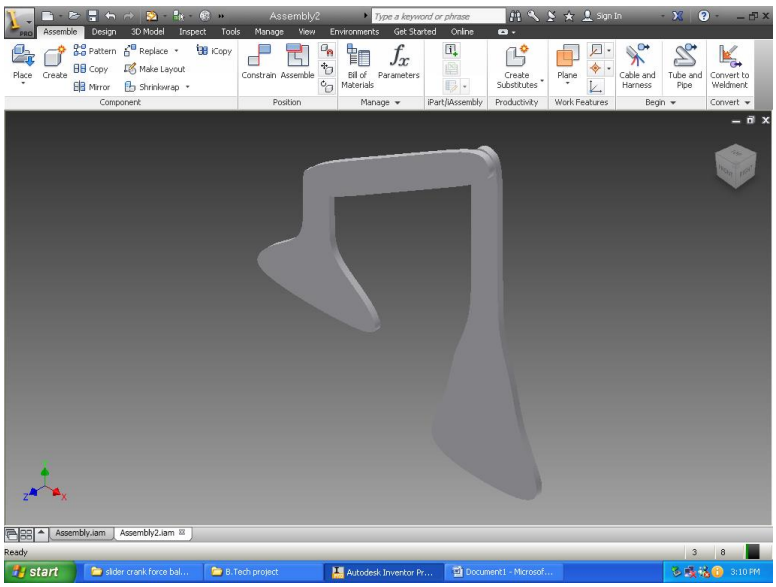

(case 1)

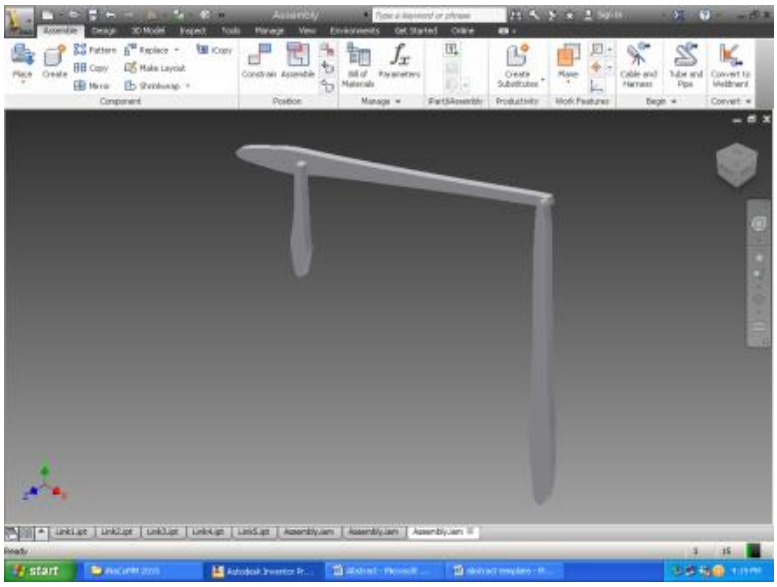

(case 2)

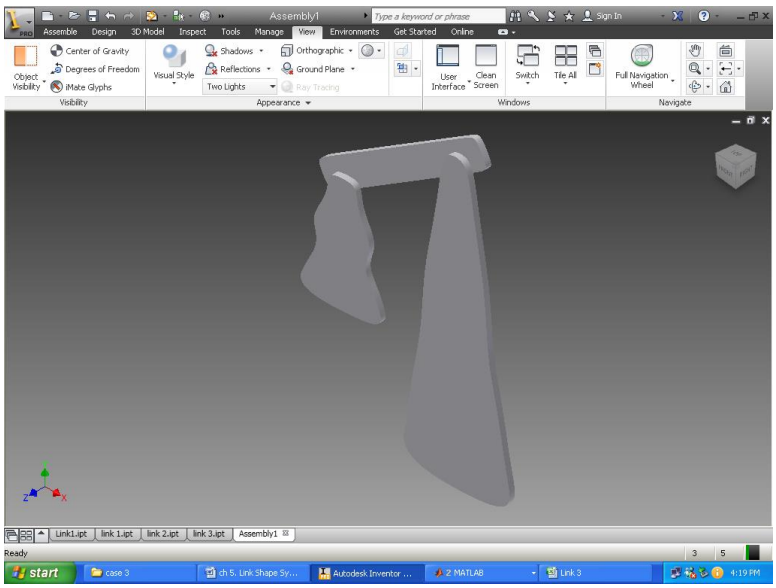

(case 3)

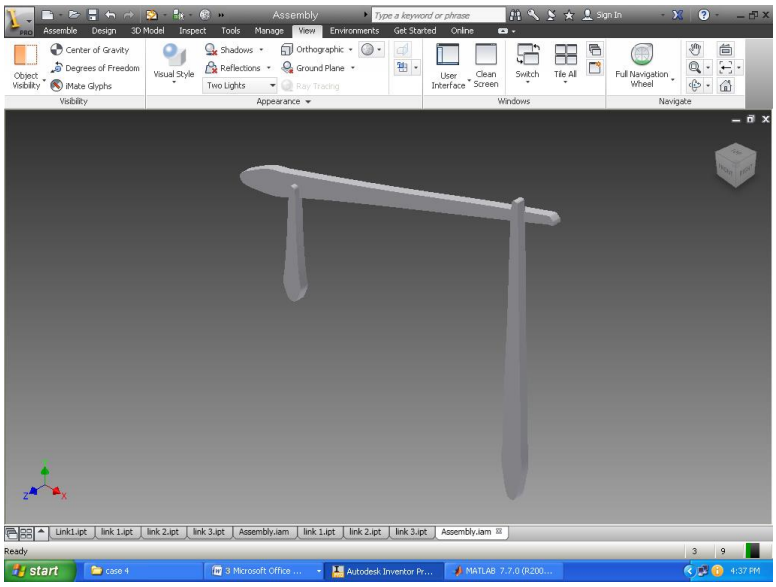
Assembly
Assemble
Design
3D Model
Inspect
Tools
Manage
View
Environments
Get Started
Online
Center of Gravity
Degrees of Freedom
iMate Glyphs
Visibility
Shadows
Reflections
Two Lights
Orthographic
Ground Plane
Ray Tracing
Appearance
User Interface
Clean Screen
Switch
Tile All
Windows
Full Navigation Wheel
Navigate
Link1.ipt
link 1.ipt
link 2.ipt
link 3.ipt
Assembly.iam
Ready
start
case 4
Autodesk Inventor Pr...
MATLAB 7.7.0 (R200...
4:37 PM

(case 4)

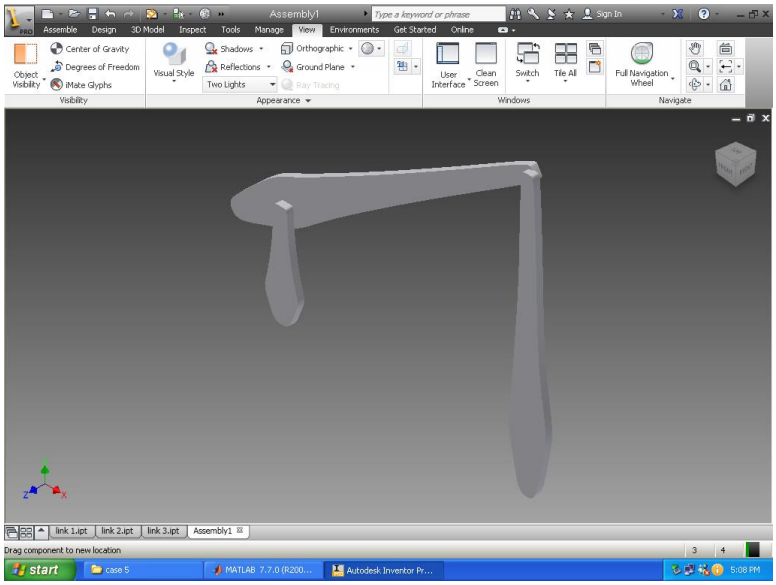
Assembly1
Assemble
Design
3D Model
Inspect
Tools
Manage
View
Environments
Get Started
Online
Center of Gravity
Degrees of Freedom
iMate Glyphs
Visibility
Shadows
Reflections
Two Lights
Orthographic
Ground Plane
Ray Tracing
Appearance
User Interface
Clean Screen
Switch
Tile All
Windows
Full Navigation Wheel
Navigate
link 1.ipt
link 2.ipt
link 3.ipt
Assembly1
Drag component to new location
start
case 5
MATLAB 7.7.0 (R200...
Autodesk Inventor Pr...
5:08 PM

(case 5)

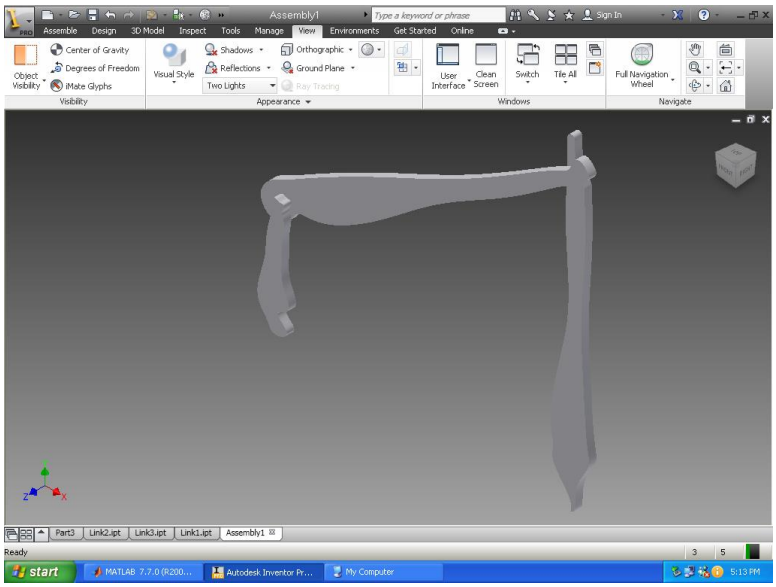

(case 6)

Fig. 5.6 *CAD model of optimally designed four-bar mechanism*

For the same problem, the physical pendulum concept was used along with the addition of force and inertia counterweights to balance the mechanism (Berkof, 1973; Farmani et al., 2011) as shown in Fig. 5.7.

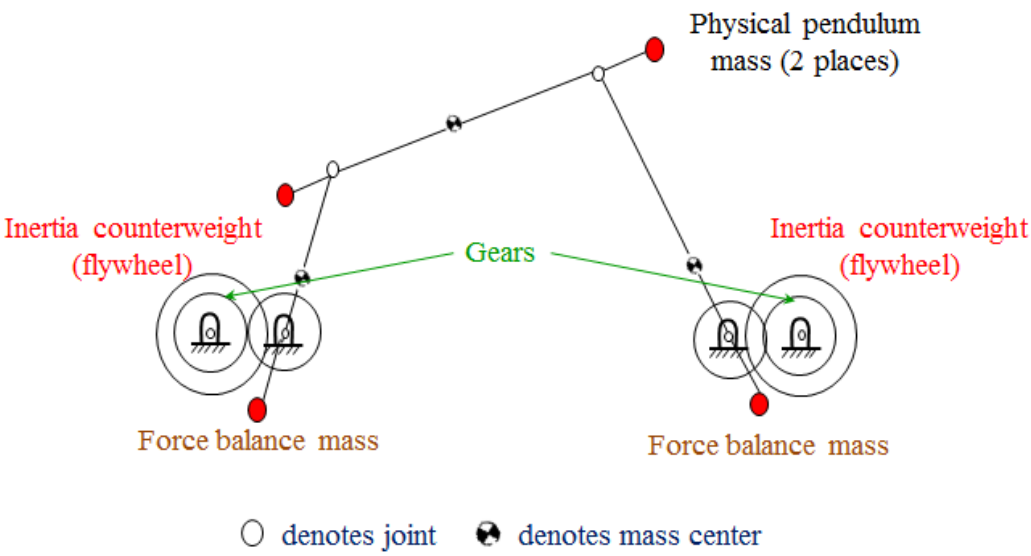

Fig. 5.7 *Fully force and moment balanced inline four-bar mechanism (Farmani et al., 2011)*

Whereas, the reductions of about 65%, 73% and 75% in RMS values of shaking force, shaking moment and driving torque, respectively, are achieved for the optimally designed mechanism (case 2) using the optimization method proposed in this chapter.

5.3.2 Five-bar Mechanism

The reduction of about 77%, 76% and 76% in the RMS values of shaking force, shaking moment and driving torque, respectively, are achieved for the optimally balanced five-bar mechanism obtained in chapter 4. The corresponding optimum link shapes for the balanced mechanism are found using the methodology proposed in this chapter and is shown in Fig. 5.8. Table 5.2 presents the optimum values of the design variables corresponding to the optimum shape obtained for five-bar mechanism whereas the CAD model of the optimally designed mechanism is shown in Fig. 5.9.

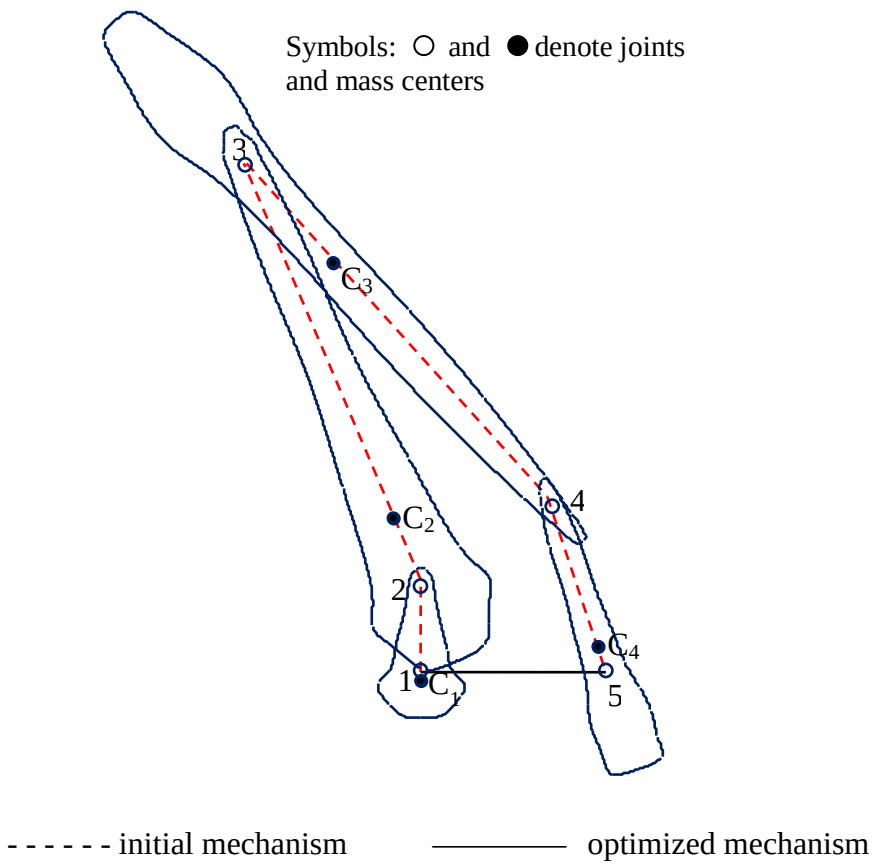

Fig. 5.8 *Original and optimally designed five-bar mechanism [figure drawn on scale]*

Table 5.2 *Design variables for optimally designed five-bar mechanism (all parameters are in meters)*

DV / Link	y_1	y_2	y_3	y_4	y_5	y_6	y_7	y_8	y_9	y_{10}	y_{11}	y_{12}	y_{13}	x_0	x_{13}
1	0.001	0.001	0.002	0.002	0.003	0.003	0.004	0.006	0.006	0.010	0.009	0.007	0.004	0.003	0.010
2	0.002	0.002	0.002	0.004	0.004	0.006	0.005	0.008	0.010	0.015	0.012	0.010	0.008	0.006	0.019
3	0.001	0.002	0.002	0.003	0.003	0.005	0.006	0.005	0.006	0.010	0.010	0.006	0.005	0.012	0.039
4	0.001	0.001	0.001	0.002	0.002	0.004	0.003	0.004	0.004	0.006	0.007	0.006	0.007	0.004	0.022

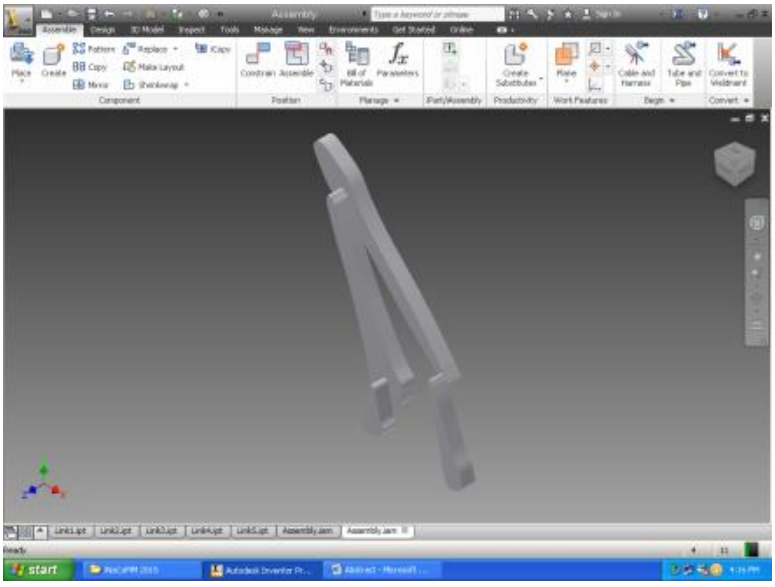

Fig. 5.9 *CAD model of optimally designed five-bar mechanism*

For the same problem, Ilia and Sinatra (2009) balanced only the shaking force through optimizing the center of mass parameters of the moving links. Whereas, the shaking force, shaking moment and driving torque for the mechanism are reduced significantly here by finding the optimum shapes of the mechanism links.

5.3.3 Stephenson Six-bar Mechanism

For optimally balanced Stephenson six-bar mechanism obtained in chapter 4, the reduction of about 70%, 73% and 58% were found in the RMS values of shaking force, shaking moment and driving torque, respectively. Figure 5.10 shows the optimum shapes for the optimally balanced mechanism. The optimum values of the

design variables are given in Table 5.3 while Fig. 5.11 shows the CAD model of the optimally designed mechanism.

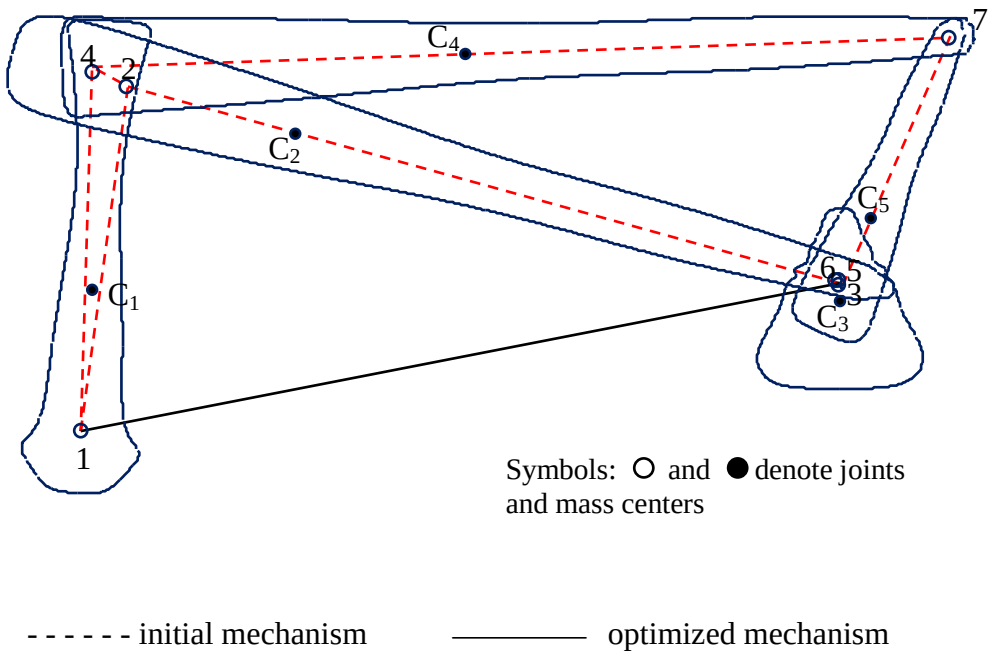

Fig. 5.10 *Original and optimized link shapes of Stephenson six-bar mechanism [figure drawn on scale]*

Table 5.3 *Design variables for optimally designed Stephenson six-bar mechanism (all parameters are in meters)*

DV / Link	y_1	y_2	y_3	y_4	y_5	y_6	y_7	y_8	y_9	y_{10}	y_{11}	y_{12}	y_{13}	x_0	x_{13}
1	0.007	0.006	0.006	0.005	0.005	0.003	0.004	0.006	0.006	0.010	0.009	0.007	0.004	0.010	0.010
2	0.001	0.001	0.002	0.003	0.003	0.005	0.004	0.007	0.008	0.008	0.008	0.008	0.006	0.006	0.019
3	0.002	0.003	0.004	0.005	0.005	0.008	0.007	0.008	0.009	0.009	0.012	0.014	0.011	0.009	0.017
4	0.001	0.002	0.002	0.003	0.003	0.005	0.004	0.007	0.008	0.008	0.008	0.008	0.006	0.002	0.005
5	0.001	0.001	0.001	0.002	0.002	0.004	0.003	0.005	0.006	0.006	0.006	0.006	0.005	0.003	0.008

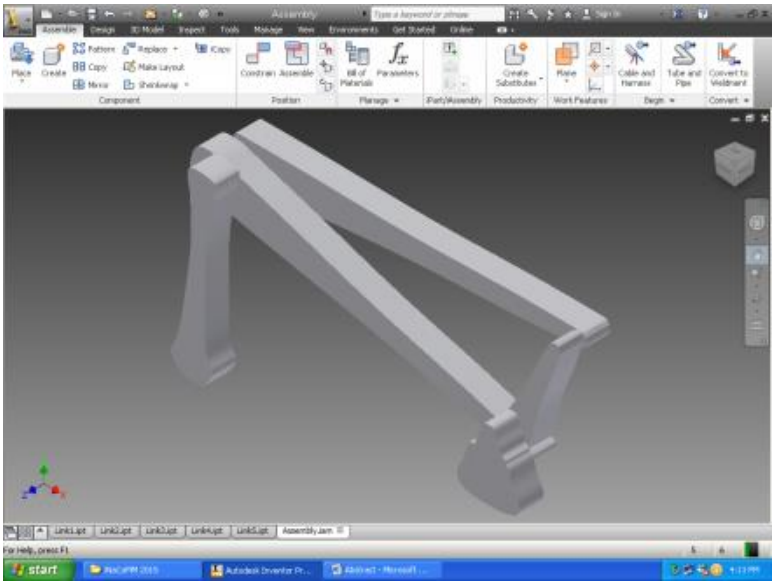

Fig. 5.11 *CAD model of optimally designed Stephenson six-bar mechanism*

Verschuure et al. (2007) used 90° sector-type counterweights to reduce the shaking force and shaking moment for the same problem (Fig. 5.12). Whereas the significant reductions of about 70%, 73% and 58% in shaking force, shaking moment and driving torque, respectively, are achieved here for the optimally designed mechanism.

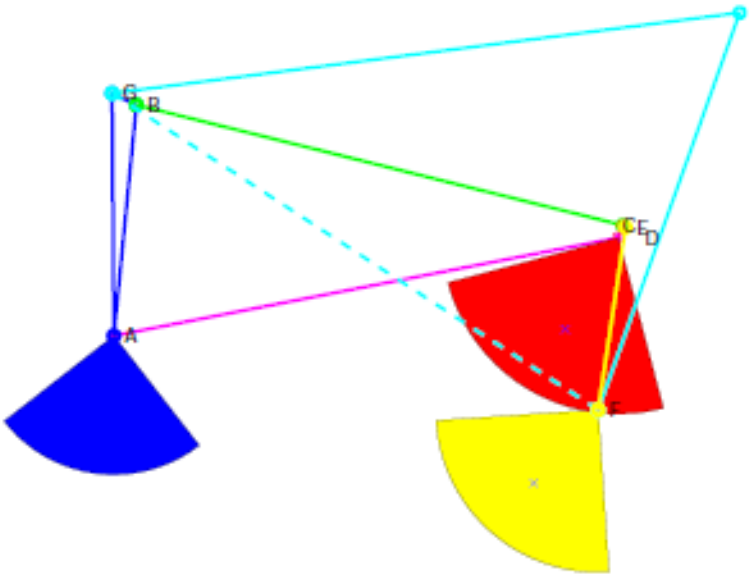

Fig. 5.12 *Balancing of shaking force and shaking moment in Stephenson six-bar mechanism using counterweights (Verschuure et al., 2007)*

5.3.4 Slider-crank Mechanism

The link shapes are synthesized using the optimization method proposed in this chapter for the force balanced slider-crank mechanism achieved in chapter 4 (Fig. 5.13). For this, the masses of the crank and the connecting rod are optimally distributed while use of the additional members like duplicate mechanism and counterweights are suggested in the traditional approach. However, the total mass is increased in both approaches. Table 5.4 presents the optimum values of the design variables corresponding to the optimum shape obtained for this mechanism whereas its CAD model is shown in n Fig. 5.14. The conditions for full force balancing (Eq. 4.43) are satisfied for the complete force balanced slider-crank mechanism achieved here (Fig. 5.13). In this case, the complete elimination of the shaking force increases the RMS value of shaking moment by about 563% while the overall mass of the mechanism is increased significantly.

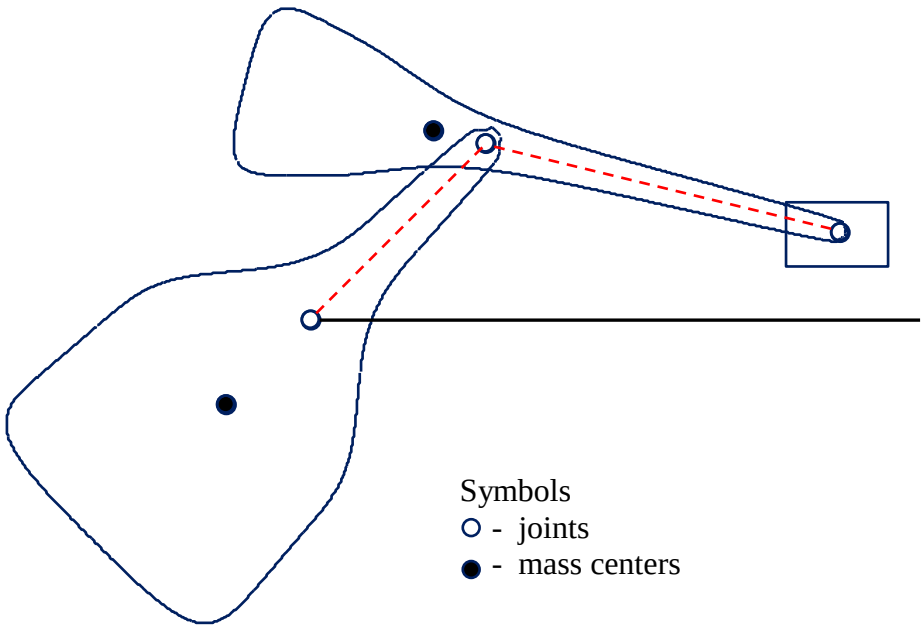

Fig. 5.13 *Original and optimally designed force balanced planar slider-crank mechanism [figure on scale]*

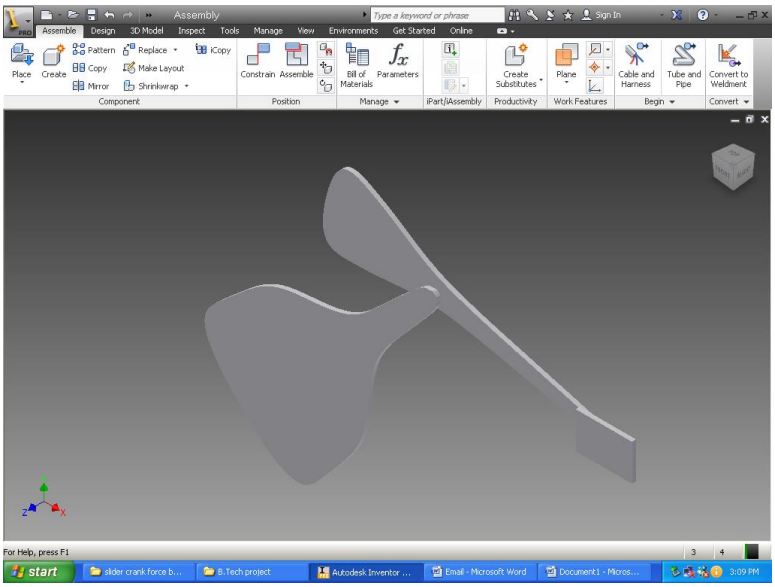

Fig. 5.14 *CAD model of optimally designed force balanced slider-crank mechanism*

Similarly, The reduction of about 48%, 44% and 35% in the RMS values of shaking force, shaking moment and driving torque, respectively, are achieved for the optimally balanced mechanism (chapter 4). The corresponding shapes of mechanism links are shown in Fig. 5.15. Table 5.4 presents the design variables defined in Fig. 5.3 for the mechanism whereas the CAD model of the optimally designed mechanism is shown in Fig. 5.16. For the same problem, use of the cam attached counterweights and spring is suggested to balance the shaking force and shaking moment in the literature (Arakelian and Briot, 2010) as shown in Fig. 5.17.

Table 5.4 *Design variables for optimally designed slider-crank mechanism (all parameters are in meters)*

Force balanced															
DV / Link	y_1	y_2	y_3	y_4	y_5	y_6	y_7	y_8	y_9	y_{10}	y_{11}	y_{12}	y_{13}	x_0	x_{13}
1	0.009	0.010	0.013	0.018	0.023	0.029	0.032	0.036	0.078	0.165	0.171	0.179	0.184	0.019	0.363
2	0.005	0.006	0.007	0.010	0.014	0.017	0.019	0.022	0.028	0.045	0.076	0.093	0.109	0.008	0.291
Force and moment balanced															
DV / Link	y_1	y_2	y_3	y_4	y_5	y_6	y_7	y_8	y_9	y_{10}	y_{11}	y_{12}	y_{13}	x_0	x_{13}
1	0.005	0.005	0.006	0.009	0.012	0.014	0.016	0.018	0.039	0.083	0.085	0.089	0.092	0.009	0.131
2	0.004	0.004	0.005	0.007	0.009	0.011	0.013	0.015	0.019	0.021	0.022	0.024	0.025	0.005	0.039

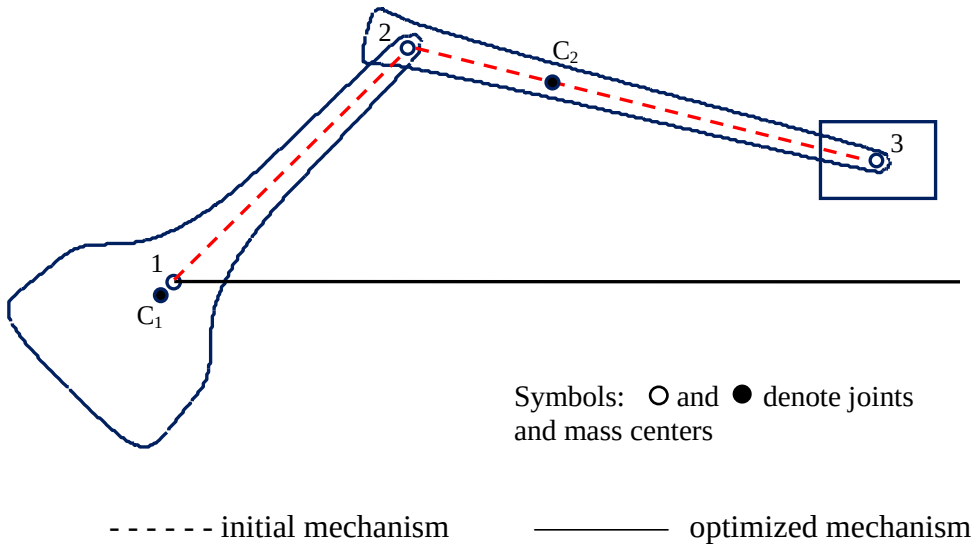

Fig. 5.15 *Original and optimally designed planar slider-crank mechanism [figure drawn on scale]*

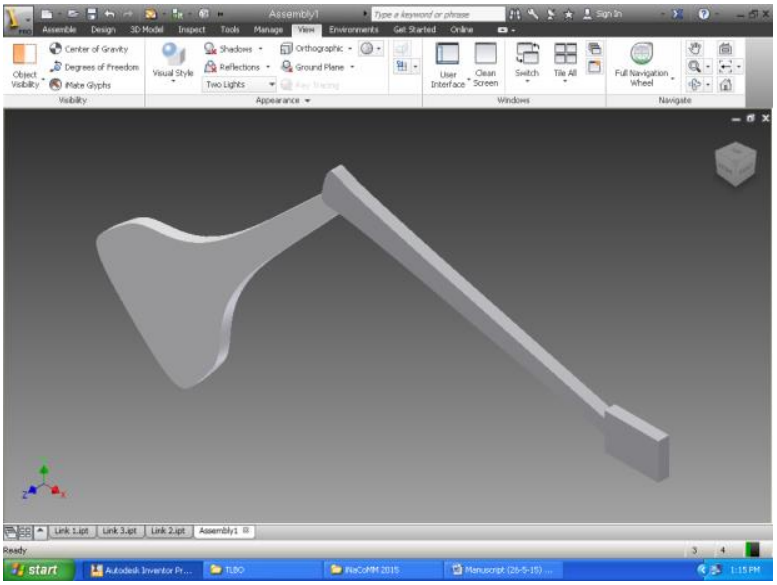

Fig. 5.16 *CAD model of optimally designed planar slider-crank mechanism*

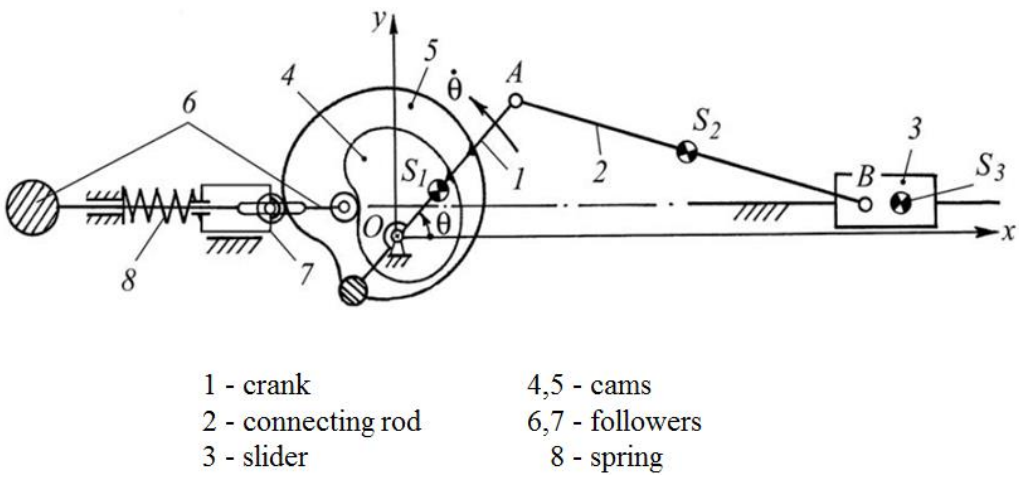

Fig. 5.17 *Complete force and moment balancing of slider-crank mechanism using cam attached counterweights (Arakelian and Briot, 2010)*

5.4 Summary

The physically possible shapes are constructed for the optimal inertial parameters of the mechanism links and the given kinematic structure. The percentage error of resulting link inertia values defined as the objective function was found within ± 5 percent. Thus, the two-stage optimization formulation including the dynamic balancing and the dynamics of mechanism has been brought in shape synthesis of links. The benefit associated with the proposed method is that the links of balanced

mechanism are of the uniform thickness while the force and inertia counterweights added to the original mechanisms in traditional methods (Berkof, 1973; Farmani et al., 2011; Berkof and Lowen, 1969) are of large thickness and radius compared to the original link parameters. Also, the proposed method doesn't require any pre-defined shapes or design domain to start with as suggested in (Farmani et al., 2011; Verschuure et al., 2007). The resulting stresses for links of the balanced mechanism can be calculated at the weakest sections under external loads.

Chapter 6

Conclusions

This thesis presents a two stage optimization methodology for optimum dynamic design of the planar mechanisms. The optimization problem formulation and various terms used by the classical and evolutionary optimization techniques are discussed in chapter 3. The popular evolutionary optimization techniques, Genetic algorithm (GA) and teaching-learning-based optimization (TLBO) algorithm are presented in details in this chapter. Both the optimization techniques are demonstrated by solving a numerical example for one iteration.

In chapter 4, an optimization problem is formulated to minimize the shaking force and shaking moment developed due to inertia forces in the planar mechanisms and solved using GA and TLBO. The balancing of the planar mechanisms is achieved through optimal mass distribution of the moving links. The inertial properties of links are represented by the equimomental point-mass system and the point-mass parameters are chosen as the design variables in the formulation of the optimization problem. The RMS values of normalised shaking force and shaking moment in planar four-bar, five-bar, six-bar and slider-crank mechanisms are reduced significantly by (65%, 73%), (77%, 76%), (70%, 73%) and (48%, 44%), respectively. It is found that TLBO is more computationally efficient and effective for mechanism balancing than that of GA. In chapter 5, the physical shapes are obtained corresponding to the optimal inertial parameters of the mechanism links found in chapter 4 for the given kinematic structure. The objective function for the shape optimization problem is formulated as the percentage error of resulting link inertia values over the optimum inertia values. The shape synthesis is obtained within ± 5 percent of the optimum

values. The resulting stresses for links of the balanced mechanism are calculated at the weakest sections under external loads.

The two-stage optimization method developed in this thesis includes the dynamic balancing and the dynamics of mechanism for shape synthesis of links. It is demonstrated that the conversion of the rigid links into the equimomental system of point-masses is more useful in solving the balancing problem for mechanism design. The optimal mass distributions of moving links by taking point-mass parameters as the design variables reduce the inertial forces and moments significantly. The links are of the uniform thickness in contrast of the traditional methods where the concept of the counterweights is used. Normally, counterweights are of large thickness and radius compared to the original link parameters. Also, the proposed method doesn't require any pre-defined shapes or design domain to start with the optimization procedure.

The method is quite general and equally applicable for all single or multiloop mechanisms where the analytical solutions are not available. The proposed method also demonstrates teaching-learning-based algorithm and genetic algorithm as a solver in mechanism balancing and design. In addition, the optimized values of link mass and inertia are effectively converted into physically possible shapes of links using closed B-spline curves. The novelty of the methodology is that it combines the dynamics and design solution for mechanisms.

The contributions of this research work are summarized as follows:

1. An optimization problem formulation is proposed for the dynamic balancing and link shape synthesis of the planar multiloop mechanisms.

2. The optimum mass distribution for the moving links for the optimally balanced mechanisms is proposed instead of the counterweights and/or additional members' methodology.
3. The computer aided design principles are integrated in a novel design methodology for links shapes formation for the optimally balanced mechanisms.
4. Implementation of evolutionary optimization techniques for mechanism design is explored.
5. Genetic algorithm (GA) and Teaching-learning-based optimization algorithm (TLBO) are applied for the mechanism design problem. It is established that TLBO is computationally more efficient than GA.

Future Scope of Work

This research work has given rise to some useful directions which forms the future scope of research. They are as follows:

1. Application of other advanced and hybridized optimization techniques to further improve the results.
2. Consideration of the flexibility, elastic deformation and joint clearance for the mechanism links.
3. Consideration of dynamic stresses due to variable loading and fatigue failure.
4. Application of equimomental system of more than three point-masses for mechanism links and their effects on dynamic balancing results.
5. Application of the proposed method to optimally design the spatial mechanisms considering feasibility constraints.

References

Alici, G., and Shirinzadeh, B., 2006, "Optimum Dynamic Balancing of Planar Parallel Manipulators Based on Sensitivity Analysis", Mechanism and Machine Theory, 41, pp. 1520-1535.

Arakelian, V., and Briot, S., 2010, "Simultaneous Inertia Force/Moment Balancing and Torque Compensation of Slider-Crank Mechanisms", Mechanics Research Communications, 37, pp. 265–269.

Arakelian, V., and Briot, S., 2015, *Balancing of Linkages and Robot Manipulators – Advanced Methods with Illustrative Examples*, Springer International Publishing.

Arakelian, V., and Dahan, M., 2001, "Partial Shaking Moment Balancing of Fully Force Balanced Linkages", Mechanism and Machine Theory, 36, pp. 1241-1252.

Arakelian, V., and Makhsudyan, N., 2010, "Generalized Lanchester balancer", Mechanics Research Communications, 37(7), pp. 647–649.

Arakelian, V.H., 2006, "Shaking Moment Cancellation of Self-Balanced Slider-Crank Mechanical Systems By Means of Optimum Mass Redistribution", Mechanics Research Communications, 33, pp. 846–850.

Arakelian, V.H., and Smith, M.R., 1999, "Complete Shaking Force and Shaking Moment Balancing of Linkages", Mechanism and Machine Theory, 34, pp. 1141-1153.

Arakelian, V.H., and Smith, M.R., 2005, "Shaking Force and Shaking Moment Balancing of Mechanisms: A Historical Review With New Examples", ASME Journal of Mechanical Design, 127, pp. 334-339.

Arora, J.S., 1989, *Introduction to optimum design*, McGraw-Hill Book Company, Singapore.

Attia, H. A., 2003, "A Matrix Formulation for the Dynamic Analysis of Spatial Mechanisms Using Point Coordinates and Velocity Transformation", Acta Mechanica, 165, pp. 207-222.

Azegami, H., Zhou, L., Umemura, K., and Kondo, N., 2013, "Shape Optimization for a Link Mechanism", Structural Multidiscipline Optimization, 48 (1), pp. 115-125.

Bagci, C., 1979, "Shaking Force Balancing of Planar Linkages With Force Transmission Irregularities Using Balancing Idler Loops", Mechanism and Machine Theory, 14(4), pp. 267-284.

Bagci, C., 1982, "Complete Shaking Force and Shaking Moment Balancing of Link

Mechanisms Using Balancing Idler Loops", ASME Journal of Mechanical Design, 104, pp. 482-493.

Bagci, C., 1995, "A Simplified Approach for Balancing of Multi-Cylinder Engines", Proc. of 13th International Modal Analysis Conference, Nashville, Tennessee.

Berkof, R.S., 1973, "Complete Force and Moment Balancing of Inline Four-bar Linkage", Mechanism and Machine Theory", 8, pp. 397-410.

Berkof, R.S., and Lowen, G.G., 1969, "A New Method For Completely Force Balancing Simple Linkages", ASME Journal of Engineering for Industry, 91(1), pp. 21-26.

Berkof, R.S., and Lowen, G.G., 1971, "Theory of Shaking Moment Optimization of Forced-Balanced Four-bar Linkages", ASME Journal of Engineering for Industry, 93B (1), pp. 53-60.

Brlek, S., labelle, G., and Lacasse, A., 2005, "The Discrete Green Theorem and Some Applications in Discrete Geometry", Theoretical Computer Science, 346, pp. 220-225.

Carson, W.L., and Stephenes, J.M., 1978, "Feasible Parameter Design Spaces for Force and Root-Mean-Square Moment Balancing An In-Line 4R 4-Bar Synthesized for Kinematic Criteria", Mechanism and Machine Theory, 13, pp. 649-658.

Castillo, J.J., Giner, P., Sim´on, A. and Cabrera, J.A., 2013, "Optimal Design of Motorcycle Rear Suspension Systems Using Genetic Algorithms", Viadero F. and Ceccarelli M. (eds.), *New Trends in Mechanism and Machine Science*, Mechanisms and Machine Science 7, Springer Science+Business Media Dordrecht, pp. 181-190.

Chaudhary, H., and Saha, S.K., 2006, "Equimomental System and Its Applications", Proc. of 8th Biennial ASME Conference on Engineering Systems Design and Analysis, July 4-7, 2006, Torino, Italy.

Chaudhary, H., and Saha, S.K., 2007, "Balancing of Four-bar Linkages Using Maximum Recursive Dynamic Algorithm", Mechanism and Machine Theory, 42(2), pp. 216-232.

Chaudhary, H., and Saha, S.K., 2008, "Balancing of Shaking Forces and Shaking Moments For Planar Mechanisms Using The Equimomental Systems", Mechanism and Machine Theory, 43, pp. 310–334.

Chaudhary, H., and Saha, S.K., 2009, *Dynamics and Balancing of Multibody Systems*, Springer-Verlag, Berlin.

Chiou, S. T., and Davies, T. H., 1994, "The Ideal Locations for the Contra-Rotating Shafts of Generalized Lanchester Balancers", Proceeding of Institution of

Mechanical. Engineering. Part C: Journal of Mechanical Engineering Science, 208 (1), pp. 29–37.

Chiou, S. T., and Davies, T. H., 1997, “Partial Cancellation of Shaking Force Harmonics By Cam Modification”, Proceeding of Institution of Mechanical Engineering. Part C: Journal of Mechanical Engineering Science, 211, pp. 253–263.

Chiou, S.T., Bai, G.J., and Chang, W.K., 1998, “Optimum Balancing Designs of The Drag-Link Drive of Mechanical Presses for Precision Cutting”, International Journal of Machine Tools and Manufacture, 38 (3), pp. 131-141.

Conte, F.L., George, G.R., Mayne, R.W., and Sadler, J.P., 1975, “Optimum Mechanism Design Combining Kinematic and Dynamic-Force Considerations”, ASME Journal of Engineering for Industry, 95(2), pp. 662-670.

Crisco, J.J., and McGovern, R.D., 1998, “Effective Calculation of Mass Moments of Inertia For Segmented Homogenous Three-Dimensional Objects”, Journal of Biomechanics, 31, pp. 97-101.

Davies, T. H., and Niu, G. H., 1994, “On the Retrospective Balancing of Installed Planar Mechanisms”, Proceeding of Institution of Mechanical Engineering. Part C: Journal of Mechanical Engineering Science, 208, pp. 39–45.

Deb, K., 2000, “An Efficient Constraint Handling Method for Genetic Algorithm”, Computer Methods in Applied Mechanics and Engineering, 186, pp. 311-336.

Deb, K., 2010, *Optimization for Engineering Design – Algorithms and examples*, PHI Learning Private Limited, New Delhi.

Demeulenaere, B., 2004, “Dynamic Balancing of Reciprocating Machinery With Application To Weaving Machines”, Ph.D. Thesis, Department of Mechanical Engineering, University of Leuven, Belgium.

Demeulenaere, B., Aertbelien, E., Verschuure, M., Swevers, J., and Schutter, J.D., 2006, “Ultimate Limits for Counterweight Balancing of Crank-Rocker Four-bar Linkages”, ASME Journal of Mechanical Design, 128, pp. 1272-1284.

Demeulenaere, B., Swevers, J., and Schutter, J.D., 2004, “A Convex Optimization Framework For Dynamic Balancing of Planar Linkages”, Proceeding of ISMA 2004, 1997-2010.

Demeulenaere, B., Verschuure, M., Swevers, J. and Schutter, J.D., 2010, “A General and Numerically Efficient Framework to Design Sector-Type and Cylindrical Counterweights For Balancing of Planar Linkages”, ASME Journal of Mechanical Design, 132, pp. 011002(1-10).

Dresig, H., and Holzweibig, F., 2010, *Dynamics of Machinery – Theory and applications*, Springer-Verlag Berlin Heidelberg.

Dresig, H., and Dien, N.P., 2011, "Complete Shaking Force and Shaking Moment Balancing of Mechanisms Using a Moving Rigid Body", Technische Mechanik, 31(2), pp. 121-131.

Elliott, J. L., and Tesar, D., 1977, "The Theory of Torque, Shaking Force, and Shaking Moment Balancing of Four Link Mechanisms", ASME Journal of Engineering for Industry, 99(3), pp. 715-722.

Elliott, J. L., and Tesar, D., 1982, "A General Mass Balancing Method for Complex Planar Mechanisms", Mechanism and Machine Theory, 17(2), pp. 153-172.

Erkaya, S., 2013, "Investigation of Balancing Problem For A Planar Mechanism Using Genetic Algorithm", Journal of Mechanical Science and Technology, 27 (7), pp. 2153-2160.

Erkaya, S., and Uzmay, I., 2008, "A Neural-genetic Approach for Optimizing Mechanisms Having Joints with Clearance", Multibody Systems Dynamics, 20, pp. 69-83.

Erkaya, S., and Uzmay, I., 2009, "Investigation on Effect of Joint Clearance on Dynamics of Four-bar Mechanism", Nonlinear Dynamics, 58, pp. 179-198.

Esat, I., and Bahai, H., 1999, "A Theory of Complete Force and Moment Balancing of Planar Linkage Mechanisms", Mechanism and Machine Theory, 34, pp. 903-922.

Farmani, M.R., Jaamialahmadi, A., and Babaie, M., 2011, "Multiobjective Optimization For Force and Moment Balance of A Four-bar Linkage Using Evolutionary Algorithms", Journal of Mechanical Science and Technology, 25 (12), pp. 2971-2977.

Feng, B., Morita, N., and Torii, T., 2002, "A New Optimization Method for Dynamic Design of Planar Linkage with Clearances at Joints", ASME Journal of Mechanical Design, 124, pp. 68-73.

Feng, B., Morita, N., Torii, T., and Yoshida, S., 2000, "Optimum Balancing of Shaking Force and Shaking Moment for Spatial RSSR Mechanism Using Genetic Mechanics", JSME International Journal, Series C, 43 (3), pp. 691-696.

Feng, G., 1990, "Complete Shaking Force and Shaking Moment Balancing of 26 Types of Four-, Five- and Six-bar Linkages with Prismatic Pairs", Mechanism and Machine Theory, 25(2), pp. 183-192.

Feng, G., 1991, "Complete Shaking Force and Shaking Moment Balancing of 17 Types

of Eight-bar Linkages Only with Revolute Pairs", Mechanism and Machine Theory, 26(2), pp. 197-206.

Freudenstein, F., 2010, "Approximate Synthesis of Four-bar Linkages", Resonance, 15 (8), pp. 740-767.

Gao, Y., Shi, L., and Yao P., 2000, "Study on Multi-Objective Genetic Algorithm", Proc. of 3rd World Congress on Intelligent Control and Automation, June 28-July 2, Hefei, P R China.

Garrett, T.K., Newton, K., and Steeds, W., 2001, *The Motor Vehicle*, Reed Educational and Professional Publishing Ltd and Society of Automotive Engineers Inc.

Gill, G.S., and Freudenstein, F., 1983a, "Minimization of Inertia-Induced Forces in Spherical Four-bar Mechanisms. Part 1: The General Spherical Four-bar Linkage", ASME Journal of Mechanisms, Transmissions, and Automation in Design, 105, pp. 471-477.

Gill, G.S., and Freudenstein, F., 1983b, "Minimization of Inertia-Induced Forces in Spherical Four-bar Mechanisms. Part 2: Wobble-Plate Engines", ASME Journal of Mechanisms, Transmissions, and Automation in Design, 105, pp. 478-483.

Gosselin, C.M., Moore, B., and Schicho, J., 2009, "Dynamic Balancing of Planar Mechanisms Using Toric Geometry", Journal of Symbolic Computation, 44, pp. 1346-1358.

Guo, G., Morita, N., and Torii, T., 2000, "Optimum Dynamic Design of Planar Linkage Using Genetic Algorithms", JSME International Journal Series C, 43 (2), pp. 372-377.

Haines, R.S., 1981, "Minimum RMS Shaking Moment or Driving Torque of a Force-balanced 4-Bar Linkage Using Feasible Counterweights", Mechanism and Machine Theory, 16 (3), pp. 185-195.

Han, C., 1967, "Balancing of High Speed Machinery", ASME Journal of Engineering for Industry, 89(1), pp. 111–117.

Hoag, K.L., 2006, *Vehicular Engine Design*, Springer-Verlag, Wien, and the Society of Automotive Engineers International.

Holland, J.H., 1992, *Adaptation in Natural and Artificial Systems, An Introductory Analysis with Applications to Biology, Control, and Artificial Intelligence*, The MIT Press, USA.

Hsieh, W., and Tsai, C., 2009, "A Study on A Novel Quick Return Mechanism", Transactions of the Canadian Society for Mechanical Engineering, 33 (3), pp. 487-

500.

Huang, N.C., 1983, “Equimomental System of Rigidly Connected Equal Particles”, Journal of Guidance, Control and Dynamics, 16(6), pp. 1194-1196.

Hüsing, M., Braune, R. and Corves, B., 2015, “Dimensional Synthesis with Mechanism Processing Strategy”, Flores P. and Viadero F. (eds.), New Trends in Mechanism and Machine Science - From Fundamentals to Industrial Applications, Mechanisms and Machine Science 24, Springer International Publishing Switzerland, pp. 139-146.

Ilia, D., and Sinatra, R., 2007, “A Novel Formulation of The Dynamic Balancing of Five-bar Linkages”, 12th IFToMM World Congress, Besancon, France, June, 2007.

Ilia, D., and Sinatra, R., 2009, “A Novel Formulation of The Dynamic Balancing of Five-bar Linkages with Application To Link Optimization”, Multibody Systems Dynamics, 21, pp. 193-211.

Kamenskii, V.A., 1968a, “On The Questions of The Balancing of Plane Linkages”, Journal of Mechanisms, 3 (4), pp. 303-322.

Kamenskii, V.A., 1968b, “On The Problem of The Number of Counterweights In The Balancing of Plane Linkages”, Journal of Mechanisms, 3(4), pp. 323–333.

Kim, Y., Tan, A., Yang, B., Kim, W., Choi, B. and An, Y., 2007, “Optimum Shape Design of Rotating Shaft By ESO Method”, Journal of Mechanical Science and Technology, 21, pp. 1039-1047.

Kochev, I.S., 1988, “A New General Method For Full Force Balancing of Planar Linkages”, Mechanism and Machine Theory, 23(6), pp. 475-480.

Kochev, I.S., 1992, “Active Balancing of The Frame Shaking Moment In High Speed Planar Machines”, Mechanism and Machine Theory, 27(1), 53–58.

Kochev, I.S., 2000, “General Theory of Complete Shaking Moment Balancing of Planar Linkages: A Critical Review”, Mechanism and Machine Theory, 35, pp. 1501-1514.

Lee, T.W., and Cheng C., 1984, “Optimum Balancing of Combined Shaking Force, Shaking Moment, and Torque Fluctuations In High Speed Linkages”, ASME Journal of Mechanisms, Transmissions, and Automation in Design, 106(2), pp. 242-251.

Lee, T.W., and Freudenstein, F., 1976a, “Heuristic Combinatorial Optimization in The Kinematic Design of Mechanisms; Part 1, Theory”, ASME Journal of Engineering for Industry, 98 (4), pp. 1277-1280.

Lee, T.W., and Freudenstein, F., 1976b, “Heuristic Combinatorial Optimization in The Kinematic Design of Mechanisms; Part 2, Application”, ASME Journal of

Engineering for Industry, 98 (4), pp. 1281-1284.

Li, Z., 1998, “Sensitivity and Robustness of Mechanism Balancing”, Mechanism and Machine Theory, 33(7), pp. 1045-1054.

Lowen, G.G., and Berkof, R.S., 1968, “Survey of Investigations Into The Balancing of Linkages”, Mechanism and Machine Theory, 3(4), pp. 221-231.

Lowen, G.G., and Berkof, R.S., 1971, “Determination of Force-Balanced Four-bar Linkages With Optimum Shaking Moment Characteristics”, Journal of Engineering for Industry, Feb 1971, pp. 39-46.

Lowen, G.G., Tepper, F.R., and Berkof, R.S., 1974, “The Quantitative Influence of Complete Force Balancing on The Forces and Moments of Certain Families of Four-bar Linkages”, Mechanism and Machine Theory, 9, pp. 299-323.

Lowen, G.G., Tepper, F.R., and Berkof, R.S., 1983, “Balancing of Linkages – An Update”, Mechanism and Machine Theory, 18 (3), pp. 213-220.

Mallipeddi, R., and Suganthan, P.N., 2010, “Ensemble of Constraint Handling Techniques”, IEEE Transactions of Evolutionary Computation, 14, pp. 561–579.

Mariappan, J., and Krishnamurty, S., 1996, “A Generalised Exact Gradient Method for Mechanism Synthesis”, Mechanism and Machine Theory, 31(4), pp. 413-421.

Marler, R.T., and Arora, J.S., 2004, “Survey of Multi-Objective Optimization Methods for Engineering”, Structural and Multidisciplinary Optimization, 26 (6), pp. 369-395.

Marler, R.T., and Arora, J.S., 2010, “The Weighted Sum Method for Multi-Objective Optimization: New Insights”, Structural and Multidisciplinary Optimization, 41, pp. 853-862.

Martini, A., Troncossi, M., and Rivola, A., 2013, “Elastodynamic Effects of Mass-Balancing: Experimental Investigation of A Four-bar Linkage”, Advances in Mechanical Engineering, pp. 1-10.

Martini, A., Troncossi, M., Carricato, M., and Rivola, A., 2014, “Elastodynamic Behavior of Balanced Closed-Loop Mechanisms: Numerical Analysis of A Four-bar Linkage”, Meccanica, 49(3), pp. 601-614.

MATLAB Optimization Toolbox, version 7.7.0.471 (R2008b).

Molian, S., 1973, “Kinematics and Dynamics of the RSSR Mechanism”, Mechanism and Machine Theory, 8, pp. 271-282.

Montes, E., Coello, C.A.C., 2005, “A Simple Multi-Membered Evolution Strategy to Solve Constrained Optimization Problems”, IEEE Transactions of Evolutionary Computation, 9(1), pp. 1-17.

Moore, B., 2009, “Dynamic Balancing of Linkages By Algebraic Methods”, Ph.D. Thesis, Research Institute for Symbolic Computation, Johannes-Kepler University Linz, Austria.

Mortenson, M.E., 2006, *Geometric Modeling*, McGraw Hill Education (India) Private Limited, New Delhi, India.

Norton, R.L., 2011, *Kinematics and Dynamics of Machinery*, Tata McGraw Hill Education Private Limited, New Delhi, India.

Ouyang, P.R., and Zhang, W.J., 2005, “Force Balancing of Robotic Mechanisms Based on Adjustment of Kinematic Parameters”, ASME Journal of Mechanical Design, 127 (3), pp. 433-440.

Ouyang, P.R., Li, Q., and Zhang, W.J., 2003, “Integrated Design of Robotic Mechanisms for Force Balancing and Trajectory Tracking”, Mechatronics, 13, pp. 887-905.

Park, C., and Kwak, B., 1987, “Counterweight Optimization For Reducing Dynamic Effects of Clearance At A Revolute Joint”, Mechanism and Machine Theory, 22(6), pp. 549-556.

Park, J.G., Jeong, W.B., Seo, Y.S., and Yoo, W.S., 2007, “Optimization of Crank Angles To Reduce Excitation Forces and Moments In Engines”, Journal of Mechanical Science and Technology, 21 (2), pp. 272-281.

Raghu, E., and Balasubramonian, A., 1990, “Experimental Study on The Elastodynamic Behavior of The Unbalanced and The Counterweighted Four-bar Mechanisms”, Journal of Mechanical Design, 112(3), pp. 271-277.

Rahman, S., 1996, “Reduction of Inertia-Induced Forces In A Generalized Spatial Mechanism”, Ph.D. Thesis, Department of Mechanical Engineering, The New Jersey Institute of Technology.

Rao, R.V., and Savsani, V.J., 2012, *Mechanical Design Optimization Using Advanced Optimization Techniques*, Springer-Verlag London, UK.

Rao, R.V., and Waghmare, G.G., 2014, “A Comparative Study of a Teaching–Learning-Based Optimization Algorithm on Multi-Objective Unconstrained and Constrained Functions”, Journal of King Saud University – Computer and Information Sciences, 26, pp. 332–346.

Rao, R.V., Savsani, V.J., and Vakharia, D.P., 2011, “Teaching-Learning-Based Optimization: A Novel Method for Constrained Mechanical Design Optimization Problems”, Computer-Aided Design, 43, pp. 303-315.

Rao, R.V., and Patel, V., 2013, “Multi-Objective Optimization of Heat Exchangers Using A Modified Teaching-Learning-Based Optimization Algorithm”, Applied Mathematical Modelling, 37, pp. 1147–1162.

Rao, R.V., and Patel, V., 2013, “Multi-Objective Optimization of Two Stage Thermoelectric Cooler Using A Modified Teaching–Learning-Based Optimization Algorithm”, Engineering Applications of Artificial Intelligence, 26, pp. 430–445.

Routh, E.J., 1905, *A Treatise on The Dynamics of A System of Rigid Bodies*, Elementary Part I, Dover Publication Inc., New York.

Runarsson, T.P., and Yao, X., 2005, “Search Biases In Constrained Evolutionary Optimization”, IEEE Transactions on Systems, Man and Cybernatics, 35, pp. 233–243.

Sandor, G.N., and Erdman, A.G., 1984, *Advanced Mechanism Design – Analysis and Synthesis*, Vol. 2, Prentice Hall, New Jersey.

Sen, D., Chowdhury, S., and Pandey S.R., 2004, “Geometric Design of Interference-Free Planar Linkages”, Mechanism and Machine Theory, 39, pp. 737-759.

Shchepetilnikov, V.A., 1968, “The Determination of The Mass Centres of Mechanisms In Connection With The Problem of Mechanism Balancing”, Mechanism and Machine Theory, 3(4), pp. 367-389.

Sherwood, A.A., and Hockey, B.A., 1968, “The Optimization of Mass Distribution in Mechanisms Using Dynamically Similar Systems”, Journal of Mechanisms, 4, pp. 243-260.

Smith, M., 1975, “Dynamic Analysis and Balancing of Linkages With Interactive Computer Graphics”, Computer Aided Design, 7(1), pp. 15–19.

Soong, R.C., and Hsu K.S., 2007, “A Design Combining Kinematic and Dynamic Balancing Considerations With Bi-Material Links For Four-bar Linkages”, Journal of Information and Optimization Sciences, 28(4), pp. 663-686.

Soriano, E., Rubio, H., Castejón C., and García-Prada J.C., 2015, “Design of a Low-Cost Manipulator Arm for Industrial Fields”, Flores P. and Viadero F. (eds.), New Trends in Mechanism and Machine Science - From Fundamentals to Industrial Applications, Mechanisms and Machine Science 24, Springer International Publishing Switzerland, pp. 839-850.

Stevensen, E.N., 1973, “Balancing of Machines”, ASME Journal of Engineering for Industry, May 1973, pp. 650-656.

Takahama, T., and Sakai, S., 2006, “Constrained Optimization by the Constrained

Differential Evolution with Gradient-Based Mutation and Feasible Elites", Proceedings of IEEE congress on evolutionary computation, Vancouver, BC, Canada, pp. 1–8.

Tepper, F.R., and Lowen, G.G., 1972, "General Theorems Concerning Full Force Balancing of Planar Linkages By Internal Mass Redistribution", ASME Journal of Engineering for Industry, 94 (3), pp. 789-796.

Tepper, F.R., and Lowen, G.G., 1975, "Shaking Force Optimization of Four-bar Linkage With Adjustable Constraints On Ground Bearing Forces", ASME Journal of Engineering for Industry, May 1975, pp. 643-651.

Tessema, B., and Yen, G., 2006, "A Self Adaptive Penalty Function Based Algorithm for Constrained Optimization", Proceedings of IEEE congress on evolutionary computation, Vancouver, BC, Canada, pp. 246–253.

Tricamo, S.J., and Lowen, G.G., 1983a, "A Novel Method For Prescribing The Maximum Shaking Force of A Four-bar Linkage With Flexibility In Counterweight Design", Journal of Mechanisms, Transmissions, and Automation in Design, 105, pp. 511-519.

Tricamo, S.J., and Lowen, G.G., 1983b, "Simultaneous Optimization of Dynamic Reactions of A Four-bar Linkage With Prescribed Maximum Shaking Force", Journal of Mechanisms, Transmissions, and Automation in Design, 105, pp. 520-525.

Tsai, L., 1984, "Oldham-coupling Second-harmonic Balancer", ASME Journal of Mechanisms, Transmissions, and Automation in Design, 106(3), pp. 285–290.

Verschuure, M., 2008, "Counterweight Balancing For Vibration Reduction of Elastically Mounted Machine Frames: A Second-order Cone Programming Approach", ASME Journal of Mechanical Design, 130, pp. 022302(1-11).

Verschuure, M., 2008, "Optimal Counterweight Balancing of Spatial Mechanisms Using Voxel-based Discretizations", Proceeding of ISMA 2008, International Conference on Noise and Vibration Engineering. Leuven, Belgium. 15-17 Sep, 2008.

Verschuure, M., 2009, "Counterweight Balancing of Mechanisms Using Convex Optimization Techniques", Ph.D. Thesis, Department of Mechanical Engineering, University of Leuven, Belgium.

Verschuure, M., Demeulenaere, B., Swevers, J., and Schutter, J.D., 2007, "On the Benefits of Partial Shaking Force Balance in Six-bar Linkages", Proc. of 12th IFToMM World Congress, June 18-21, Besancon.

Walker, M.J., and Oldham, K., 1978, "A General Theory of Force Balancing Using Counterweights", Mechanism and Machine Theory, 13, pp. 175-185.

Walker, M.J., and Oldham, K., 1979, "Extensions To The Theory of Balancing Frame Forces In Planar Linkages", Mechanism and Machine Theory, 14, pp. 201-207.

Wenglarz, R.A., Fogarasy, A.A., and Maunder, L., 1969, "Simplified Dynamic Models", Engineering, 208, pp. 194-195

Wiederrich, J.L., Roth, B., 1976, "Momentum Balancing of Four-bar Linkages", ASME Journal of Engineering for Industry, 98(4), pp. 1289-1295.

Wijk, V.V., Herder, J.L., and Demeulenaere, B., 2009, "Comparison of Various Dynamic Balancing Principles Regarding Additional Mass and Additional Inertia", ASME Journal of Mechanisms and Robotics, 1, pp. 041006-1-9.

Xi, F., and Sinatra, R., 1997, "Effect of Dynamic Balancing On Four-bar Linkage Vibrations", Mechanism and Machine Theory, 32(6), pp. 715-728.

Xie, Y.M., and Steven, G.P., 1993, "A Simple Evolutionary Procedure for Structural Optimization", Computers and Structures, 49(5), pp. 885-896.

Xie, Y.M., and Steven, G.P., 1996, "Evolutionary Structural Optimization for Dynamic Problems", Computers and Structures, 58(6), pp. 1067-1073.

Xu, D., and Ananthasuresh, G.K., 2003, "Freeform Skeletal Shape Optimization of Compliant Mechanisms", ASME Journal of Mechanical Design, 125, pp. 253-261.

Yan, H.S., and Soong, R.C., 2001, "Kinematic and Dynamic Design of Four-bar Linkages By Links Counterweighing With Variables Input Speed", Mechanism and Machine Theory, 36, pp. 1051-1071.

Yan, H.S., and Soong, R.C., 2004, "An Integrated Design Approach of Four-bar Linkages with Variable Input Speed", JSME International Journal, Series C, 47 (1), pp. 350-362.

Yang, B.S., Choi, S.P., and Kim, Y.C., 2005, "Vibration Reduction Optimum Design of A Steam-Turbine Rotor-Bearing System Using A Hybrid Genetic Algorithm", Structural Multidiscipline Optimization, 30, pp. 43-53.

Ye, Z., and Smith, M.R., 1994, "Complete Balancing of Planar Linkages By An Equivalent Method", Mechanism and Machine Theory, 29(5), pp. 701-712.

Yoganand, G., Sen, D., 2011, "Link Geometry Synthesis for Prescribed Inertia", Proc. of 15th National Conference on Machines and Mechanisms, Nov 30 - Dec 02, IIT Madras, India.

Yu, Y.Q., 1987a, "Research On Complete Shaking Force and Shaking Moment

Balancing of Spatial Linkages", Mechanism and Machine Theory, 22(1), pp. 27-37.

Zeid, I., and Sivasubramanian, R., 2009, *CAD/CAM – Theory and Practice*, Tata McGraw-Hill, New Delhi, India.

Zhe, L., and Shixian, B., 1992, "Optimum Balancing of Linkages with Clearances", Mechanism and Machine Theory, 27(5), pp. 535–541.

Appendix A

MATLAB codes for generating shape

A B-spline curve is made of several curve segments defined by its control points. The MATLAB codes to generate a shape using B-spline curve are presented here. For example, a circle of radius 50 mm is generated using linear, quadratic and cubic B-spline curves. The circle can be generated with a suitable number of control points depending upon the choice as higher number of control points take more computational time to generate the curve. Considering the appropriate smoothness, visualization and calculation time, the circle with 16 control points is demonstrated here as an example (Fig. A.1).

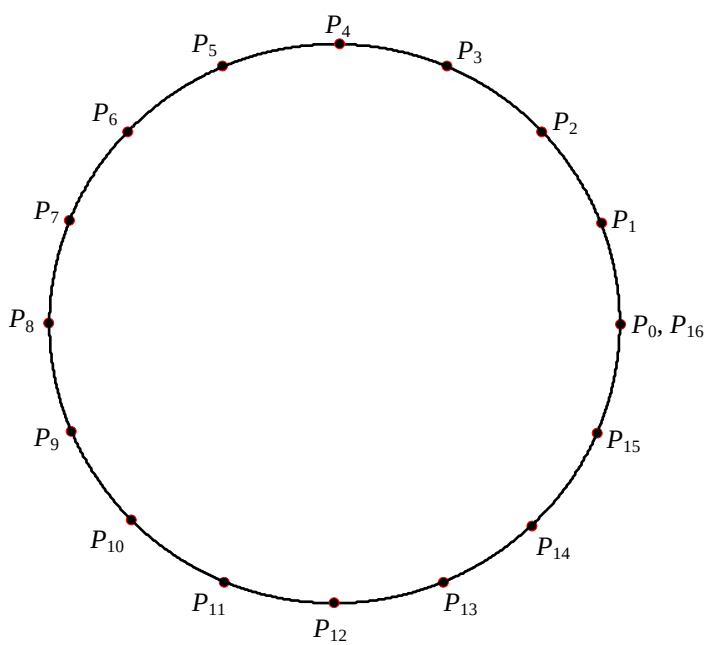

Fig. A.1 *The control points of a circle*

A.1 Control points calculation and plotting

The coordinates of the control points are calculated and plotted using the following MATLAB code.

```
% coordinates of 16 control points

x0=50*cos(0); y0=50*sin(0);
x1=50*cos(pi/8); y1=50*sin(pi/8);
x2=50*cos(2*pi/8); y2=50*sin(2*pi/8);
x3=50*cos(3*pi/8); y3=50*sin(3*pi/8);
x4=50*cos(4*pi/8); y4=50*sin(4*pi/8);
x5=50*cos(5*pi/8); y5=50*sin(5*pi/8);
x6=50*cos(6*pi/8); y6=50*sin(6*pi/8);
x7=50*cos(7*pi/8); y7=50*sin(7*pi/8);
x8=50*cos(8*pi/8); y8=50*sin(8*pi/8);
x9=50*cos(9*pi/8); y9=50*sin(9*pi/8);
x10=50*cos(10*pi/8); y10=50*sin(10*pi/8);
x11=50*cos(11*pi/8); y11=50*sin(11*pi/8);
x12=50*cos(12*pi/8); y12=50*sin(12*pi/8);
x13=50*cos(13*pi/8); y13=50*sin(13*pi/8);
x14=50*cos(14*pi/8); y14=50*sin(14*pi/8);
x15=50*cos(15*pi/8); y15=50*sin(15*pi/8);
x=[x0 x1 x2 x3 x4 x5 x6 x7 x8 x9 x10 x11 x12 x13 x14 x15];
y=[y0 y1 y2 y3 y4 y5 y6 y7 y8 y9 y10 y11 y12 y13 y14 y15];
plot(x,y,'or');
xlabel('x'); ylabel('y')
```

This MATLAB code generates control points of the circle.

A.2 Generation of circle using linear B-spline curve

The circle is generated using 16 linear B-spline curve segments corresponding to the control points obtained in the last section. Following is the MATLAB code:

```
% coordinates for linear B-spline curve

Lx=[x0 x1 x2 x3 x4 x5 x6 x7 x8 x9 x10 x11 x12 x13 x14 x15 x0];
Ly=[y0 y1 y2 y3 y4 y5 y6 y7 y8 y9 y10 y11 y12 y13 y14 y15 y0];
LB=eq_linear_B_spline(Lx,Ly);
```

```
for i = 1 : 16;
linear_B_spline=ezplot(LB(1, i),LB(2, i), [i - 1, i]);
end
```

The function for generating piecewise linear B-spline curve used in this code is as follows:

```
function eq_linear=eq_linear_B_spline(x,y)
syms u real;
p=[x; y];
eq_linear=[ ];
for i=1:16;
yi=linear_B_spline(p(1, i : i + 1), p(2, i : i + 1));
eq_linear = [eq_linear, simplify(subs(yi, u, u - i + 1))];
end
end
```

The function used for elementary linear B-spline curve equation is given as:

```
function equation = linear_B_spline(x,y)
syms u real;
n1 = (1 - u);
n2 = u;
equation = ([x; y]*[n1, n2]');
end
```

The circle composed of linear B-spline curve segments along with control points' using this code is shown in Fig. A.2. The resulting shape is a sequence of straight-line segments connecting the control points.

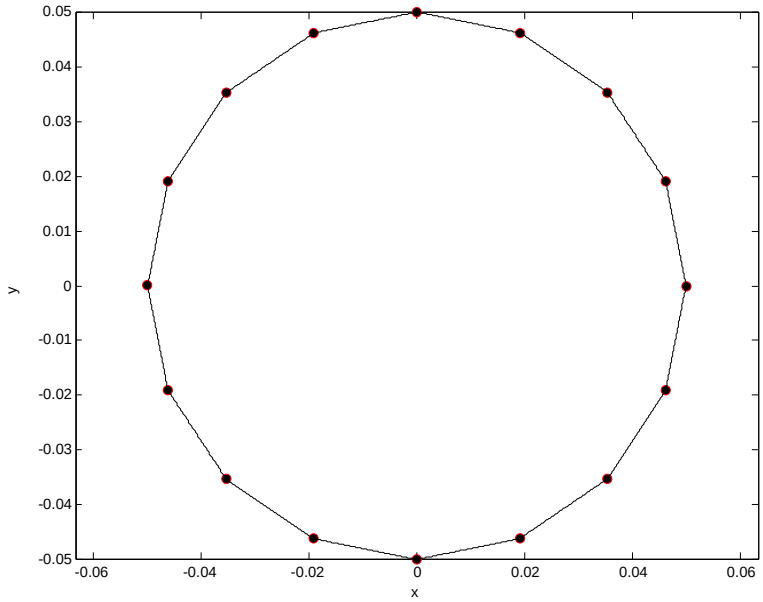

Fig. A.2 *Circle generated using linear B-spline curve segments*

A.3 Generation of circle using quadratic B-spline curve

The circle is generated using 16 quadratic B-spline curve segments corresponding to the control points obtained in section A.1. Following is the MATLAB code:

```
% coordinates for quadratic B-spline curve

Qx=[x0 x1 x2 x3 x4 x5 x6 x7 x8 x9 x10 x11 x12 x13 x14 x15 x0 x1];
Qy=[y0 y1 y2 y3 y4 y5 y6 y7 y8 y9 y10 y11 y12 y13 y14 y15 y0 y1];
QB=eq_quadratic_B_spline(Qx,Qy);
for i = 1 : 16;
quadratic_B_spline=ezplot(QB(1, i), QB(2, i), [i - 1, i]);
end
```

The function for generating piecewise quadratic B-spline curve used in this code is as follows:

```
function eq_quadratic=eq_quadratic_B_spline(x,y)
syms u real;
p=[x; y];
```

```
eq_quadratic=[ ];
for i=1:16;
yi=quadratic_B_spline(p(1,i:i+2),p(2,i:i+2));
eq_quadratic=[eq_quadratic,simplify(subs(yi,u,u-i+1))];
end
end
```

The function used for elementary quadratic B-spline curve equation is given as:

```
function equation = quadratic_B_spline(x,y)
syms u real;
n1 = (1-u).^2;
n2 = -2*u.^2 + 2*u + 1;
n3 = u.^2;
equation = ([x; y]*[n1, n2, n3]'/2);
end
```

The circle composed of quadratic B-spline curve segments along with control points' using this code is shown in Fig. A.3.

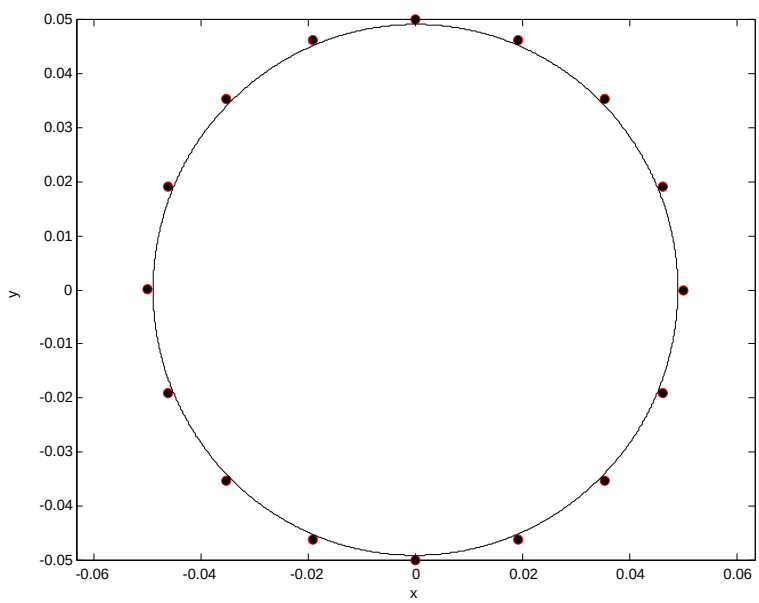

Fig. A.3 *Circle generated using quadratic B-spline curve segments*

The resulting shape has first-order parametric continuity throughout the curve.

A.4 Generation of circle using cubic B-spline curve

The circle is generated using 16 cubic B-spline curve segments using the MATLAB code given below:

```
% coordinates for cubic B-spline curve

Cx=[x0 x1 x2 x3 x4 x5 x6 x7 x8 x9 x10 x11 x12 x13 x14 x15 x0 x1 x2];
Cy=[y0 y1 y2 y3 y4 y5 y6 y7 y8 y9 y10 y11 y12 y13 y14 y15 y0 y1 y2];
CB=eq_cubic_B_spline(Cx,Cy);
for i = 1 : 16;
cubic_B_spline=ezplot(CB(1, i), CB(2, i), [i - 1, i]);
end
```

The function for generating piecewise cubic B-spline curve used in this code is as follows:

```
function eq_cubic = eq_cubic_B_spline(x,y)
syms u real;
p=[x; y];
eq_cubic=[ ];
for i = 1 : 16;
yi = cubic_B_spline(p(1, i : i + 3), p(2, i : i + 3));
eq_cubic = [eq_cubic, simplify(subs(yi, u, u - i + 1))];
end
end
```

The function used for elementary cubic B-spline curve equation is given as:

```
function equation = cubic_B_spline(x, y)
syms u real;
n1 = (1-u).^3;
n2 = 3*u.^3 - 6*u.^2 + 4;
n3 = -3*u.^3 + 3*u.^2 + 3*u + 1;
```

```
n4 = u.^3;
equation = ([x; y]*[n1, n2, n3, n4]'/6);
end
```

The circle composed of cubic B-spline curve segments along with control points using this code is shown in Fig. A.4. The resulting shape has second-order parametric continuity throughout the curve.

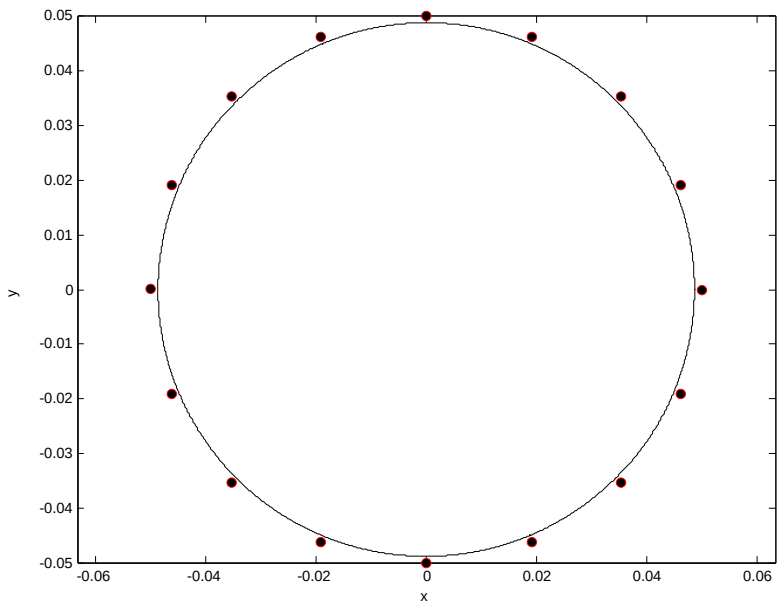

Fig. A.4 *Circle generated using cubic B-spline curve segments*

Note that both the quadratic and cubic B-spline curves are not passing through the control points as shown in Fig. A.3 and Fig. A.4. These curves are uniform and periodic in nature as their basis functions are repeated in the successive intervals. The uniform curves are preferred to generate the closed curves. The circle generated using linear, quadratic and cubic B-spline curves is shown in Fig. A.5.

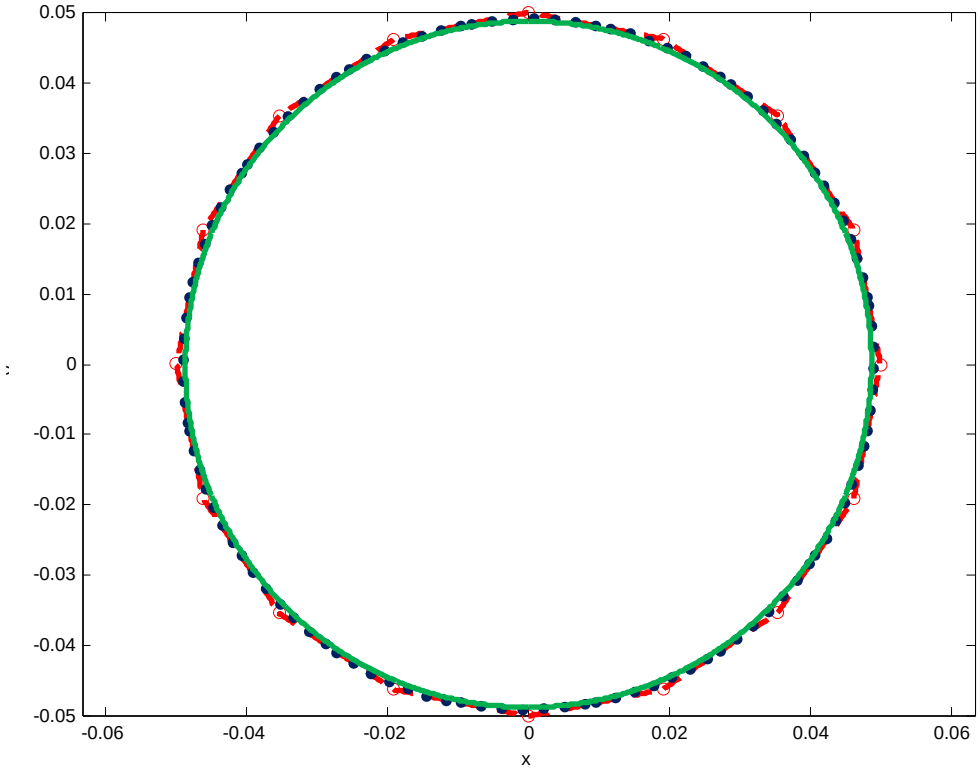

Fig. A.5 *Circle generated using linear, quadratic and cubic B-spline curve segments*

The B-spline curves are controlled within the convex hull of the control polygon connecting the control points. In Fig. A.5, linear, quadratic and cubic B-spline curves are shown by dashed line (red), dotted line (blue) and bold line (green), respectively. The control points are shown as the circles in red colour.

Appendix B

MATLAB codes for calculating inertial properties of a shape

The MATLAB programs to calculate the inertial properties using green's theorem for the shape generated using B-spline curves are given here. The inertial properties are calculated for a circle generated in Appendix A using linear, quadratic and cubic B-spline curves. The area A, centroid ($\bar{x}$, $\bar{y}$) and area moment of inertia about centroidal axes [I_{xx}, I_{yy}, I_{zz}] of a closed curve made of n B-spline curve segments are defined in Eqs. (5.20) – (5.25) as:

$$A = \sum_{i=1}^{n} \int_{u_{i-1}}^{u_i} x_i(u) y_i^{'}(u)\, du \tag{5.20}$$

$$\bar{x} = \frac{1}{2A_i} \sum_{i=1}^{n} \int_{u_{i-1}}^{u_i} x_i^2(u) y_i^{'}(u)\, du \tag{5.21}$$

$$\bar{y} = -\frac{1}{2A_i} \sum_{i=1}^{n} \int_{u_{i-1}}^{u_i} y_i^2(u) x_i^{'}(u)\, du \tag{5.22}$$

$$I_{xx} = -\frac{1}{3} \sum_{i=1}^{n} \int_{u_{i-1}}^{u_i} y_i^3(u) x_i^{'}(u)\, du \tag{5.23}$$

$$I_{yy} = \frac{1}{3} \sum_{i=1}^{n} \int_{u_{i-1}}^{u_i} x_i^3(u) y_i^{'}(u)\, du \tag{5.24}$$

$$I_{zz} = I_{xx} + I_{yy} \tag{5.25}$$

The parameters for circle are taken as:

(i) Radius, r = 0.05 m, (ii) Thickness, t = 0.01 m, (iii) Density, ρ = 7860 kg/m^3

Using standard formulas, the geometric and inertial properties of the circle are found as:

Area = $A = \pi r^2$ = 0.00785 m^2;

Mass = $m = At\rho$ = 0.6170 kg;

Mass center = $CG_x = CG_y = 0$;

Mass moment of inertia about mass center = $I = mr^2/2 = 7.7125 \times 10^{-4}$ kg-m^2

The MATLAB codes are developed using Eqs. (5.20) – (5.25) to calculate these properties for the shape generated using linear, quadratic and cubic B-spline curves.

1. For the circle generated using linear B-spline curve, the inertial properties are calculated using the following MATLAB code:

```
Lx=[x0 x1 x2 x3 x4 x5 x6 x7 x8 x9 x10 x11 x12 x13 x14 x15 x0]/1000;      % in meters
Ly=[y0 y1 y2 y3 y4 y5 y6 y7 y8 y9 y10 y11 y12 y13 y14 y15 y0]/1000;      % in meters
LB=eq_linear_B_spline(Lx,Ly);
for i = 1 : 16;
LX(i)=LB(1,i);
LY(i)=LB(2,i);
LX_dot(i)=diff(LX(i),sym('u'));
LY_dot(i)=diff(LY(i),sym('u'));
LA(i)=LX(i)*LY_dot(i);
Larea(i)=int(LA(i),sym('u'),i-1,i);
LCGx(i)=LX(i)^2*LY_dot(i);
Lcentroid_x(i)=int(LCGx(i),sym('u'),i-1,i);
LCGy(i)= LY(i)^2*LX_dot(i);
Lcentroid_y(i)=int(LCGy(i),sym('u'),i-1,i);
LIxx(i)=LY(i)^3*LX_dot(i);
LIxx(i)=-int(LIxx(i),sym('u'),i-1,i)/3;
LIyy(i)=LX(i)^3*LY_dot(i);
LIyy(i)=int(LIyy(i),sym('u'),i-1,i)/3;
LIzz(i)=LIxx(i)+LIyy(i);
end
Larea=sum(Larea);                                   % area in meter^2 using Eq. (5.20)
```

```
Lcentroid_x=sum(Lcentroid_x)/(2*Larea);          % centroid in meters using Eq. (5.21)
Lcentroid_y=-sum(Lcentroid_y)/(2*Larea);         % centroid in meters using Eq. (5.22)
Lmass=Larea*t*rho;                                                    % mass in kg
LIxx=sum(LIxx);
LIyy=sum(LIyy);
LIzz=sum(LIzz);
LIzz=sum(LIzz) *t*rho;                 % moment of inertia in Kg-meter^2 using Eq. (5.25)
```

The function, eq_linear_B_spline, used for generating piecewise linear B-spline curve is defined in Appendix A.

2. For the circle generated using quadratic B-spline curve, the inertial properties are calculated using the following MATLAB code:

```
Qx=[x0 x1 x2 x3 x4 x5 x6 x7 x8 x9 x10 x11 x12 x13 x14 x15 x0 x1]/1000;   % in meters
Qy=[y0 y1 y2 y3 y4 y5 y6 y7 y8 y9 y10 y11 y12 y13 y14 y15 y0 y1]/1000;   % in meters
QB=eq_quadratic_B_spline(Qx,Qy);
for i = 1 : 16;
QX(i)=QB(1,i);
QY(i)=QB(2,i);
QX_dot(i)=diff(QX(i),sym('u'));
QY_dot(i)=diff(QY(i),sym('u'));
QA(i)=QX(i)*QY_dot(i);
Qarea(i)=int(QA(i),sym('u'),i-1,i) ;
QCGx(i)=QX(i)^2*QY_dot(i);
Qcentroid_x(i)=int(QCGx(i),sym('u'),i-1,i);
QCGy(i)= QY(i)^2*QX_dot(i);
Qcentroid_y(i)=int(QCGy(i),sym('u'),i-1,i);
QIxx(i)=QY(i)^3*QX_dot(i);
QIxx(i)=-int(QIxx(i),sym('u'),i-1,i)/3;
QIyy(i)=QX(i)^3*QY_dot(i);
```

```
QIyy(i)=int(QIyy(i),sym('u'),i-1,i)/3;
QIzz(i)=QIxx(i)+QIyy(i);
end;
Qarea=sum(Qarea);                                   % area in meter^2 using Eq. (5.20)
Qcentroid_x=sum(Qcentroid_x)/(2*Qarea);             % centroid in meters using Eq. (5.21)
Qcentroid_y=-sum(Qcentroid_y)/(2*Qarea);            % centroid in meters using Eq. (5.22)
Qmass=Qarea*t*rho;                                  % mass in Kg
QIxx=sum(QIxx);
QIyy=sum(QIyy);
QIzz=sum(QIzz);
QIzz=sum(QIzz) *t*rho;                              % moment of inertia in Kg-meter^2 using Eq. (5.25)
```

The function, eq_quadratic_B_spline, used for generating piecewise quadratic B-spline curve is defined in Appendix A.

3. For the circle generated using cubic B-spline curve, the inertial properties are calculated using the following MATLAB code:

```
Cx=[x0 x1 x2 x3 x4 x5 x6 x7 x8 x9 x10 x11 x12 x13 x14 x15 x0 x1 x2]/1000;
% in meters
Cy=[y0 y1 y2 y3 y4 y5 y6 y7 y8 y9 y10 y11 y12 y13 y14 y15 y0 y1 y2]/1000;
% in meters
CB=eq_cubic_B_spline(Cx,Cy);
for i = 1 : 16;
CX(i)=CB(1,i);
CY(i)=CB(2,i);
CX_dot(i)=diff(CX(i),sym('u'));
CY_dot(i)=diff(CY(i),sym('u'));
CA(i)=CX(i)*CY_dot(i);
Carea(i)=int(CA(i),sym('u'),i-1,i) ;
CCGx(i)=CX(i)^2*CY_dot(i);
Ccentroid_x(i)=int(CCGx(i),sym('u'),i-1,i);
```

```
CCGy(i)=CX(i)*CY(i)*CY_dot(i);
Ccentroid_y(i)=int(CCGy(i),sym('u'),i-1,i);
CIxx(i)=CY(i)^3*CX_dot(i);
CIxx(i)=-int(CIxx(i),sym('u'),i-1,i)/3;
CIyy(i)=CX(i)^3*CY_dot(i);
CIyy(i)=int(CIyy(i),sym('u'),i-1,i)/3;
CIzz(i)=CIxx(i)+CIyy(i);
end;
Carea=sum(Carea);                                   % area in meter^2 using Eq. (5.20)
Ccentroid_x=sum(Ccentroid_x)/(2*Carea);             % centroid in meters using Eq. (5.21)
Ccentroid_y=sum(Ccentroid_y)/Carea;                 % centroid in meters using Eq. (5.22)
Cmass=Carea*t*rho;                                  % mass in Kg
CIxx=sum(CIxx);
CIyy=sum(CIyy);
CIzz=sum(CIzz);
CIzz=sum(CIzz) *t*rho;                              % moment of inertia in Kg-meter^2 using Eq. (5.25)
```

The function, eq_cubic_B_spline, used for generating piecewise cubic B-spline curve is defined in Appendix A.

The inertial properties calculated for the circle generated using linear, quadratic and cubic B-spline curves are given in Table B.1.

Table B.1 *Inertial properties of the circle*

	Original	Linear B-spline	Quadratic B-spline	Cubic B-spline
Area (m^2)	0.0078	0.0077	0.0076	0.0075
CGx (m)	0.0000	0.0000	0.0000	0.0000
CGy (m)	0.0000	0.0000	0.0000	0.0000
Mass (kg)	0.6170	0.6016	0.5939	0.5864
Mass moment of inertia (kg-m^2)	7.7125e-4	7.3289e-4	7.1432e-4	6.9617e-4

Papers published based on this work

SCI Journals

1. Chaudhary K., Chaudhary H., 2015, "Optimal Dynamic Balancing and Shape Synthesis of Links in Planar Mechanisms", *Mechanism and Machine Theory*, 93, pp. 127-146. ISSN: 0094-114X. DOI 10.1016/j.mechmachtheory.2015.07.006.
2. Chaudhary K., Chaudhary H., 2014, "Dynamic Balancing of Planar Mechanisms using Genetic Algorithm", *Journal of Mechanical Science and Technology*, 28 (10), pp. 4213-4220. ISSN: 1738-494X. DOI 10.1007/s12206-014-0934-4.
3. Chaudhary K., Chaudhary H., 2015, "Optimal Design of Planar Slider-crank Mechanism Using Teaching-learning-based Optimization Algorithm", *Journal of Mechanical Science and Technology*, 29(12), pp. 5189-5198. ISSN: 1738-494X. DOI 10.1007/s12206-015-1119-5.
4. Chaudhary K., Chaudhary H., 2015, "Optimal Dynamic Design of Planar Mechanisms using Teaching-learning-based Optimization Algorithm", *Proceedings of the Institution of Mechanical Engineers, Part C: Journal of Mechanical Engineering Science*, ISSN: 0954-4062, published online Oct 2015. Sage Publications Ltd., England.

Non SCI Journals

1. Chaudhary K., Chaudhary H., 2016, "Computer Aided Design of Links in Planar Mechanisms", *International Journal of Advance Engineering and Research Development*, 3(3), pp. 369-376. ISSN: 2348-6406.
2. Chaudhary K., Chaudhary H., 2015, "Dynamic Balancing and Link Shape Synthesis of Slider-crank Mechanism for Multi-cylinder Engines", *International Journal of Mechanisms and Robotic Systems*, 2(3), pp. 254-275. ISSN: 2047-7252. Inderscience Publishers, Switzerland.
3. Chaudhary K., Chaudhary H., 2015, "Shape Optimization of Dynamically Balanced Planar Four-bar Mechanism", *Procedia Computer Science*, 57, pp. 519-526. ISSN: 1877-0509, DOI 10.1016/j.procs.2015.07.378.
4. Chaudhary K., Chaudhary H., 2014, "Optimum Balancing of Slider-crank Mechanism using Equimomental System of Point-masses", *Procedia Technology*, 14, pp. 35-42. ISSN: 2212-0173. DOI

10.1016/j.protcy.2014.08.006.

Book Chapter

1. Chaudhary H., Chaudhary K., 2015, "Design of Reactionless Mechanisms Based on Constrained Optimization Procedure" in *Dynamic Balancing of Mechanisms and Synthesizing of Parallel Robots*, chapter 11, pp. 273-298. Published by Springer International Publishing, Switzerland. DOI 10.1007/978-3-319-17683-3_11. ISBN 978-3-319-17682-6.

Conferences

1. Chaudhary K., Chaudhary H., 2015, "Optimum Dynamic Balancing of a Planar Five-bar Mechanism using Genetic Algorithm", in proceeding of *International Conference on Advances in Materials and Product Design* (AMPD2015), NIT Surat, Gujarat, India, Jan 10-11, pp. 73-80. ISBN 978-93-5196-956-3
2. Chaudhary K., Chaudhary H., 2013, "Minimization of Shaking Force and Shaking Moment in Multiloop Planar Mechanisms", in proceeding of *1st International and 16th National Conference on Machines and Mechanisms* (iNaCoMM2013), IIT Roorkee, Dec. 18-20, pp. 346-352.
3. Chaudhary K., Chaudhary H., 2013, "Concept of Equimomental System for Dynamic Balancing of Mechanisms", in proceeding of *1st International Conference on Automation and Mechanical Systems* (ICAMS2013), Lingaya's University, Faridabad, India, March 21-22, pp. 124-132. ISBN 978-81-909732-9-8
4. Chaudhary K., Chaudhary H., 2013, "Kinematic and Dynamic Analysis of Stephenson Six Bar Mechanism using HyperWorks", in proceeding of *India Altair Technology Conference* 2013, Altair Engineering India Pvt Ltd. Pune, July 18-19, 2013.

Brief Bio-data of the author

Name : **Kailash Chaudhary**

Date of birth : March 28, 1980

Address for correspondence : P.N. 12, Opposite Shiv Market, Saran Nagar, Jodhpur (Rajasthan), India - 342001

Education:

Degree	Discipline	Institute	Board/University	Percentage	Year	Division
Secondary	--	Saint Paul's Ajmer	RBSE Ajmer Rajasthan	87.64	1997	First
Senior Secondary	PCM	Saint Paul's Ajmer	RBSE Ajmer Rajasthan	67.54	1999	First
B.E.	Mechanical Engineering	GSET Jaipur	University of Rajasthan Jaipur	77.68	2004	First
M.E.	Production and Industrial Engineering	MBM Jodhpur	JNVU Jodhpur Rajasthan	72.33	2012	First
Ph.D.	Mechanical Engineering	Malaviya National Institute of Technology Jaipur	Autonomous	---	Thesis submitted in Dec 2015	---

Teaching Experience:

Organisation	Designation	Service Period
Raj Engineering College, Jodhpur	Assistant Professor	06-07-2010 to 23-12-2011
SKIT Jaipur	Lecturer	22-07-2006 to 07-04-2007
GSET Jaipur	Lecturer	02-08-2004 to 21-07-2006

Industrial Experience:

Organisation	Designation	Service Period
SURFEX Jodhpur	Design Engineer	09-04-2007 to 05-07-2010

Membership of Professional Society: Association for Machines and Mechanisms India

Awards and achievements

- 30th position in RBSE state merit in secondary examination
- Qualified GATE 2007
- Young scientist award in National Conference on Environmental Pollution, Restoration and Management organized by Govt. College of Engineering and Technology Bikaner, 2011
- Scholarship awarded by the Ministry of Human Resource Development, Government of India to carry out PhD. research work in MNIT Jaipur